# Palynological investigation of Holocene climatic and oceanic variability in South Africa and the southern Benguela upwelling system

Dissertation for the Doctoral Degree in Natural Sciences

**Dr. rer. nat**

in the Faculty of Geosciences

at the University of Bremen

submitted by

**Xueqin Zhao**

Bremen, February, 2017

# PRÜFUNGSAUSSCHUSS

## Gutachter

Herr Prof. Dr. Dr. Gerold Wefer

Herr Prof. Dr. Hermann Behling

## Tag des Prüfungskolloquiums

04 May 2017

## Mitglieder der Kommission

Herr Prof. Dr. Dr. Gerold Wefer

Herr Prof. Dr. Hermann Behling

Herr Prof. Dr. Michal Kucera

Frau Dr. Lydie Dupont

Frau Dr. Annette Hahn

Herr Oliver Helten

# Versicherung an Eides Statt

## gem.§ 5 Abs. 5 der Promotionsordnung vom 15.07.2015

---

Ich, **Xueqin Zhao**

Anschrift: Carl-Severing-Str. 40, 28329, Bremen

Matr.-Nr.: 2973412

Versichere an Eides Statt durch meine Unterschrift, dass ich die vorstehende Arbeit selbständig und ohne fremde Hilfe angefertigt und alle Stellen, die ich wörtlich dem Sinne nach aus Veröffentlichungen entnommen habe, als solche kenntlich gemacht habe, mich auch keiner anderen als der angegebenen Literatur oder sonstiger Hilfsmittel bedient habe, und die zu Prüfungszwecken beigelegte elektronische Version der Dissertation mit der abgegebenen gedruckten Version identisch ist.

Ich versichere an Eides Statt, dass ich die vorgenannten Angaben nach besten Wissen und Gewissen gemacht habe und dass die Angaben der Wahrheit entsprechen und ich nichts verschwiegen habe.

Die Strafbarkeit einer falschen eidesstattlichen Versicherung ist mir bekannt, namentlich die Strafandrohung gemäß § 156 StGB bis zu drei Jahren Freiheitsstrafe oder Geldstrafe bei vorsätzlicher Begehung der Tat bzw. gemäß § 161 Abs. 1 StGB bis zu einem Jahr Freiheitsstrafe oder Geldstrafe bei fahrlässiger Begehung.

_____ _____

Ort, Datum Unterschrift

# Contents

# Abstract

South Africa is very sensitive to climate change, because it is located between two atmospheric systems (subtropical and warm-temperate systems) and two oceanic systems (Benguela Current and Agulhas Current). Presently, the seasonal changes of atmospheric and oceanic systems induce a pronounced rainfall seasonality comprised of three different rainfall zones (summer rainfall zone, SRZ; year-round rainfall zone, YRZ and winter rainfall zone, WRZ) over South Africa. However, the seasonality development during the Holocene in South Africa is poorly understood and the driving forces of the climate change are debated. Therefore, this study aims to provide a detailed reconstruction of Holocene climate and vegetation variability of South Africa, palaeoceanographic changes in the southern Benguela upwelling system as well as the land-ocean linkages. It is based on the high-resolution palynological analysis (pollen, microcharcoal and organic-walled dinoflagellate cysts) of marine sediment samples offshore of the west coast of South Africa.

Although pollen preserved in undisturbed marine sediments has the potential to provide long continuous information integrating a large area of continental vegetation and climate history, the pollen distribution in marine sediments is very complex. Thus, it is crucial to characterize the pollen distribution in the marine sediments and the source of the pollen before we turn into the interpretation of fossil records. In the first part of this thesis, the spatial distribution of pollen in marine surface sediments was investigated based on a transect of 12 marine surface sediment samples retrieved from north (29.12°S) to south (32.50°S) of the Namaqualand mudbelt off western South Africa. The distinct pollen spectra reflect vegetation communities on the adjacent continent with a marked north-south gradient of pollen concentration. The distribution of specific pollen taxa suggests that the Orange River is a major contribution of pollen to the northern mudbelt declining southwards. Whereas the seasonal inputs of pollen from offshore berg winds and local ephemeral Namaqualand rivers have a great contribution to the central mudbelt. In the southern mudbelt, the dominated Fynbos elements indicate a main pollen source from the Fynbos vegetation in the southwestern Cape of South Africa.

The study of pollen distribution in the Namaqualand mudbelt demonstrates that pollen records from marine sediment cores in the mudbelt have the potential to be a reliable tool to decipher vegetation history in this region. The approach in the first part of this thesis allows for climate reconstructions of the SRZ and WRZ using specific pollen taxa from a single marine archive. Therefore, in the second part of this thesis, the Holocene vegetation and climate variability in South Africa was reconstructed using pollen and microcharcoal records of two marine core sites GeoB8331 and GeoB8323 from the Namaqualand mudbelt offshore

of the west coast of South Africa covering the last 9900 and 2200 years, respectively. Three different climate periods were described with apparently contrasting climate developments between the SRZ and WRZ: during the early Holocene (9900-7800 cal. yr BP), a minimum of grass pollen suggests lower summer rainfall in the SRZ, while relatively wet conditions in the WRZ were indicated by the initial presence of Renosterveld vegetation. During the middle Holocene (7800-2400 cal. yr BP), a maximum in grass pollen suggests an expansion of rather moist savanna/grassland. This is probably associated with higher summer rainfall in the SRZ resulting from increased austral summer insolation. In the WRZ, a decline of Fynbos vegetation accompanied by an expansion of Succulent Karoo vegetation indicate warmer and drier conditions, which possibly suggests a southward shift of the southern westerlies. Comparing the results of the two sites for the last 2200 years show a more stable climate in the WRZ than in the SRZ. In addition, the 'Little Ice Age' (LIA) event (ca. 700-200 cal. yr BP) was detected with colder and drier conditions in the SRZ but colder and wetter conditions in the WRZ.

To assess the land-sea linkages in this region, in the third part of this thesis, the Holocene palaeoceanographic and palaeoenvironmental changes in the southern Benguela upwelling system was investigated based on the organic-walled dinoflagellate cyst analysis of 12 marine surface sediment samples and gravity core GeoB8331-4 from the Namaqualand mudbelt offshore of the west coast of South Africa. The results were compared with pollen and geochemical records from the same samples. Three main phases were identified with significantly distinct oceanographic conditions during the Holocene: during the early Holocene (9900-8400 cal. yr BP), warm and stratified conditions were indicated by high percentages of autotrophic taxa suggesting reduced upwelling likely due to a northward shift of the southern westerlies. In contrast, during the middle Holocene (8400-3100 cal. yr BP), cool and nutrient-rich waters with active upwelling were indicated by a strong increase in heterotrophic taxa at the expense of autotrophic taxa. This is probably caused by a southward shift of the southern westerlies. During the late Holocene (3100 cal. yr BP to modern), strong river discharge with high nutrient supply between 3100-640 cal. yr BP was implied by high percentages of *Brigantedinium* spp. and other fluvial-related taxa such as *Protoperidinium americanum* and *Lejeunecysta oliva*.

# Zusammenfassung

Südafrika reagiert sehr sensibel auf Klimaveränderungen, da es zwischen zwei atmosphärische Systemn (subtropisches und warm temperates Klima) und zwei ozeanische Systemen (Benguela und Agulhas Strömung) liegt. Heutzutage verursachen die saisonalen Veränderungen der atmosphärischen und ozeanischen Systeme eine ausgeprägte Saisonalität des Niederschlags mit zwei verschiedenen Niederschlagszonen (Sommerregenzone, SRZ; ganze Jahrezone, YRZ und Winterregenzone, WRZ) über Südafrika. Die Entwicklung dieser Saisonalität im Holozän ist bis jetzt jedoch nicht gut untersucht und die Auslöser des Klimawandels sind umstritten. Die vorliegende Studie ist eine detaillierte Rekonstruktion von Klima- und Vegetationsveränderungen des Holozäns in Südafrika. Außerdem werden paläozeanographische Veränderungen des südlichen Benguela Auftriebssystems sowie Land-Ozean-Interaktionen untersucht. Ziel der Arbeit basiert auf hochaufgelösten palynologischen Analysen (Pollen, Mikro-Holzkohle und Dinoflagellaten-Zysten) aus marinen Sedimentproben, die vor der Westküste Südafrikas genommen wurden.

Generell können Pollen aus ungestörte marinen Sedimenten, kontinuierliche Informationen über kontinentale Vegetation und Klima über einen langen Zeitraum liefern. Die Pollenverteilung in Meeressedimenten wird jedoch verändert. Deshalb ist es wichtig, zunächst die Pollenverteilung in Meeressedimenten und die Ursprung zu definieren, bevor der Datensatz interpretiert werden kann. Im ersten Teil dieser Arbeit wurde die räumliche Verteilung von Pollen in Meeressedimenten basierend auf einem Nord-Süd-Transekt von 12 marinen Oberflächenproben aus dem Namaqualand Schlammgürtel vor der Westküste Südafrikas untersucht. Die unterschiedlichen Pollenspektra reflektieren Pflanzengesellschaften des angrenzenden Kontinents mit einem ausgeprägten Nord-Süd-Gradienten der Pollenkonzentration. Die Verbreitung bestimmter Pollentaxa deutet darauf hin, dass der Orange River eine Hauptquelle für Pollen im nördlichen Schlammgürtel ist und südwärts abnimmt. Hingegen leistet der saisonale Polleneintrag von küstennahen „berg winds“ und lokalen ephemeren Namaqualand Flüssen einen großen Beitrag zu der Gemeinschaft im zentralen Schlammgürtel. Im südlichen Schlammgürtel zeigen die dominierenden Fynboselemente die Fynbos-Vegetation im südwestlichen Kap von Südafrika als Hauptpollenquelle an.

Die Untersuchung der Pollenverbreitung im Namaqualand Schlammgürtel demonstriert, dass die Pollenanalyse mariner Sedimentkerne des Schlammgürtels zur Rekonstruktion der Paläovegetation dieser Region geeignet ist. Die Ergrbnisse aus dem ersten Teil dieser Arbeit ermöglichen die Klimarekonstruktion der SRZ und der WRZ mithilfe von bestimmter

Pollentaxa aus demselben Probensatz. Im zweiten Teil dieser Arbeit wurde die Vegetation und Klimavariabilität des Holozäns in Südafrika mithilfe von Pollen und Mikro-Holzkohle der beiden Sedimentkerne GeoB8331 und GeoB8323 aus dem Namaqualand Schlammgürtel vor der Westküste Südafrikas über den Zeitraum der letzten 9900 bzw. 2200 Jahre rekonstruiert. Drei verschiedene Klimaperioden mit auffälligen klimatischen Unterschieden zwischen der SRZ und der WRZ während des frühen Holozäns (9900-7800 cal. yr BP) wurden beschrieben. Ein Minimum an Graspollen deutet auf niedrigere Niederschläge in der SRZ hin, während feuchtere Bedingungen in der WRZ durch das erstmalige Auftreten von Renosterveld Vegetation erkennbar werden. Während des mittleren Holozäns (7800-2400 cal. yr BP) deutet ein Maximum von Graspollen auf eine Expansion von eher feuchten Savannen/Grasländern mit vielen Gräsern hin. Dies hängt wahrscheinlich mit höheren Sommerniederschlägen in der SRZ zusammen, die sich aus erhöhter Insolation im Südsommer ergeben. In der WRZ zeigt eine Abnahme der Fynbos-Vegetation begleitet von einer Ausweitung der sukkulenten Karoo-Vegetation wärmere und trockenere Bedingungen an, die vermutlich auf eine Südwärtsverlagerung der südlichen Westwinde hindeuten. Der Vergleich der beiden oben genannten Standorte über die letzten 2200 Jahre zeigt ein stabileres Klima in der WRZ im Vergleich zur SRZ an. Außerdem konnten für das „Little Ice Age“ Ereignis (ca. 700-200 cal. yr BP) kältere und trockenere Bedingungen in der SRZ sowie kältere und nassere Bedingungen in der WRZ ausgemacht werden.

Um die Land-Ozean-Interaktionen der Region zu beurteilen, wurden im dritten Teil der Arbeit paläozeanographische und Paläoumweltveränderungen des südlichen Benguela Auftriebssystems mithilfe der Analyse von Dinoflagellaten-Zysten in 12 marinen Oberflächenproben und dem Schwerelotkern GeoB8331-4 aus dem Namaqualand Schlammgürtel vor der Westküste Südafrikas untersucht. Die Ergebnisse werden mit Pollen und geochemischen Daten derselben Proben verglichen. Drei Hauptphasen mit signifikant unterschiedlichen ozeanographischen Bedingungen wurden für das Holozän identifiziert: Im frühen Holozän (9900-8400 cal. yr BP) deuten hohe prozentuale Anteile von autotrophen Taxa auf warme und stratifizierte Bedingungen hin. Dies lässt auf verringerten Auftrieb, wahrscheinlich aufgrund einer Nordwärtsverlagerung der südlichen Westwinde schließen. Im Gegensatz dazu lässt im mittleren Holozän (8400-3100 cal. yr BP) ein starker Anstieg heterotropher Taxa auf Kosten autotropher Taxa, auf kaltes und nährstoffreiches Wasser mit aktivem Auftrieb schließen. Dies wird wahrscheinlich von einer Südwärtsverlagerung der südlichen Westwinde verursacht. Im späten Holozän (3100 cal. yr BP bis heute) deuten hohe prozentuale Anteile von *Brigantedinium* spp. und anderen fluvial-bezogenen Taxa wie *Protoperidinium americanum* und *Lejeunecysta oliva* auf hohe Abflussmengen mit hohem Nährstoffeintrag zwischen 3100-640 cal. yr BP hin.

# Chapter 1 Introduction

## 1.1 Holocene climate variations in South Africa

Global climate change which has been broadly discussed by the governments and scientists all over the world, is one of the hottest topic and greatest challenges of the 21st century. Research of global climate change is one of the effective methods to accurately predict future climate trend drawing lots of attention in the world, especially in recent years when the global warming and natural disasters occur very frequently. The Holocene time period is the witness of all humanity's recorded history and its civilization is very crucial for our understanding of the palaeoclimate evolution. Early studies show that variations in the global average temperatures during the Holocene have been relatively small in comparison with the ice age cycle (Houghton et al., 1990). However, small variations known as Holocene Climate Optimum (ca. 7000-5000 cal. yr BP), Medieval Warm Period (ca. 950-1250 AD) and Little Ice Age (ca. 1300-1850 AD) are documented.

South Africa, located at the interface between subtropical and warm-temperate climate zones and between the Indian and Atlantic oceans, is very sensitive to climate change and thus a critical region for Holocene environmental research in the Southern Hemisphere (Chase and Meadows, 2007; Scott et al., 2012). It is principally divided into three different rainfall zones due to the seasonal changes of atmospheric and oceanic systems inducing a pronounced rainfall seasonality: a winter rainfall zone (WRZ) at the southwestern tip of the continent, a transitional year-round rainfall zone (YRZ) and a summer rainfall zone (SRZ) in the remainder of the continent (Figure 1.1). However, due to the unfavorable conditions for the preservation of the climate archives in such dry regions, palaeoenvironmental evidence is very difficult to obtain. In particular, Holocene records are still scarce and mostly situated in the eastern part of South Africa (Neumann et al., 2010, 2014; Stager et al., 2013). The existing long continuous records are widely distributed over South Africa and have been recovered from distinct local environments, which sometime lead to contradictory results (Baker et al., 2014; Kristen et al., 2007; Norström et al., 2014). This might be associated with the dynamic interaction of two different rainfall zones (WRZ and SRZ) from west to east over the South Africa (Chase and Meadows, 2007). Therefore, the research questions about climate variability, regional comparison and driving forces during the Holocene in South Africa are still open for us to investigate.

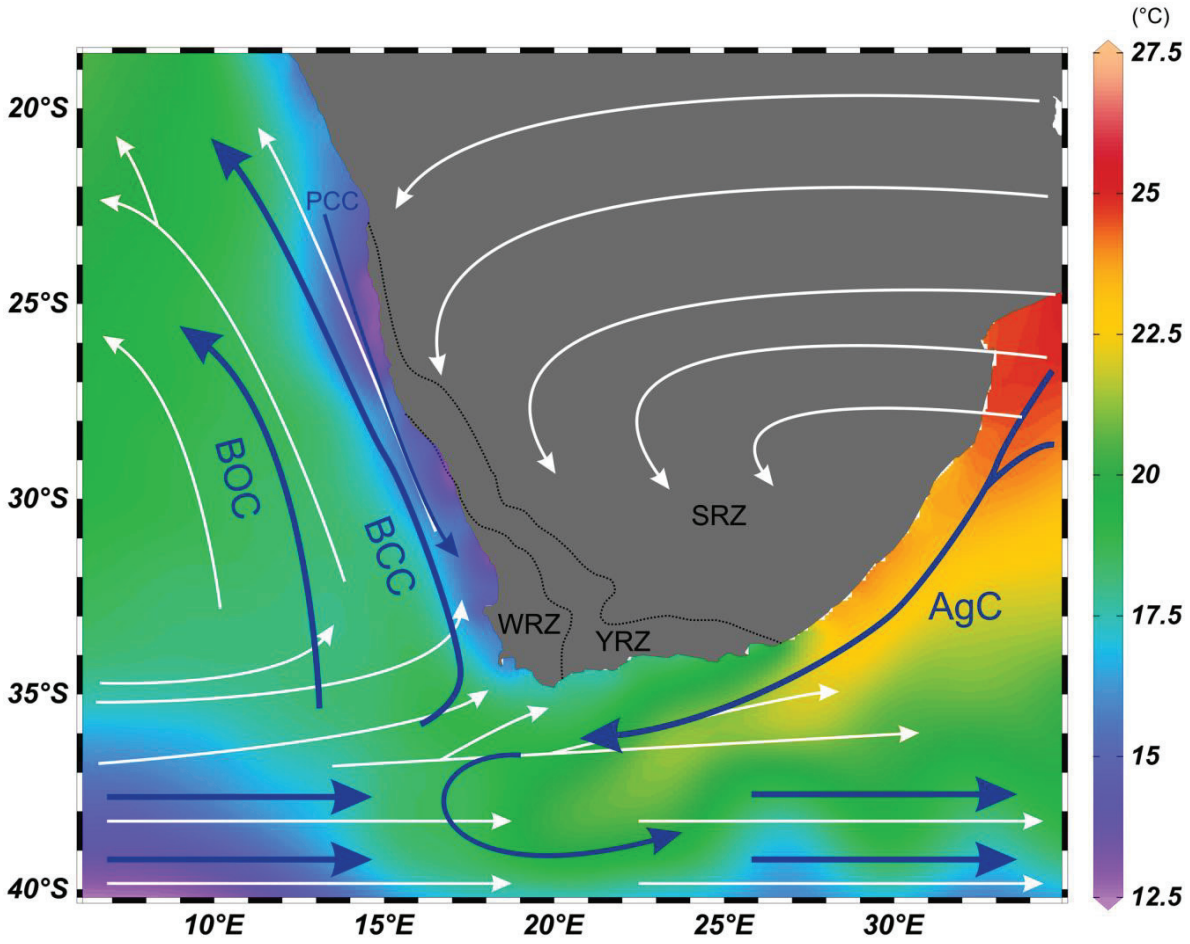


**Figure 1.1** Major atmospheric (white arrows) and oceanic (blue arrows, AgC: Agulhas Current, BCC: Benguela Coastal Current, BOC: Benguela Ocean Current, PCC: poleward countercurrent) circulation systems over southern Africa with the mean annual sea surface temperatures in colours (Ocean Data View, U.S. NODC World Ocean Atlas 2013). Three rainfall zones of southern Africa are indicated: winter rainfall zone (WRZ), year-round rainfall zone (YRZ) and summer rainfall zone (SRZ).

For the WRZ, it is known to having glacial-interglacial variability and may have experienced increased humidity during the last glacial maximum (LGM) (Cowling et al., 1999a; Meadows and Baxter, 1999; Scott and Woodborne, 2007a). Most studies attribute it to an equatorward expansion of the WRZ during the glacials (Chase and Meadows, 2007; Dupont et al., 2007) resulting from a northward shift of the southern westerlies (Cockcroft et al., 1987). Unfortunately, little is known about the Holocene hydrological changes in the WRZ due to limited information from mostly short and non-continuous terrestrial archives. Evidences indicating the position of the southern westerlies or the extension of the WRZ only cover the late Holocene or even the past few decades (Biastoch et al., 2009; Granger, 2016; Stager et al., 2012). Considering the large role of the southern westerlies in hydrological systems of South Africa, a high-resolution Holocene record would help to improve our understanding of their dynamics. In contrast to the WRZ, the climate of the SRZ was arid during the glacial and

humid during the interglacial as in most regions of the world. This glacial-interglacial climate variability is assumed to be mainly driven by fluctuations in orbital variation (Hopley et al., 2007; Partridge et al., 1997), while the insolation forcing on shorter time scales during the Holocene (Chase et al., 2009, 2010; Chevalier and Chase, 2015; Schefuß et al., 2011) may have occurred as the primary driver of hydrological variations in the SRZ. Other driving forces on continental vegetation and hydrology are effects of ocean sea surface temperature (SST). Strong southeast trade winds drive upwelling in the southern Benguela region. The lower evaporation of the cold waters of the Benguela upwelling region induce a strong decrease in SST and cause aridity over the western coastal areas, thereby affect the coastal vegetation. However, since now, the high-resolution sea surface conditions records are still missing which is crucial for the understanding of land-sea linkages. Another possible driver is human activities which has been addressed by many other studies concerning the impact of humans such as Iron-Age people (Evers, 1975; Klapwijk, 1974) and Khoikhoi people (Bousman and Scott, 1994; Bousman, 1998), and particularly later of European settlement since late 17$^{th}$ century (Neumann et al., 2010, 2011). In summary, the uncertain mechanisms of climate variability in South Africa indicate that high-resolution Holocene records for palaeoclimate and palaeoceanography reconstruction are essential to investigate the climate system of the study area.

## 1.2 Scientific objectives

Overall, the high-resolution Holocene climatic evolution of South Africa and its main driving forces remain uncertain. The major objective of this thesis is to reconstruct Holocene climatic variability in South Africa and the southern Benguela upwelling system off western South Africa. This will provide a better understanding of the palaeoclimate system (climate variability and driving forces) of the study area.

To be more specifically, the following objectives are addressed:

(1) What are the possible sources of mudbelt pollen and to what degree can pollen distribution of the mudbelt reflect the adjacent continental vegetation?

(2) How did the Holocene vegetation and climate vary in the winter and summer rainfall zones of South Africa?

(3) Were the variabilities in the two zones consistent? If not, what were their mechanisms, respectively?

(4) How was the land-sea interaction during the Holocene?

## 1.3 Regional setting

The Namaqualand mudbelt (Figure 1.2) stretches over 500 km along the western coast of southern Africa from 20 km north of the Orange River mouth to south of St Helena Bay (Rogers and Bremner, 1991). This mudbelt is an inner continental shelf suite of generally fine-grained Holocene sediments. It lies in water depths of 80-140 m under the action of the poleward countercurrent. The mudbelt is broadly cohesive, continuous and thicker in the Orange River prodelta area where it is dominated by laminated silt, while it tends to be thinner and consisting of homogeneous mud towards the south (Mabote et al., 1997; Meadows et al., 1997, 2002).

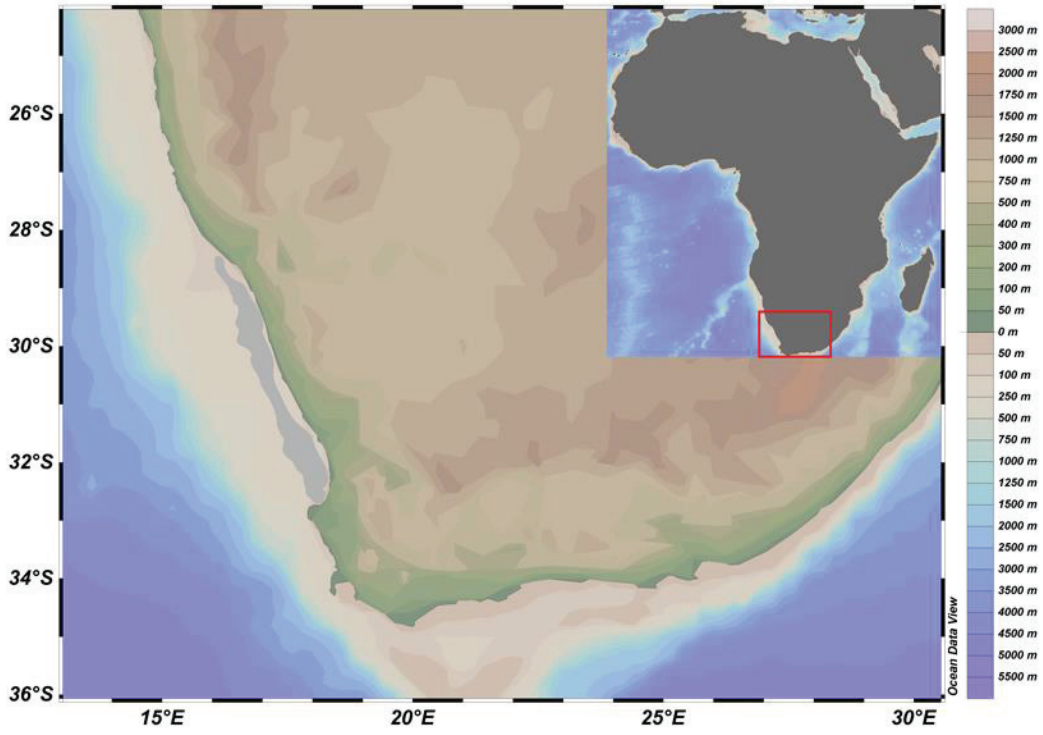


**Figure 1.2** Map of southern Africa showing bathymetry and topography. The grey shaded area indicates the location of the Namaqualand mudbelt.

### 1.3.1 Oceanic circulation

Oceanographic conditions on the west coast of southern Africa have been well reviewed in detail by e.g., Nelson and Hutchings (1983), Shannon and Nelson (1996), Peterson and Stramma (1991). The ocean circulation in the study area (Figure 1.1) is dominated by the northward flowing of the Benguela Current (BC) stretching from 34°S to 15°S along the west coast of southern Africa. Two branches of the Benguela Current can be distinguished: the

Benguela Coastal Current (BCC), flowing along the coast in depth varying from a few meters nearest to the coast to about 120 m along the outer shelf. The Benguela Oceanic Current (BOC) is a north-westward flowing branch diverging from the coast at about 28°S. Below the BCC, there is a weak and seasonal poleward countercurrent (PCC). Our study sites are located on the Namaqualand mudbelt. It is in the southern part of the Benguela upwelling system driven by the trade wind system which is controlled by the position and the intensity of the South Atlantic anticyclone (Schell, 1968). In the southern Benguela upwelling system, main upwelling of cold and nutrient-rich water originating from the body of the South Atlantic Central Water at depths of 150-330 m occurs during austral spring and summer (Shannon, 1985). Three upwelling centers with enhanced productivity can be distinguished: Namaqua cell (30°S), Cape Columbine cell (33°S) and Cape Peninsula cell (34°S). During austral winters, when the South Atlantic anticyclone is far to the north, the southern westerlies move to their northernmost position. This blocks the influence of southeast trade winds and reduces upwelling in the southern Benguela region. During austral summers, the poleward retreat of the South Atlantic anticyclone and the southern westerlies allows the influence of the southeast trade winds. They promote upwelling and water mixing processes driving increased productivity (Andrews and Hutchings, 1980; Hutchings et al., 2009).

At the southern boundary of the Benguela upwelling system, the relatively cool and oligotrophic waters of South Atlantic Current and the cold waters of the Antarctic Circumpolar Current meet the south-westward flow of warm and saline waters of the Agulhas Current (AgC) from the Indian Ocean (Figure 1.1). One part of the AgC, which forms eddies and transports relatively warm and saline water of the Indian Ocean into the South Atlantic Ocean, is at a maximum during austral summers when the southern westerlies shift polewards and southeast trade winds coincide with maximum upwelling (Shannon and Nelson, 1996).

### 1.3.2 Climate and vegetation

South Africa is located at the interface between subtropical and warm-temperate climate zones and between the Indian and Atlantic oceans. It is dominated by specific atmospheric and oceanic circulation systems across the region (Shannon and Nelson, 1996; Tyson and Preston-Whyte, 2000) resulting in three main rainfall zones (Figure 1.1): a summer rainfall zone (SRZ) in the north and east of southern Africa, a winter rainfall zone (WRZ) at the south-western tip of the continent extending northward from the Cape Peninsula along the west coast to about 28°C and a transitional year-round rainfall zone (YRZ) between these two regions (Chase and Meadows, 2007; Tyson and Preston-Whyte, 2000). During the austral summer, the rainfall in the SRZ is generated mainly by warm and moist easterly winds associated with the South Indian Anticyclone and more than 66% of the annual

precipitation falls between October and March. In the WRZ, precipitation is minimized in summer when the southern westerlies are located south due to alongshore winds resulting from a southern position of the South Atlantic Anticyclone. In contrast, during the austral winter, dry conditions and high pressure prevail over the SRZ. The southern westerlies are at their northernmost position over the southwestern Cape supplying rainfall to the WRZ and more than 66% of the annual precipitation falls between April and September. Westward to south-westward directed offshore winds (known as Berg winds) are very limited because they are blocked by the southern westerlies and almost no dust plumes can be observed south of 28°S (Eckardt and Kuring, 2005). Between these two regions, the YRZ receives both summer and winter rainfall all the year where the summer rainfall progressively increases eastward along the south coast of South Africa (Tyson and Preston-Whyte, 2000). Temperature and precipitation are highly variable, with annual values ranging from 11 to 20°C and 25-970 mm/yr in the WRZ, and 7-24°C and 10-1380 mm/yr in the SRZ (Hijmans et al., 2005). Along the west coast area, more than 65% of the precipitation falls in austral winter and varies between 50 and 400 mm/yr (Cowling et al., 1999b).

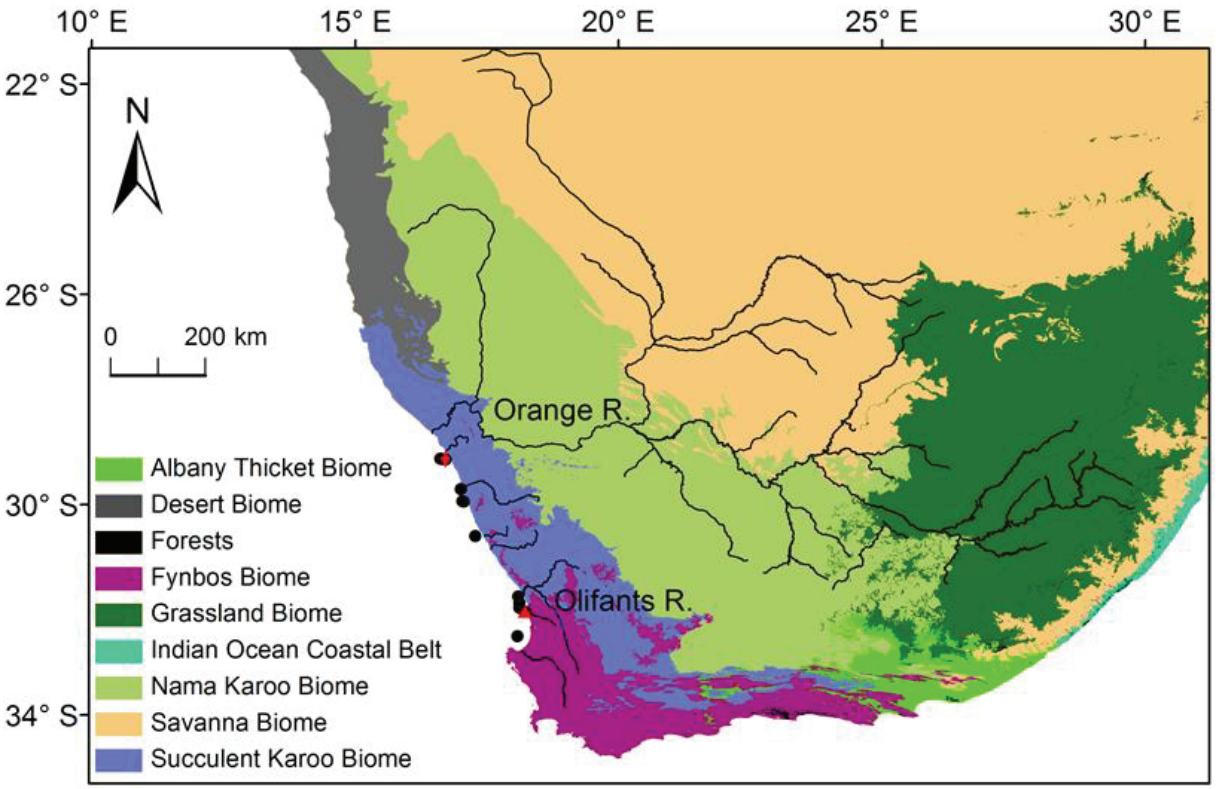


**Figure 1.3** Modern vegetation of southern Africa (after Mucina and Rutherford, 2006; Scott et al., 2012), Orange River catchment, Olifants River and other main rivers on the west coast with the location of 12 multicores (black dots) and two gravity cores GeoB8331-4 (in red diamond) and GeoB8323-2 (in red triangle).

The vegetation of southern Africa is spatially diverse and there are nine biomes in southern Africa, which reveal a marked east to west gradient driven by rainfall amount and seasonality (Figure 1.3) (Bredenkamp et al., 1996; Cowling et al., 1997; Mucina and Rutherford, 2006; White, 1983). The Savanna Biome, which is the most extensive one in southern Africa occupying 46% of its area, is characterized by a grassy ground layer and a distinct upper layer of woody elements associated with mean annual rainfall varying from 235 to 1000 mm/yr. The Grassland Biome, situated on the cooler and higher interior plateau, is dominated by a single layer of grasses and trees are largely absent except in a few localized habitats. It spans a large rainfall gradient from 400 to 1200 mm/yr. The Forest Biome, which is restricted to areas with mean annual rainfall of more than 725 mm in the SRZ and more than 525 mm in the WRZ (Mucina and Rutherford, 2006) comprises mostly of evergreen trees in multi-layered canopies, while the ground layer is often poorly developed due to the dense shade. The Nama Karoo Biome is semi-desert grassy and dwarf shrubland on the central plateau and is dominated by members of the Asteraceae, Poaceae, Aizoaceae, Liliaceae and Scrophulariaceae families. The rain in this biome falls mainly during austral summer varying between 100 and 520 mm/yr. The Succulent Karoo Biome, located in a narrow strip along the west coast and south of the escarpment, is characterized by dwarf leaf-succulents of which Aizoaceae (including Mesembryanthemaceae) and Crassulaceae are particularly prominent, where Asteraceae, Amaranthaceae, Euphorbiaceae (*Euphorbia*) and Zygophyllaceae (*Zygophyllum*) (Wheeler, 2010) are relatively common. Grasses are rare except in some sandy areas. This biome is primarily determined by low winter rainfall and extreme summer aridity with rainfall varying between 20 and 290 mm/yr. The Desert Biome, found under very harsh environmental conditions, is characterized by dominance of annual plants (often annual grasses like *Stipagrostis sabulicola*). The climate is characterized by occasional summer rainfall, but high levels of summer aridity with mean annual rainfall from approximately 10 mm in the west to 70 or 80 mm on the inland margin of the desert. The Fynbos Biome, which is an evergreen shrubland in the southwest Cape, is typified by the presence of Restionaceae, Ericaceae and Proteaceae with rainfall usually varying from 600 to 800 mm/yr. Renosterveld is another type of shrubland occurring within the Fynbos Biome and is dominated by Asteraceae, in particular by one species - renosterbos (*Elytropappus rhinocerotis*), together with other important shrubs of different families including Rubiaceae (*Anthospermum*), Thymelaeaceae (*Passerina*), Rosaceae (*Cliffortia*), Boraginaceae, Fabaceae and Malvaceae (Goldblatt and Manning, 2002). The rainfall in the Renosterveld is between 250 and 600 mm/yr of which at least 30% falls during austral winter. Other two biomes (Albany Thicket Biome and Indian Ocean Coastal Belt) are located in the southeastern South Africa, which are not relevant for this study and thus not described here.

### 1.3.3 Orange River and Olifants River

The Orange basin (Figure 1.3) is the most important drainage system in southern Africa covering an area of about 950,000 $km^2$. The perennial Orange River arises in the Drakensberg Mountains of Lesotho running 2160 km westwards through South Africa to the Atlantic Ocean. The Orange River has a discharge of 11 $km^3$/yr and is the world's fourth most turbid river (Milliman et al., 1995). The catchment of the Orange River is dominated spatially by grassland in the uppermost catchment, Nama Karoo and Savanna towards the middle and lower catchment and Succulent Karoo in the lowermost catchment. There are also local riparian wetlands along the Orange River, dominated by sedges and aquatics, primarily Cyperaceae, *Phragmites*, *Typha* and *Gunnera*.

The Olifants River (Figure 1.3) discharges into the Atlantic approximately 250 km north of Cape Town at the southern boundary of the Namaqualand. It is the second largest perennial river in South Africa with a catchment area of 46,220 $km^2$ rising 280 km sourced from the Witzenberg plateau at about 800 m altitude. Although having a much smaller catchment, the discharge of the Olifants River (7.4 $km^3$/yr) (Basson et al., 1998) is within the same order of magnitude as that of the Orange River (11 $km^3$/yr). The vegetation in the catchment of the Olifants River is dominated by the Fynbos Biome in the upper catchment and by the Succulent Karoo Biome in the lower catchment.

## 1.4 Materials and methods

### 1.4.1 Marine sediment samples

The samples used in this study (Figure 1.3) are from 12 multicores and two gravity cores which were obtained in January-February of 2003 during the M57/1 *Meteor* cruise (Schneider et al., 2003). Marine surface sediments from multicores are along a north-south transect of the Namaqualand mudbelt. The upper 3 cm of twelve multicores were assessed for their pollen composition. The two gravity cores GeoB8331-4 (29°08.12'S, 16°42.99'E, 887 cm long) and GeoB8323-2 (32°01.70'S, 18°12.21'E, 285 cm long) were retrieved at 97 m water depth from the northern Namaqualand mudbelt off the Holgat River (just south of the estuary of the Orange River), and at 92 m water depth from the southern Namaqualand mudbelt off the Olifants River, respectively. The GeoB8331-4 sedimentary sequence consists of olive brown mud from 887 to 15 cm and dark laminated layers within olive brown mud above 15 cm. The GeoB8323-2 sedimentary sequence consists of dark greenish gray sandy mud with bilvalve shell fragments, and shell layers from 182 to 178 cm. Additionally, considering the disturbance and compaction of the uppermost parts of the gravity cores during coring, two

multicores GeoB8331-2 (35 cm long, same site as GeoB8331-4) and GeoB8323-1 (45 cm long, same site as GeoB8323-2) were processed to extend the coverage of both records towards the present.

### 1.4.2 Palynological preparation

The samples were decalcified with diluted HCl (~12%) and two *Lycopodium* spore tablets (each containing 18584 ± 372 markers) were added during the decalcification step. After washing, the samples were treated with HF (~ 40%). The samples were shaken for 2 hours, and then kept standing for two days to remove silicates. Samples were sieved ultrasonically to remove particles smaller than 10-15 µm. Samples were stored in water, mounted in glycerol and identified under a light microscope (magnification 400 and 1000×) for pollen, spores, fresh-water algae, dinoflagellate cysts ("dinocysts" here after) and microcharcoal. Morphologies of pollen and spores, dinocysts and fresh-water algae are attached in Appendix I. Pollen grains were identified using the African pollen reference collection of the Department of Palynology and Climate Dynamics of the University of Göttingen and the Department of Environmental and Geographical Science of the University of Cape Town, African Pollen Database and after Scott (1982), Bonnefille and Riollet (1980). Dinocyst were identified following Zonneveld (1997), Head et al. (2005), Fensome et al. (2008) and the online modern dinoflagellate cyst determination key of Zonneveld and Pospelova (2015). Samples volumes were measured using water displacement to calculate concentration values. Accumulation rates were calculated by multiplying the concentration by the sedimentation rate for each sample. Microcharcoal particles (5-150 µm) were counted on the same slides for pollen and dinocyst analysis using the 202 touch point-count method (Clark, 1982) to calculate the microcharcoal concentration as $cm^2/cm^3$.

### 1.4.3 Terrestrial palynomorphs

With the further application of marine sediments in palaeoclimate reconstruction, various proxies such as pollen and spores, charcoal, stable isotopes, diatoms, cocolithophorids, planktonic foraminifera, grain size, magnetic susceptibility and organic carbon have been developed very well. Pollen and spores have been proved to be a useful tool to reconstruct palaeovegetation and palaeoclimate as they are taxon specific, small (generally between 10 and 100 µm), often produced in large quantities, easily transported, well preserved in suitable sediments, and may thus provide a good indication of the vegetation. Pollen preserved in undisturbed marine sediments has the potential to provide long continuous information which integrates a large area of continental vegetation and climate developments (Dupont, 1999). However, due to the remarkably varied pollen productivities of different plants, large scale

mixing possibility of pollen transportation by winds and rivers, displacement by ocean currents, sedimentation and taphonomic processes (Dupont, 1999), the pollen sources and the relationship between pollen and vegetation are very complicated suggesting that the interpretation of pollen records in marine sediments should be done with caution.

### 1.4.4 Microcharcoal

Charcoal is the black and opaque inorganic carbon residue which persists after the incomplete combustion (or pyrolysis) of plants tissue and other organic materials. Although the analysis has a wide application (Scott and Damblon, 2010), the most important one is that charcoal can be used as a proxy for fire. Fossil charcoal which is preserved in sediments after the burning of fires in the surrounding vegetation can be used for reconstruction of the past fire frequencies and magnitudes (Clark, 1988). Generally, charcoal concentration depends on the fire intensity which is not only associated with the climate conditions (dry or wet) but can also be affected by the biomass (Whitlock and Millspaugh, 1996). As vegetation and climate change through time, the frequency and intensity of fires also change, thus the relationship among charcoal, fire, vegetation and climate is very complicated. This study focuses on microscopic charcoal (black, opaque, rectangular shaped, smaller than 125 μm) analysis which potentially reflects the regional fire history (MacDonald et al., 1991; Tinner et al., 1998).

### 1.4.5 Marine palynomorphs

Dinoflagellates are single-celled organisms with two distinctive flagella which have a heterotrophic, autotrophic, mixtrophic, symbiotic or parasitic life strategy (Schnepf and Elbrächter, 1992). As part of their life cycle, many dinoflagellate species can produce a non-motile (cyst) stage, whose walls are made of organic, calcareous or siliceous substances (Marret and Zonneveld, 2003). This study focuses on organic-walled dinocysts. Of the 2000 dinoflagellate species ~90% are known to live in the marine environment (e.g. Stover et al., 1996) and only about 20% of these can produce a highly resistant organic-walled cyst during their lifecycle which can be well preserved in the sediment (Head, 1996; Wall et al., 1977). During the last decades, the spatial and seasonal distribution of organic-walled dinocysts found in recent marine sediments around the world can be well related to sea surface conditions such as sea surface temperature, sea surface salinity, nutrients and sea-ice cover (Bouimetarhan et al., 2009b; Dale, 1996; de Vernal et al., 1994, 2005; Holzwarth et al., 2007; Wallet al., 1977; Zonneveld et al., 2001a, 2013). Therefore, it has become evident that organic-walled dinocysts can be a valuable tool for palaeoclimatic and palaeoceanographic reconstructions, especially in coastal high productive environments where the other

calcareous plankton proxies (e.g., calcareous dinoflagellate cysts, planktonic forminifera, diatoms and coccolithophores) are often problematic due to the high degradation of the organic matter (Dale, 1996; Zonneveld et al., 1997).

## 1.5 Thesis Outline

This thesis is presented in three manuscripts of which two are published in international peer-reviewed journals and one is submitted to an international peer-reviewed journal. The three manuscripts correspond to Chapter 2, 3 and 4 of this thesis, respectively.

**Chapter 2- Pollen distribution in the marine surface sediments of the mudbelt along the west coast of South Africa (Published in Quaternary International)**

Xueqin Zhao, Lydie Dupont, Michael E. Meadows and Gerold Wefer.

This study presents the spatial pollen distribution offshore of the west coast of South Africa based on a transect of marine surface sediment samples retrieved from the Namaqualand mudbelt. The results indicate distinctive pollen spectra reflecting vegetation communities on the adjacent continent. This investigation is to aid in the interpretation of marine fossil pollen records of onshore palaeovegetation changes demonstrating that pollen records from marine sediment cores in the Namaqualand mudbelt have the potential to be a tool for palaeovegetation reconstruction of South Africa.

**Chapter 3- Holocene vegetation and climate variability in the winter and summer rainfall zones of South Africa (Published in The Holocene)**

Xueqin Zhao, Lydie Dupont, Enno Schefuß, Michael E. Meadows, Annette Hahn and Gerold Wefer.

This study focuses on Holocene vegetation and hydrological changes in South Africa using pollen and microcharcoal records of two marine sites GeoB8331 and GeoB8323 from the Namaqualand mudbelt offshore of the west coast of South Africa covering the last 9900 and 2200 years, respectively. The results show that climate developments apparently contrast between the summer rainfall zone and winter rainfall zone over the last 9900 years driven by different mechanisms.

**Chapter 4- Palynological evidence for Holocene climatic and oceanographic changes off western South Africa (Published in Quaternary Science Reviews)**

Xueqin Zhao, Lydie Dupont, Enno Schefuß, Ilham Bouimetarhan and Gerold Wefer

To obtain a better knowledge of palaeoceanographic and palaeoenvironmental changes in the southern Benguela upwelling system during the Holocene, this study presents dinocyst

records of 12 marine surface sediment samples and the gravity core GeoB8331-4 from the Namaqualand mudbelt offshore of the west coast of South Africa. The results show three distinct oceanographic conditions during the Holocene associated with climate changes on land.

# Chapter 2 Pollen distribution in the marine surface sediments of the mudbelt along the west coast of South Africa

Xueqin Zhao[1], Lydie Dupont[1], Michael E. Meadows[2], Gerold Wefer[1]

[1] MARUM - Center for Marine Environmental Sciences, University of Bremen, P.O. Box 330 440, D-28334, Bremen, Germany

[2] Department of Environmental and Geographical Science, University of Cape Town, Rondebosch 7701, Cape Town, South Africa

**Published as:** Zhao X., Dupont L., Meadows M.E., Wefer G., 2016. Quaternary International 404, 44-56.

## 2.1 Abstract

The distribution of pollen in marine surface sediments offshore of the west coast of South Africa has been investigated to aid in the interpretation of marine pollen records of onshore vegetation changes. A transect of sediment surface pollen samples retrieved from the Namaqualand mudbelt from just south of the Orange River mouth (29°S) to St Helena Bay (33°S) indicates distinctive pollen spectra reflecting vegetation communities on the adjacent continent. Pollen concentration increases southwards, partly in relation to greater pollen productivity due to higher biomass and density of Fynbos vegetation and of sedimentary processes and low pollen concentrations consequent to dilution with silt and clay from the Orange River. The distribution of specific pollen taxa suggests that the Orange River is a major contributor of pollen to the northern mudbelt declining southwards, while the pollen distribution in the central mudbelt is largely attributable to seasonal inputs of pollen from offshore berg winds and local ephemeral Namaqualand rivers. The typical Fynbos elements dominate in the southern mudbelt indicating a pollen source mainly in the Fynbos vegetation types. These conclusions support a companion analysis of fossil pollen records of two marine sediment cores from the northern and southern mudbelt respectively. This study demonstrates that pollen records from marine sediment cores in the Namaqualand mudbelt have the potential to be a tool to reconstruct palaeovegetation on the adjacent continent. However, to better reconstruct the palaeoclimate of South Africa and fully understand the relations between terrestrial and marine deposits, more marine surface

sediments along the western coast of South Africa as well as more terrestrial surface sediments need to be studied.

## 2.2 Introduction

Palaeoenvironmental evidence based on terrestrial pollen records in a relatively dry region such as southern Africa is often difficult to obtain due to the paucity of lakes or swamps, although the palaeoenvironmental archive of rock hyrax middens is ideally suited to the reconstruction of dryland palaeoenvironments (Chase et al., 2012; Scott and Cooremans, 1992). Still, the terrestrial records are often discontinuous (Neumann et al., 2011), have a low temporal resolution (Meadows et al., 2010), cover short periods (Baxter and Meadows, 1994; Meadows et al., 1996; Stager et al., 2012), or are widely distributed over the continent with distinct local environment or have different proxies which generally lead to contradicted results or make them difficult for comparison even with long continuous records (Baker et al., 2014; Kristen et al., 2007; Meadows and Baxter, 2001; Neumann et al., 2014; Norström et al., 2014). Albeit less detailed, pollen preserved in undisturbed marine sediments has the potential to provide long continuous information integrating a large area of continental vegetation and climate developments (Dupont, 1999). Due to the large scale mixing possibility of pollen from diverse sources (Shi et al., 1998), checking whether or to what degree the sediments were disturbed is essential. The continental shelf off the west coast of southern Africa is a key region for palaeoenvironmental research and the understanding of climate change of southern Africa (Birch, 1977; Herbert and Compton, 2007; Oboh-Ikuenobe and de Villiers, 2003).

For the interpretation of sediment records of the continental shelf, it is crucial to characterize the source of its terrigenous sediments which would have been brought in mainly by the Orange River (Rogers, 1977; Rogers and Bremner, 1991). Much of the terrigenous sediment is redistributed in the high-energy coastal environment. The coarser fraction sand and gravel is transported northward by wave-induced littoral drift, and the finer fraction silt and clay (mud) is transported southward by the poleward countercurrent (Nelson, 1989; Rogers, 1977). The latter forms a Holocene mud deposit referred to as the Namaqualand mudbelt (Birch et al., 1991). However, the study of Mabote et al. (1997) revealed that the Orange River might be only a major source of sediments near the Orange River mouth, while further south along the mudbelt input of terrigenous sediments from both offshore berg winds and local ephemeral Namaqualand rivers becomes increasingly important.

Basically, pollen distribution in sediments is related to environmental and sedimentological factors including the vegetation composition, pollen production,

dispersal, transportation (including fluvial, aeolian and ocean current transport), deposition and preservation. The mechanisms of pollen sedimentation on the Atlantic continental margin should be similar to the sedimentation processes of terrigenous fine particles (Heusser, 1983). This suggests that the marine pollen signal may indicate the source and transportation of fine-grained terrigenous sediments within which pollen is associated.

Rather few marine palynological studies have been conducted on the marine surface sediments of this region (Davey, 1971; Davey and Rogers, 1975; Gray et al., 2000). Preliminary studies (Davey, 1971; Davey and Rogers, 1975) of palynomorphs in a traverse of the Orange River mouth region demonstrate the importance of turbulence of the Orange River in palynomorph deposition. Pollen analysis of two sediment cores from the Namaqualand mudbelt (Gray, 2009) shows distinctive pollen composition, suggesting a major fluvial contribution near the Orange River mouth, while near the Buffels River mouth pollen elements originated mainly from the nearshore vegetation. Unfortunately, the interpretation of the data was hampered by inconsistencies in the chronology (Gray, 2009; Gray et al., 2000; Meadows et al., 1997, 2002). An accurate and detailed interpretation of regional marine pollen records, as well as other proxies, needs better data about the distribution and mechanisms of pollen transport in modern marine sediments of the mudbelt. In addressing this shortcoming, marine surface sediments (sampled by multicorer, which takes multiple cores at every deployment and is hydraulically damped enabling the samples tubes to be lowered gently sampling soft surface sediments with minimum disturbance) were obtained from the Namaqualand mudbelt (Fig. 1a, Table 1). Dating of four multicores in the mudbelt all suggest that the top samples are modern (Leduc et al., 2010; Taylor, 2004).

The primary aim of this study is to describe and explain the modern pollen distribution of the Namaqualand mudbelt, with the following specific objectives: (1) to characterize the pollen concentrations and distribution in the Namaqualand mudbelt surface sediments, (2) to determine the possible sources of mudbelt pollen, and to assess the degree to which the characteristic pollen concentrations and distribution reflect the adjacent continental vegetation, (3) to assess the significance of pollen preserved in mudbelt sediments during the Holocene as proxies of terrestrial palaeovegetation in the region and to assist in the interpretation of fossil pollen records.

## 2.3 Regional setting

The Namaqualand mudbelt (Figure 2.1a) along the western coast of southern Africa extends from 20 km north of the Orange River mouth and 500 km to the south off St Helena Bay (Rogers and Bremner, 1991). This mudbelt is an inner continental shelf

suite of generally fine-grained sediments lying in water depths of 80-140 m. The mudbelt is broadly cohesive, continuous and thicker in the Orange River prodelta area where it is dominated by laminated silt, while it tends to be thinner and consisting of homogeneous mud towards the south (Mabote et al., 1997; Meadows et al., 1997, 2002).

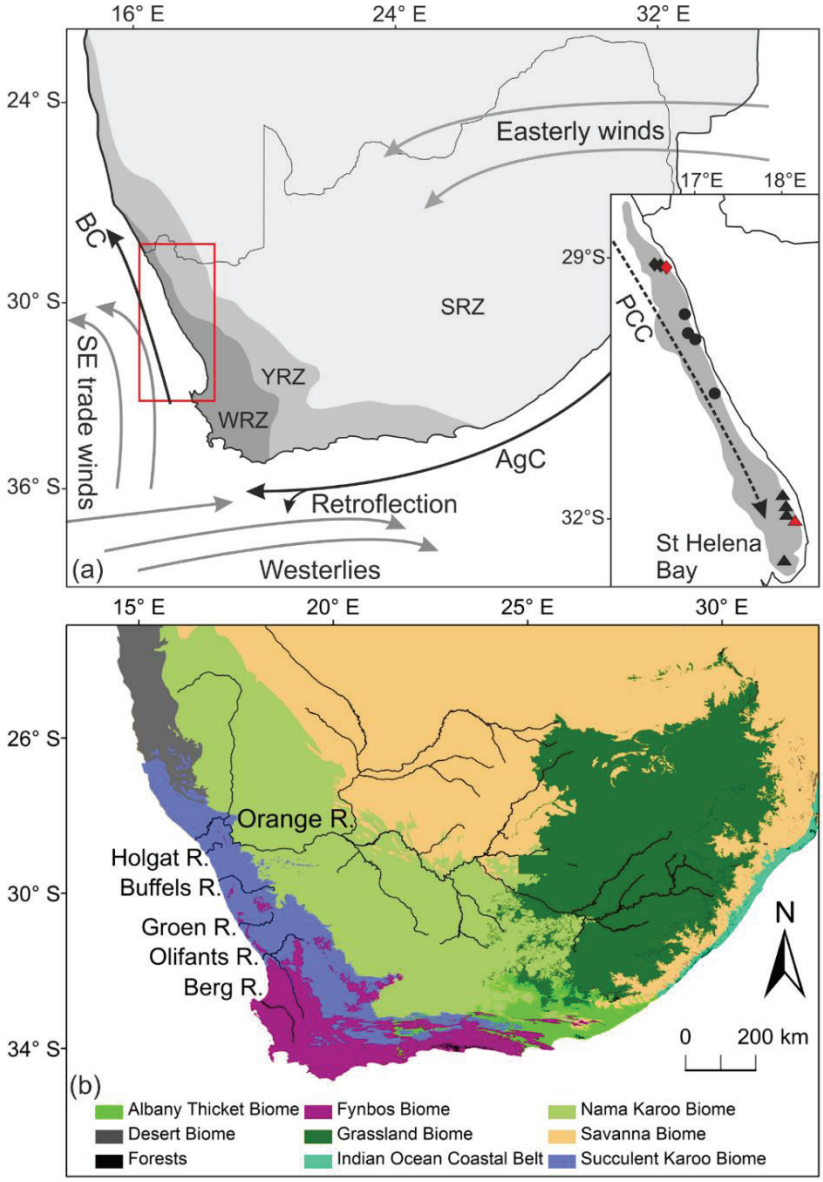


**Figure 2.1** Maps of southern Africa showing: (a) modern austral summer atmospheric (gray arrows) and oceanic (black arrows) circulation systems, three rainfall zones of southern Africa are indicated: summer rainfall zone (SRZ), year-round rainfall zone (YRZ) and winter rainfall zone (WRZ). Major representations of oceanic circulation, Benguela Current (BC), Agulhas Current (AgC) are shown. The inset denotes the Namaqualand mudbelt (shading) after Birch et al. (1991), poleward countercurrent (PCC) and multicore locations (diamonds represent samples from the northern mudbelt, dots represent samples from the central mudbelt and triangles represent samples from the southern mudbelt, two gravity cores GeoB8331-4 and GeoB8323-2 are marked in red). (b) Modern vegetation of southern Africa (after Mucina and Rutherford, 2006; Scott et al., 2012), Orange River catchment and main rivers on the west coast.

### 2.3.1 Oceanic circulation

Oceanographic conditions on the west coast of South Africa have been well described (Nelson, 1989; Nelson and Hutchings, 1983; Shannon and Nelson, 1996), which are dominated by the northward flowing cold Benguela Current (BC) (Figure 2.1a). This current is induced by offshore prevailing southeast trade winds driving a coastal upwelling process especially during the austral spring and summer in the southern Benguela region. Below the BC, a poleward countercurrent (PCC) is positioned permanently south of 33°S while the northward boundary varies seasonally. In the southern boundary of the Benguela system, elements of the warm and saline Agulhas Current (AgC) water from the Indian Ocean are shed into the South Atlantic Ocean and filaments of AgC water enter the BC.

### 2.3.2 Climate and vegetation

In southern Africa, the climate is variable due to the alternating seasonal dominance of atmospheric and oceanic circulation systems across the region resulting in three main rainfall zones (Figure 2.1a): winter rainfall zone (WRZ), year-round rainfall zone (YRZ) and summer rainfall zone (SRZ) (Chase and Meadows, 2007; Tyson and Preston-Whyte, 2000). During the austral summer, the WRZ is controlled by strong southeast trade winds inducing an intensive upwelling zone and low sea surface temperatures along the west coast, which minimizes summer precipitation over the west coast of southern Africa. The rainfall in the SRZ is mainly brought by warm and moist easterly winds associated with the South Indian Anticyclone. During the austral winter, the southern westerlies are situated over the southwestern Cape supplying rainfall to the WRZ, while high pressure dry conditions prevail over the SRZ. Temperature and precipitation are highly variable, with annual values ranging from 11 to 20°C and 25 to 970 mm/yr in the WRZ, and 7 to 24°C and 10 to 1380 mm/yr in the SRZ (Hijmans et al., 2005). Along the west coastal area, more than 65% of the precipitation falls in austral winter and varies between 50 and 400 mm/yr (Cowling et al., 1999b).

The vegetation of southern Africa is spatially diverse, but very strongly related to the rainfall amount and seasonal distribution as well as the influence of the altitude and temperature over the continent (Figure 2.1b). Seven major biomes in southern Africa have been described by White (1983), Bredenkamp et al.(1996), Cowling et al. (1997) and Mucina and Rutherford (2006). The Fynbos Biome, in the southwest Cape, is an evergreen shrubland typified by the presence of restios (Restionaceae), a high cover of ericoid shrubs (Ericaceae, Asteraceae and Thymelaeaceae) and the common occurrence of proteoid shrubs (Proteaceae). Another vegetation type is Renosterveld,

which is dominated by Asteraceae, specifically *Elytropappus rhinocerotis* (renosterbos). Other important shrub families represented in renosterveld include Rubiaceae (*Anthospermum*), Rosaceae (*Cliffortia*), Fabaceae, Boraginaceae and Malvaceae (Goldblatt and Manning, 2002). The Succulent Karoo Biome, located in a narrow strip inland of the west coast, is characterized by dwarf leaf-succulents of which Aizoaceae (including Mesembryanthemaceae) and Crassulaceae are particularly prominent; many other families are also common including Asteraceae, Amaranthaceae, Euphorbiaceae (*Euphorbia*) and Zygophyllaceae (*Zygophyllum*) (Wheeler, 2010) but grass cover is low. The Nama Karoo Biome, which is semi-desert dwarf and grassy shrubland found on the central plateau, is dominated by Asteraceae, Poaceae, Aizoaceae, Liliaceae and Scrophulariaceae. The Desert Biome, found under very harsh environmental conditions, is characterized by dominance of annual plants (often annual grasses like *Stipagrostis sabulicola*). The Grassland Biome, situated on the cooler and elevated interior plateau, is dominated by grasses, geophytes and herbaceous plants, since trees are largely absent. Savanna, which is the largest biome in southern Africa, is characterized by woody elements forming the upper layer and a grassy-rich ground layer. The catchment of the Orange River is dominated spatially by grassland, mostly of the C4 type. There are also local riparian wetlands along the Orange River, dominated by sedges and aquatics, primarily Cyperaceae, *Phragmites, Typha* and *Gunnera*.

## 2.4 Materials and methods

The samples used in this study (Figure 2.1a, Table 2.1) are from multicores and gravity cores which were obtained in January-February of 2003 during the M57/1 *Meteor* cruise (Schneider et al., 2003) along a north-south transect of the Namaqualand mudbelt, as well as the dated multicore samples mentioned in the introduction which were also obtained on the same cruise. Three of these samples from GeoB8331-2, GeoB8332-3 and GeoB8333-1, all situated very close to each other near the Orange River and Holgat River mouth, form a short offshore traverse. The distance to the shore of these three samples are 11 km for GeoB8331-2, 16 km for GeoB8332-3 and 20 km for GeoB8333-1. The upper 3 cm of twelve multicores were assessed for their pollen composition. 31 samples from gravity core GeoB8331-4 (accompanied by multicore GeoB8331-2) and 22 samples from gravity core GeoB8323-2 (accompanied by multicore GeoB8323-1) were processed for pollen analysis of late Holocene sediments.

The samples were decalcified with diluted HCl (~12%). Two *Lycopodium* spore tablets (each containing 18584±372 markers) were added during the decalcification step. After washing, the samples were treated with HF (~40%). The samples were shaken for 2 hours, and then kept standing for two days to remove silicates. Samples were sieved

ultrasonically to remove particles smaller than 10-15 µm. Samples were stored in water, mounted in glycerol and identified under a light microscope (magnification 400 and 1000×) for pollen, spores and marine palynomorphs (organic-walled dinoflagellate cysts). At least 300 pollen grains were counted per sample except for three marine surface samples, and the total pollen count is shown in Table 1. Percentages are based on a terrestrial pollen sum (excluding aquatic taxa, sedges and spores, Table 2.1). Sample volumes were measured using water displacement, so that concentration values can be calculated. The 95% confidence intervals of percentage and concentration were determined following Maher (1972, 1981). Pollen grains were identified using the African pollen reference collection of the Department of Palynology and Climate Dynamics of the University of Göttingen, and after Scott (1982) and Bonnefille and Riollet (1980). Counts are stored in Pangaea, available from www.pangaea.de.

**Table 2.1** Core sites, water depths, pollen sums and pollen concentrations of multicore top samples. (Core locations are shown in Figure 2.1a)

| Core name | Longitude (°E) | Latitude (°S) | Water depth (m) | Pollen sum | Terrestrial pollen sum | Pollen concentration (grains/cm$^3$) |
|---|---|---|---|---|---|---|
| GeoB8333-1 | 16.61 | 29.12 | 20 | 307 | 260 | 3962 |
| GeoB8332-3 | 16.66 | 29.13 | 116 | 305 | 243 | 2314 |
| GeoB8331-2 | 16.71 | 29.14 | 88 | 313 | 231 | 2011 |
| GeoB8327-1 | 17.01 | 29.70 | 88 | 205 | 182 | 2762 |
| GeoB8329-1 | 17.03 | 29.93 | 111 | 323 | 284 | 2792 |
| GeoB8328-1 | 17.06 | 29.94 | 112 | 305 | 272 | 2710 |
| GeoB8325-1 | 17.28 | 30.60 | 39 | 305 | 274 | 4310 |
| GeoB8324-1 | 18.09 | 31.75 | 100 | 317 | 286 | 8816 |
| GeoB8321-1 | 18.12 | 31.86 | 104 | 220 | 200 | 7571 |
| GeoB8322-1 | 18.12 | 31.95 | 105 | 302 | 266 | 9594 |
| GeoB8323-1 | 18.22 | 32.03 | 90 | 305 | 273 | 7686 |
| GeoB8319-1 | 18.08 | 32.50 | 69 | 267 | 241 | 6760 |

## 2.5 Results

### 2.5.1 Results of marine surface sediments

Twelve marine surface sediments were processed for this study. All samples were used to establish pollen concentration. In total, 64 pollen and spore taxa were identified in the sediments, and the 16 most common taxa were selected to represent the pollen

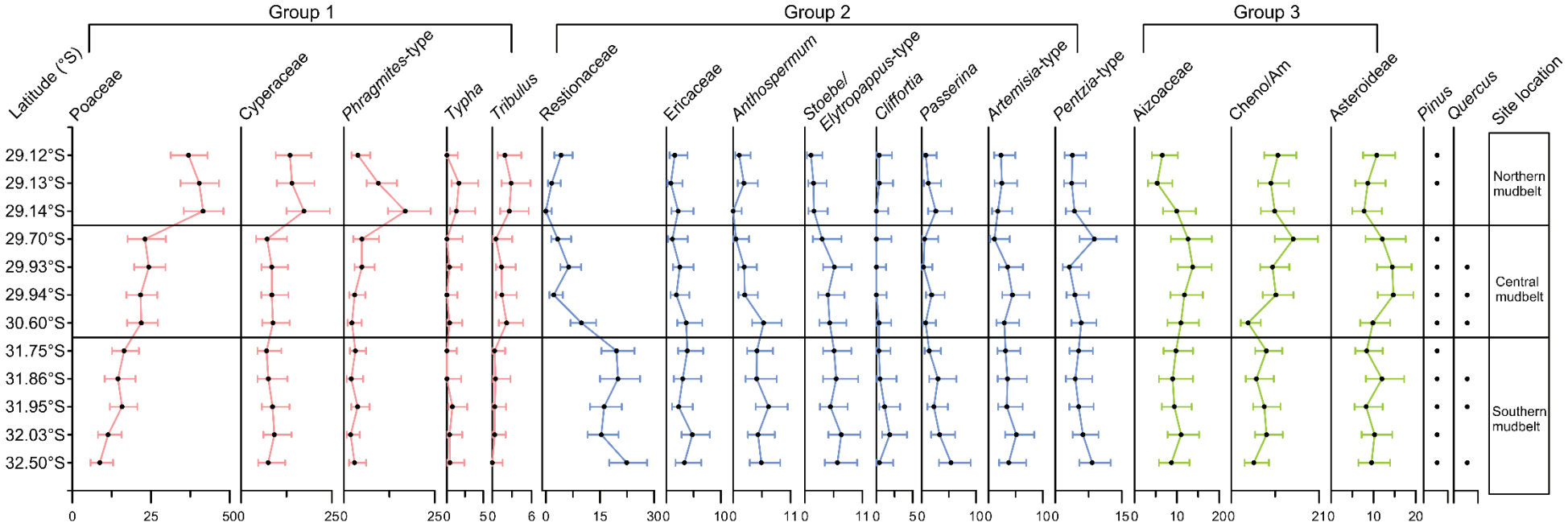


**Figure 2.2** Relative abundance of selected pollen taxa in marine surface sediments (multicores) from the Namaqualand mudbelt, plotted against latitude. The error bars denote 95% confidence intervals of pollen percentages.

distribution patterns in the mudbelt since the other pollen types are represented in low abundances.

Two of the multicores (GeoB8331-2 and GeoB8332-3) from the northern mudbelt have been dated based on $^{210}Pb_{ex}$ measurements (Leduc et al., 2010) and the upper 3 cm of core material turn out to be probably no older than 10 years. Dating of another two multicores (GeoB8322-1 and GeoB8319-1) in the southern mudbelt were based on radiocarbon ages (Taylor, 2004). The $^{14}C$ age of GeoB8322-1 is 1260 ± 35 years at 43 cm (630-670 cal. yr BP) and the $^{14}C$ age of GeoB8319-1 is 685 ± 35 years at 11-14 cm (110-240 cal. yr BP). Although the chronology is only available for four multicores, the marine surface sediments can be identified as modern or recent according to the presence of neophytes (e.g., *Pinus*, *Quercus*, Figure 2.2) derived from trees which were introduced into South Africa by the end of 17th century (Campbell and Moll, 1977; Richardson, 2000). Additionally, no reworked pollen or dinoflagellate cysts have been found in any of our samples.

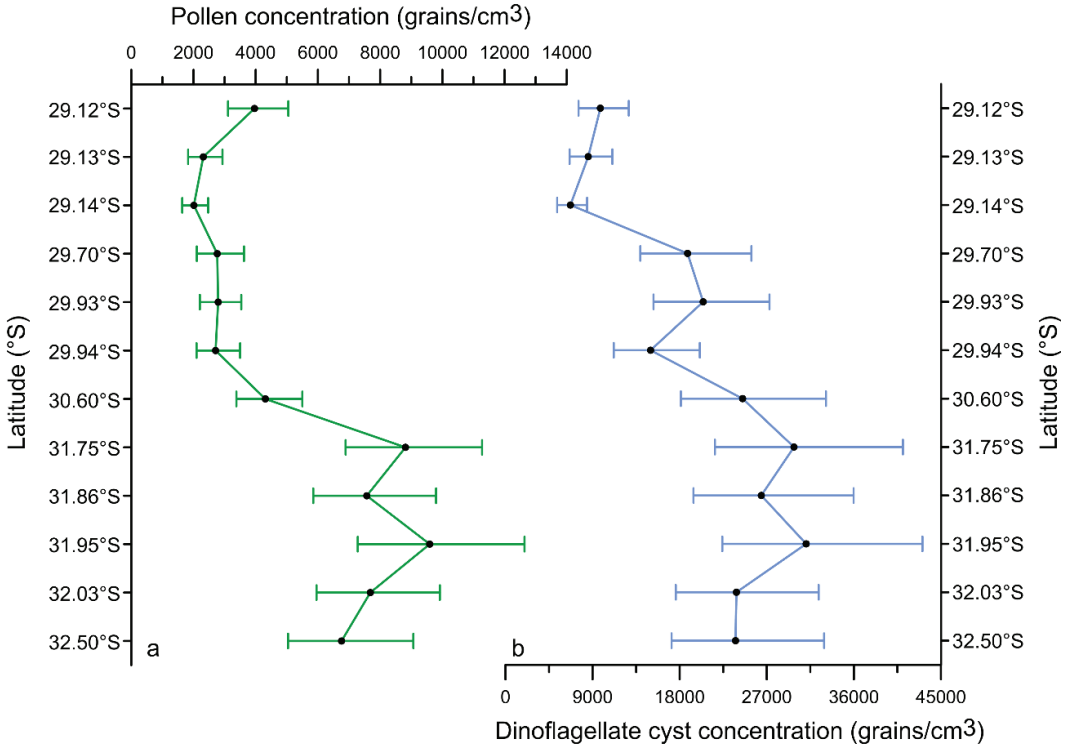


**Figure 2.3** Pollen and organic-walled dinoflagellate cyst concentrations (grains/cm$^3$) in the marine surface sediments from the Namaqualand mudbelt, plotted against latitude. The error bars denote 95% confidence intervals of pollen and organic-walled dinoflagellate cyst concentration.

#### *2.5.1.1 Pollen concentration*

The pollen concentrations in marine surface sediments show a clear pattern, indicating an increase from north to south (Figure 2.3a). In the northern and central mudbelt (29-31°S), the pollen concentrations remain below 4300 grains/cm$^3$ (with an average of 3000 grains/cm$^3$) with a slight increase for the offshore traverse of northernmost three samples from 2000 to 4000 grains/cm$^3$. In the southern mudbelt (31-33°S), the pollen concentrations are never lower than 6700 grains/cm$^3$ (with an average of 8100 grains/cm$^3$). The organic-walled dinoflagellate cyst (that is cysts mainly from marine dinoflagellates) concentrations show also high values in the southern mudbelt and decline gradually northwards, although absolute values are much higher (Figure 2.3b).

#### *2.5.1.2 Pollen distribution*

Figure 2.2 shows the distribution in relative abundance of 16 selected pollen taxa (For more detailed relative abundance of pollen taxa, please see the Supplementary Figure 2.1). The multicore locations are depicted in north-south direction according to their latitudes.

Poaceae pollen, which is ubiquitous in all the marine surface sediments, has percentage values between 9-42%. Maximum percentage values (37-42%) of Poaceae pollen are found in the northern mudbelt with a steep decrease southwards to minimum percentage values of 9-16% in the southern mudbelt. Cyperaceae pollen, which is from sedges being abundant in local riparian wetland vegetation, has percentage values between 7-17%. Percentage values of this pollen type are higher in the northern mudbelt and decrease southwards similar to the pattern in Poaceae pollen. Small Poaceae pollen grains (<25 µm), possibly originating from *Phragmites* (reed) (Bonnefille and Riollet, 1980) which is an important constituent of local riparian vegetation, are concentrated in the northern mudbelt with maximum percentage values of 10-17%, decreasing sharply southwards to much lower percentage values of 2-4%. *Typha* pollen, mostly likely also sourced from local riparian wetland vegetation (along with Cyperaceae and *Phragmites*-type), has maximum percentage values (1-2%) in the northern mudbelt, except for one sample where it is absent. *Typha* pollen is rare in the central and southern mudbelt except for one sample with a percentage value of almost 1%. *Tribulus* pollen is likely attributable to pioneer vegetation of disturbed places along the Orange River and essentially restricted to the sediments in the northern and central mudbelt with maximum percentage values of 2-3%. *Tribulus* pollen is almost absent in the southern mudbelt with percentage values of less than 0.5%.

Pollen of Aizoaceae, Cheno/Am (Chenopodiaceae and Amaranthaceae) and Asteroideae (undifferentiated Asteraceae) is more evenly distributed in the mudbelt. However, these groups are better represented in the central mudbelt with maximum percentage values of 11-14%, 10-15% and 10-15%, respectively (Figure 2.2).

Highest percentage values (15-22%) of Restionaceae pollen which is the most common pollen type among Fynbos elements are recorded in the southern mudbelt and decrease sharply to the north (0-4%). This pollen taxon shows a clear contrasting distribution pattern to that exhibited by Poaceae, Cyperaceae, *Phragmites*-type, *Typha* and *Tribulus*. Ericaceae pollen, which has a very similar pattern to that of Restionaceae, is concentrated in the southern mudbelt with maximum percentage values of 2-5% decreasing northwards to 1-2% in the northern mudbelt. *Anthospermum* and *Stoebe/Elytropappus*-type pollen are also characteristic of the southern mudbelt, both with maximum percentage values of 5-7%. *Cliffortia* and *Passerina* pollen, both of which have low percentage values in the marine surface sediments, are mostly restricted to the southern mudbelt with maximum values of 2% and 5%, respectively. *Artemisia*-type and *Pentzia*-type pollen display a distinctive pattern in which there are higher percentage values in both the central and southern mudbelt (Figure 2.2).

#### *2.5.1.3 Statistical analysis*

To simplify variable taxonomic data, Principal Component Analysis (PCA) was used to allocate characteristic groups of co-varying pollen taxa into coherent assemblages. Percentage data of all the pollen and spore taxa from all the marine surface sediments were analyzed using the module of “factor analysis” in SPSS version 16.0 (SPSS, Inc., Chicago IL).

Figure 2.4a indicates that the samples can be separated into three clusters, *viz.* northern, central and southern mudbelt with two major components (PC) accounting for 89.0% of the total variance. Figure 2.4b represents the principal component loadings for the 16 selected pollen taxa which can be classified into three groups, with two majorcomponents accounting for 91.8% of the total variance in the sample dataset. The first component (PC1, axis1) accounts for 57.8% of the total variance with maximum loading values in the southern mudbelt. Poaceae, which is well associated with Cyperaceae, Phragmites-type, Typha and Tribulus pollen, dominates the negative side of this component. These five taxa are grouped together as “Group 1” (Figure 2.4b), all concentrated in the northern mudbelt. Restionaceae pollen is highly positively weighted on PC1 along with the Ericaceae, Anthospermum, Stoebe/Elytropappus-type, Passerina, Cliffortia, Artemisia-type and Pentzia-type pollen. These eight taxa are grouped together as “Group 2” (Figure 2.4b), all concentrated in the southern mudbelt.

The second component (PC2, axis2), which accounts for 34.0% of the total variance, has highest positive loading values for samples in the central mudbelt and decreases both southwards and northwards. This component is dominated by Aizoaceae, Cheno/Am and Asteroideae which are grouped together as “Group 3” (Figure 2.4b), whose maximum percentage values are found in the central mudbelt.

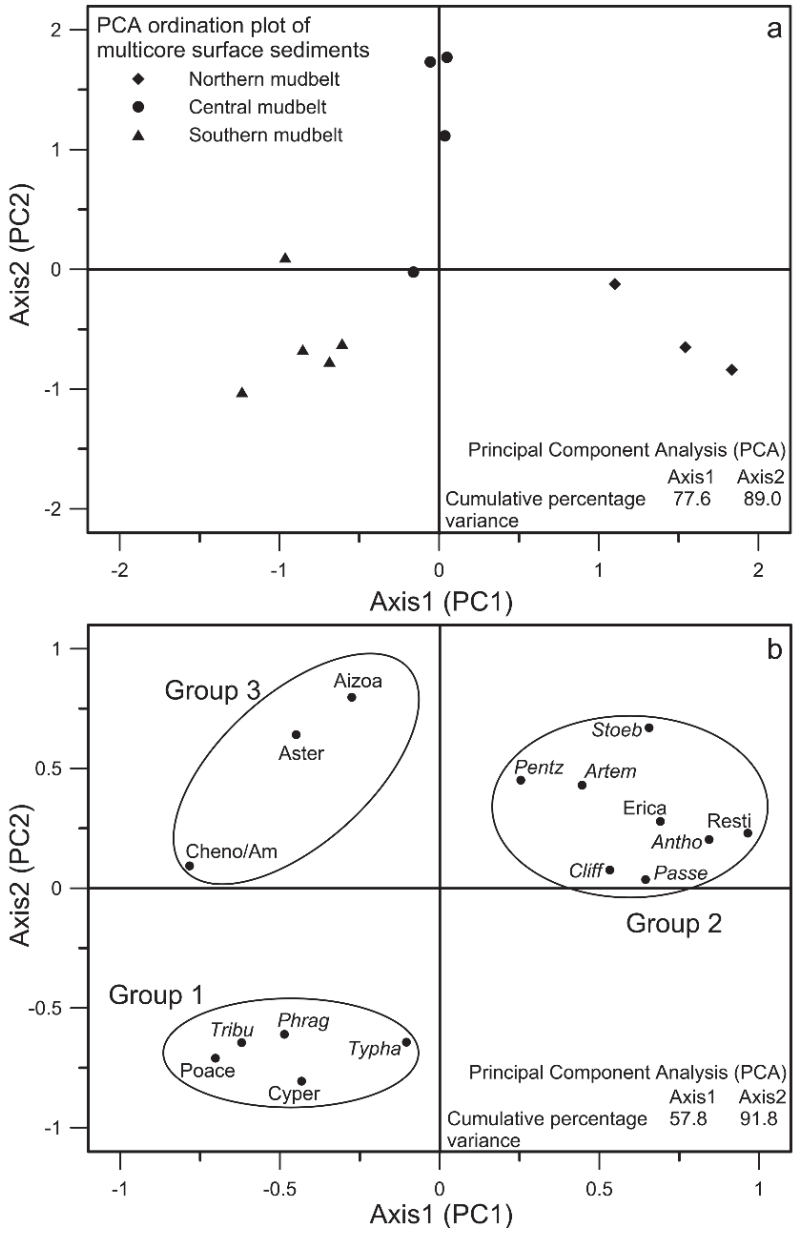


**Figure 2.4** (a) PCA ordination plot of the 12 marine surface sediment samples from the Namaqualand mudbelt using all pollen and spore taxa. Diamonds represent samples from the northern mudbelt, dots represent samples from the central mudbelt and triangles represent samples from the southern mudbelt. (b) PCA ordination plot of 16 selected pollen taxa from marine surface sediments from the Namaqualand mudbelt. Group 1: Poace (Poaceae), Cyper (Cyperaceae), *Phrag* (*Phragmites*-type), *Typha* and *Tribu* (*Tribulus*). Group 2: Resti (Restionaceae), Erica (Ericaceae), *Antho* (*Anthospermum*), *Stoeb* (*Stoebe/Elytropappus*-type),

*Cliff* (*Cliffortia*), *Passe* (*Passerina*), *Artem* (*Artemisia*-type) and *Pentz* (*Pentzia*-type). Group 3: Aizoa (Aizoaceae, incl. Mesembryanthemaceae), Cheno/Am (Chenopodiaceae, Amaranthaceae) and Aster (Asteroideae).

### 2.5.2 Pollen records of Holocene sequences

Considering the north-south gradient of modern pollen concentrations from marine surface sediments in the mudbelt, the pollen assemblages of the two sediment cores display marked consistency. The pollen concentrations of GeoB8331-4 range from 1400-11000 grains/cm$^3$ with an average of 5900 grains/cm$^3$, while the pollen concentrations of GeoB8323-2 are much higher, ranging from 7500 to 13000 grains/cm$^3$ with an average of 10000 grains/cm$^3$ (Zhao et al., 2016b).

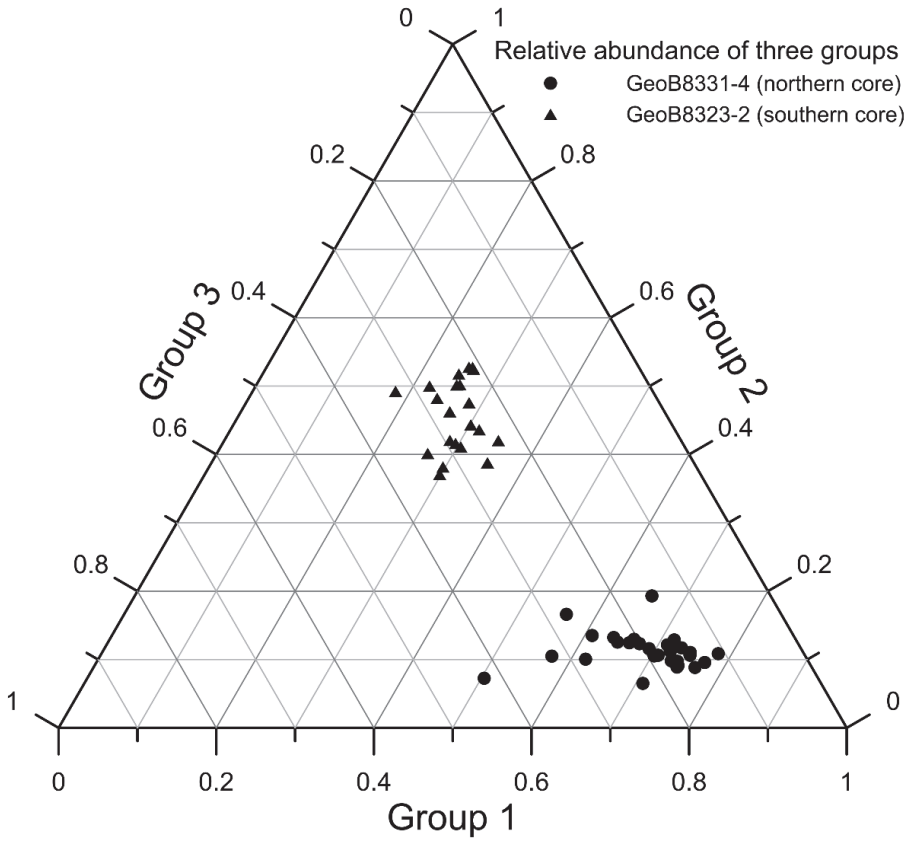


**Figure 2.5** The relative abundance of Groups 1, 2 and 3 in the gravity cores GeoB8331-4 and GeoB8323-2, percentages are based on all pollen and spore taxa. Dots represent samples from core GeoB8331-4 and triangles represent samples from core GeoB8323-2.

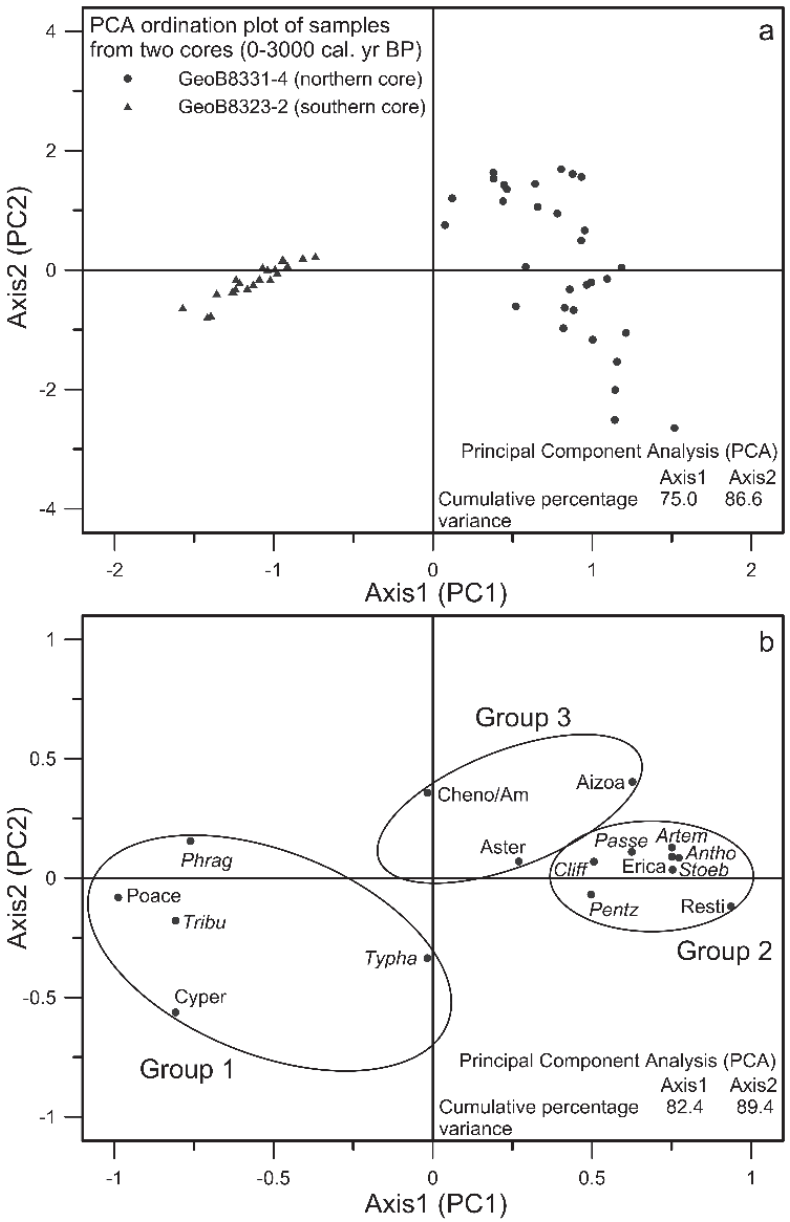


**Figure 2.6** (a) PCA ordination plot of the 31 samples from gravity core GeoB8331-4 and 22 samples from gravity core GeoB8323-2 using all pollen and spore taxa. Dots represent samples from core GeoB8331-4 and triangles represent samples from core GeoB8323-2. (b) PCA ordination plot of 16 selected pollen taxa from cores GeoB8331-4 and GeoB8323-2. Group 1: Poace (Poaceae), Cyper (Cyperaceae), *Phrag* (*Phragmites*-type), *Typha* and *Tribu* (*Tribulus*). Group 2: Resti (Restionaceae), Erica (Ericaceae), *Antho* (*Anthospermum*), *Stoeb* (*Stoebe/Elytropappus*-type), *Cliff* (*Cliffortia*), *Passe* (*Passerina*), *Artem* (*Artemisia*-type) and *Pentz* (*Pentzia*-type). Group 3: Aizoa (Aizoaceae, incl. Mesembryanthemaceae), Cheno/Am (Chenopodiaceae, Amaranthaceae) and Aster (Asteroideae).

The pollen composition (Figure 2.5) in GeoB8331-4 is dominated by Poaceae, Cyperaceae and *Phragmites*-type (i.e. Group 1) contributing 41-68% of the total. This is followed by the pollen taxa of Group 3 (Aizoaceae, Cheno/Am and Asteroideae)

contributing 9-35%, while the pollen taxa of Group 2 (Restionaceae, Ericaceae, *Anthospermum*, *Stoebe/Elytropappus*-type, *Cliffortia*, *Passerina*, *Artemisia*-type and *Pentzia*-type) are poorly represented in this core and contribute only 5-16%. In contrast, the pollen taxa of Group 2 (31-46%) dominate in GeoB8323-2 and there is a much lower representation of Group 1 (15-31%) compared to GeoB8331-4.

The analytical results using all the pollen and spore taxa indicate a strong degree of congruency with the pollen distribution pattern in marine surface sediments, since the samples from the two sediment cores can apparently be separated without any overlap (Figure 2.6a). The 16 selected pollen taxa can also be grouped into three assemblages as with the marine surface sediments (Figure 2.6b). The pollen taxa (including Poaceae, Cyperaceae, *Phragmites*-type and *Tribulus*) in Group 1 dominate the negative first component (PC1, axis1). *Typha* pollen appears to be marginal to Group 1, a result that is perhaps attributable to its low abundance in both cores. The pollen taxa classified into Group 2 are the same as those found in the marine surface sediments with positive values for PC1, but are more tightly clustered than in the marine surface sediments. The pollen taxa in Group 3 of the sediment cores score more positive on the PC1 compared to the marine surface sediments.

## 2.6 Discussion

### 2.6.1 Pollen assemblages in marine surface sediments

The distribution of specific pollen taxa in marine surface sediments reveals marked differences across the mudbelt transect from north to south. The patterns of pollen distribution in the offshore marine surface sediments and onshore vegetation exhibit strong correlations despite the limited numbers of available samples. In addition, to better determine the possible sources of mudbelt pollen and to assess the degree to which the characteristic pollen distribution reflect the adjacent continental vegetation, we also make a comparison with the terrestrial modern pollen distribution in southern Africa (Urrego et al., 2015). The terrestrial modern pollen distribution was addressed with 31 surface samples along a transect from Cape Town (South Africa) to Lüderitz (Namibia) covering the four major biomes (Fynbos, Succulent Karoo, Nama Karoo and Desert) of southwestern Africa combined with previously published pollen spectra from 150 additional surface samples collected between 22 °S and 35 °S (Gajewski et al., 2002).

The high frequencies of Poaceae pollen in the northern mudbelt sediments is most likely due to transport by the Orange River from the Nama Karoo, grassland and savanna vegetation in the catchment. The ratios of major and trace elements of the

suspended sediment load in the upper Orange River indicate a primary source derived from Karoo sediment in that area (Compton and Maake, 2007). Compton et al. (2010) also concluded that much of the fine sediment in the mudbelt was sourced from erosion of mudstones from the Elliot Formation at the base of the western Drakensberg escarpment during the Holocene. Rogers (1977) found that recent terrigenous sediments in the mudbelt are derived by erosion of poorly consolidated Karoo sediment in the upper catchment of the Orange River. However, it is not clear that, the mudbelt pollen would be transported from such a distant source, exclusively. On the other hand, it is feasible that some of the pollen may originate from the karroid vegetation in the middle Orange River catchment where the grasses (Poaceae) are also abundant. Both the field observations and the surface samples in the Nama Karoo and Savanna support the view that grasses are dominated in the Savanna as well as Nama Karoo, where Poaceae pollen is as high as 70% in terrestrial surface samples (Urrego et al., 2015). The very clear trends in the distribution of Poaceae, Cyperaceae, *Phragmites*-type and *Typha* (Group 1) pollen along the mudbelt can best be explained as being a consequence of fluvial transport from the Orange River. The fact that *Tribulus* pollen is restricted to the northern mudbelt suggests that it comes from disturbance areas in sandy soils along the Orange River. On a transect of terrestrial samples, *Tribulus* pollen was also only found in the Nama Karoo surface samples (Urrego et al., 2015). Furthermore, as suggested by Mabote et al. (1997), the weak poleward countercurrent lacks the capacity to transport medium to fine silt as far south as the Buffels River mouth (29.70°S). The results suggest that transport of pollen from the Orange River mouth decreases rapidly southwards and the river is indeed the major source of pollen in sediments near the Orange River mouth in the northern mudbelt. The slight decreasing representation of Group 1 in the northernmost three samples, in particular *Phragmites*-type, also suggests an offshore decreasing pollen contribution by the Orange River. The low pollen percentage values of Poaceae and Cyperaceae in the southern part of the mudbelt suggest a relative small fluvial influence in this area in combination with limited long-distance aeolian transport from the grassland and savanna vegetation of the continental interior.

The pollen composition in the central mudbelt differs from that of the northern and southern mudbelt. Species of the Aizoaceae family are particularly prominent in the Succulent Karoo. Although vegetation represented by the Cheno/Am pollen type is more widely distributed, it is also abundant in the Succulent Karoo. Asteroideae pollen is representative of vegetation types that are widely distributed, for example, both the Nama Karoo and savanna are rich in Asteraceae. The terrestrial pollen distribution of Cheno/Am and Asteroideae indicates that high pollen percentages of them can be characteristic of the Succulent Karoo and Nama Karoo (Urrego et al., 2015). Thus, the

distribution patterns of these three pollen taxa (summed into Group 3) reflect the adjacent continental vegetation (Succulent Karoo, Nama Karoo), suggesting decreasing contributions from the Orange River and the possible increased importance of berg winds and local ephemeral Namaqualand rivers (e.g., Buffels River) (Mabote et al., 1997) as pollen sources. Gray (2009) also found distinctly different pollen compositions between different mudbelt sediment cores. Nama Karoo (Asteraceae) and Succulent Karoo (Aizoaceae) elements are more dominant in the sediment core off the Buffels River mouth, while the sediment core off the Orange River mouth is characterized by significant levels of grassland and savanna elements such as Poaceae (Gray, 2009). Coetzee (1976) also found that the pollen assemblages from the sediments of the different river mouths along the west coast of southern Africa reflected the regional vegetation type through which the rivers pass. Furthermore, the pollen assemblages in modern sediments of the lower Orange River are very similar to those in a sediment core off the Buffels River mouth, suggesting a primary pollen contribution from the Succulent Karoo and Nama Karoo vegetation (Gray, 2009).

The high values of Restionaceae pollen in the southern mudbelt surface samples fit nicely the distribution of Restionaceae in the Fynbos biome. Maximum Restionaceae pollen percentages in the southern mudbelt sharply decrease northwards with increasing distance from the Fynbos vegetation. Gray (2009) concluded that, since Restionaceae are wind-pollinated, its pollen is probably transported by the prevailing southeast trade winds and then be deposited as the ocean current dispersal of pollen is limited due to the relatively high sinking velocity of pollen in water (Fischer and Wefer, 1996). However, based on the results of the surface sediments only, it is difficult to differentiate between aeolian and fluvial sources of pollen in the southern mudbelt. Apart from the prevailing southeast trade winds, the Olifants and Berg Rivers (Fig. 1b) which are perennial rivers flowing into the Atlantic Ocean through Fynbos vegetation, probably are other non-negligible carriers of pollen to the surface sediments in the southern mudbelt. Besides Restionaceae, pollen types of Group 2 include Ericaceae, *Anthospermum*, *Stoebe/Elytropappus*-type, *Passerina* and *Cliffortia*, which are represented in low percentage values in the marine surface sediments. They exhibit similar trends to that of Restionaceae in having higher pollen percentage values in the southern mudbelt and therefore reflecting the common occurrence of these species in the Fynbos vegetation. According to the terrestrial pollen distribution within the Fynbos vegetation, pollen taxa of Ericaceae, *Anthospermum*, *Stoebe*-type and *Passerina* all reach maximum percentages, which correspond very well with our marine pollen distribution in the southern mudbelt. However, the terrestrial distribution of Restionaceae pollen was only found less than 5% in the surface samples derived from the Fynbos vegetation, while up to 5% of Restionaceae pollen was found in surface

samples from the Nama Karoo, Succulent Karoo and the Desert (Urrego et al., 2015). This is odd because Restionaceae plants are mostly found in the Fynbos vegetation and not in the Nama Karoo, Succulent Karoo or Desert (Cowling et al., 1997). However, greater taxonomic diversity can be found in the different types of terrestrial surface samples. Previous studies in the Fynbos vegetation show that Restionaceae pollen accounts for more than 25% in modern hyrax pellets, while it is much less prominent (no more than 10%) in the surface soil sediments (Scott and Woodborne, 2007a; Meadows et al., 2010). The study of more surface samples would be helpful to correct for possible biases that may be present at the individual sample level (Quick et al., 2011).

Also the pollen concentrations reveal a marked gradient from north to south, fluctuations in the concentration of the 16 selected pollen taxa are consistent with the pollen distribution patterns based on the relative percentage values (Figures 2.2 and 2.7). The concentrations of Group 2 are all much higher in the southern mudbelt, while the concentrations of Group1 show no such north-south gradient and instead dominate the pollen spectra of the northern mudbelt.

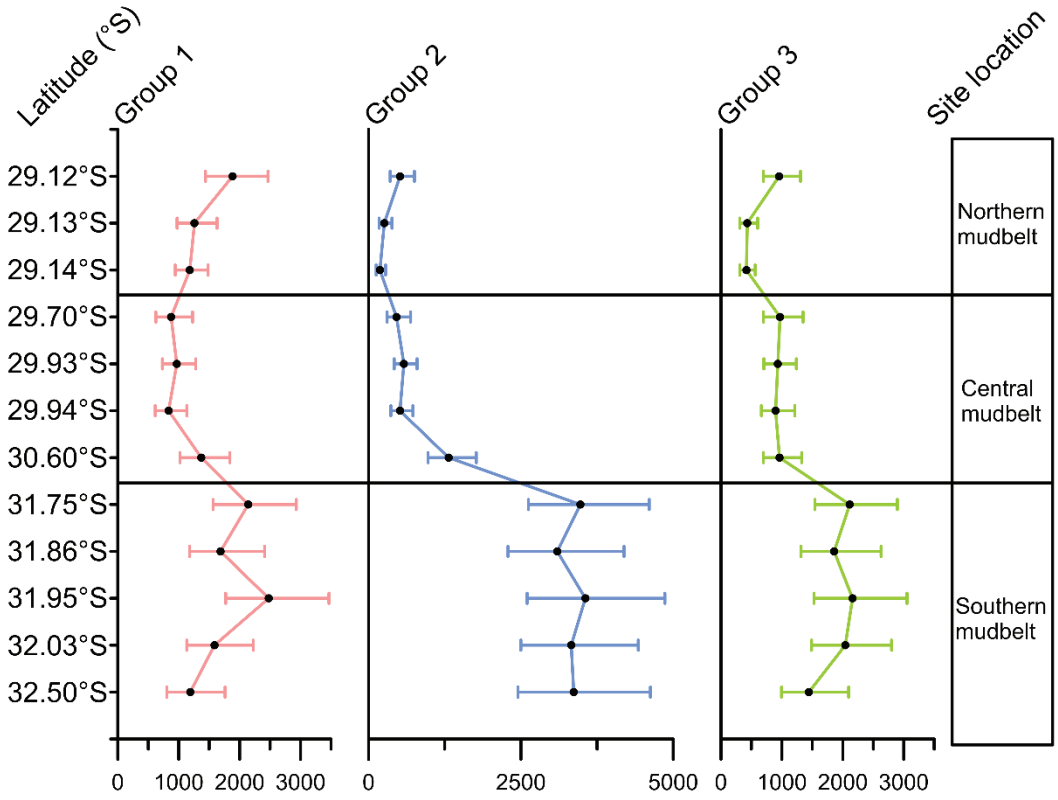


**Figure 2.7** Pollen concentration (grain/cm$^3$) diagram of Groups 1, 2 and 3 in marine surface sediments from the Namaqualand mudbelt, plotted against latitude. The error bars denote 95% confidence intervals of pollen concentration.

### 2.6.2 Dispersal of pollen over the mudbelt

In an attempt to describe the trend in pollen distribution patterns of the Namaqualand mudbelt in a more quantitative way, we first correlated the pollen of Group 3 and dinoflagellate cysts concentration with the distance to the Orange River mouth (Table 2.2). The rationale is that the source areas of marine dinoflagellate cysts and that of unspecific terrestrial Group 3 pollen are situated neither north nor south. Despite the difference between marine and terrestrial origins both records show the same linear trend declining towards the Orange River mouth (Figure 2.8). The parsimonious explanation of these similar trends is the dilution of pollen or cysts input by mud from the mudbelt being most abundant near the Orange River mouth and declining southwards. This does not imply that all mud of the mudbelt must originate from the Orange River, but only that the amount of terrestrial mud declines southwards. The southernmost multicore sample (GeoB8319-1) comes from the southern edge of the mudbelt and contains sandy mud. We, therefore, excluded this sample from the regression (Table 2.2, Figure 2.8). Organic carbon is known to be positively correlated with the abundance of fine-grained sediments because its larger surface area is conducive to the adsorption of organic carbon (Keil et al., 1994; Mayer, 1994). Weight percentages of total organic carbon (TOC) measured by Inthorn et al. (2006) on the same multicores (except GeoB8324-1) show a similar linear trend as Group 3 and dinoflagellate cysts (Figure 2.8). The decline of Group 3 pollen is about 5 grains/cm$^3$ for each km. The same rate of decline is also found for pollen concentrations of Group 1 barring the northernmost three samples in the vicinity of the Orange River (Figure 2.8). The high pollen concentration of Group 1 near the mouth of the Orange River is readily explained by fluvial input. On the other hand, the decline in pollen concentration of Group 2 is exponential instead of linear (Figure 2.8). This indicates that there is an extra decline in pollen concentration northwards explained by the increasing distance from its source.

**Table 2.2** Regression equations for pollen concentrations of Groups 2 and 3, dinoflagellate cysts concentration, total organic carbon (TOC) (Inthorn et al., 2006) and accumulation rates of Group 2 against distance to the Orange River.

| Y | X | Y = aX+b | $R^2$ | Sample Nr. | fit |
|---|---|---|---|---|---|
| Group3 (grains/cm$^3$) | distance | 4.4X + 294 | 0.93 | 13 | linear |
| Dino-cysts (grains/cm$^3$) | from the | 63.1X + 6389 | 0.80 | 13 | linear |
| TOC (wt.%) | Orange River | 0.009X + 2 | 0.74 | 10 | linear |
| Group 2 (grains/cm$^3$) | (km) | $185e^{0.007X}$ | 0.96 | 13 | exponential |
| Group 2 (grains/cm$^2$/yr) | | 0.95X + 397 | 0.93 | 13 | linear |

The simplest way to account for the dilution effect is to estimate the sedimentation rates and calculate pollen accumulation (or influx) rates. The sedimentation rates can be determined reasonably accurate for the gravity cores (age models are available; Herbert and Compton, 2007), but is more difficult for the multicore samples. We, therefore, interpolated the sedimentation rates between the values of 2.47 mm/yr (last 300 years) just south of the Orange River mouth and 1.04 mm/yr (last 250 years) at the southern end of the mudbelt in the vicinity of the Olifants River. (We think interpolation is allowed because of the linearity of the dilution effect discussed above). In Figure 2.9 pollen accumulation rates using interpolated sedimentation rates are plotted against the arbitrary distance from the southernmost core. With exception of the northernmost three samples the pollen accumulation rates of Group 1 are roughly constant varying between 165 and 270 grains/cm$^2$/yr. The accumulation rates in the vicinity of the Orange River are almost twice as high varying between 290 and 470 grains/cm$^2$/yr, suggesting that roughly half of the pollen of Group 1 is fluvial and transported by the Orange River. Dinoflagellate cyst accumulation rates are also more or less constant but for the northern samples, which have much lower rates. Here, probably the fresh water discharge of the Orange River may create unfavorable conditions for dinoflagellates (Davey and Rogers, 1975). Accumulation rates of Group 3 very slightly (not significant) decrease over the whole transect. However, accumulation rates of Group 2 exhibit a linear trend with a decline of about one grain/cm$^2$/yr for each km (Table 2.2, Figure 2.9). The linear decline of the Group 2 accumulation rates is remarkable, and indicates a wide southern source area as dispersal from a point source or from a line of point sources would result in an exponential decline.

Over all, the distinctive pollen composition in the mudbelt surface sediments suggests that the Orange River most of which lying in the SRZ is a major contributor of pollen to the northern mudbelt, while to the south pollen is probably transported by both winds and rivers from the WRZ.

Concerning differential preservation, very little is known about specific African pollen types. Hints about the little corrosiveness of the sediments can be deduced from the dinoflagellate cyst composition which is dominated by the sensitive (heterotrophic) cysts suggesting that the cyst associations have not been significantly altered by degradation processes (Zonneveld et al., 2007, 2008). Since pollen concentrations clearly increase southwards, it is necessary to consider the factors that may be involved to cause this. One possible explanation is that this is a function of greater pollen production due to higher vegetation biomass and density in Fynbos vegetation in response to winter rainfall, as has been suggested by Montade et al. (2011) working on marine surface sediments from Chilean Patagonia. However, the similar trend in

dinoflagellate cyst concentrations suggests that the vegetation density may only partly explain the pattern. An additional explanation may lie in decreasing dilution by terrigenous material with increasing distance from the Orange River, as suggested by the poleward increase of fine-silt and organic matter south of the Orange River mouth (Rau, 2002; Rogers and Bremner, 1991). This is supported by Davey and Rogers' (1975) study of palynomorphs in a traverse of the Orange River mouth region which showed that organic matter and dinoflagellate cyst concentrations were much lower in samples nearest the coast due to turbulence which is also shown in the traverse of northernmost three samples with an offshore increasing concentration. This process was also suggested by Traverse and Ginsburg (1966, 1967) in their analysis of marine surface sediments on the Great Bahama Bank where lower pollen concentrations were recorded in sandy sediments associated with relatively turbulent water. Moss et al. (2005) found higher pollen concentrations in silt-sized sediments compared to coarser grained samples in northeastern Australia and Heusser (1983) came to similar conclusions with respect to sediments of the western north Atlantic Ocean. Therefore, compared to the factor of vegetation density change, the dilution effect of the Orange River seems to be more reasonable and explainable.

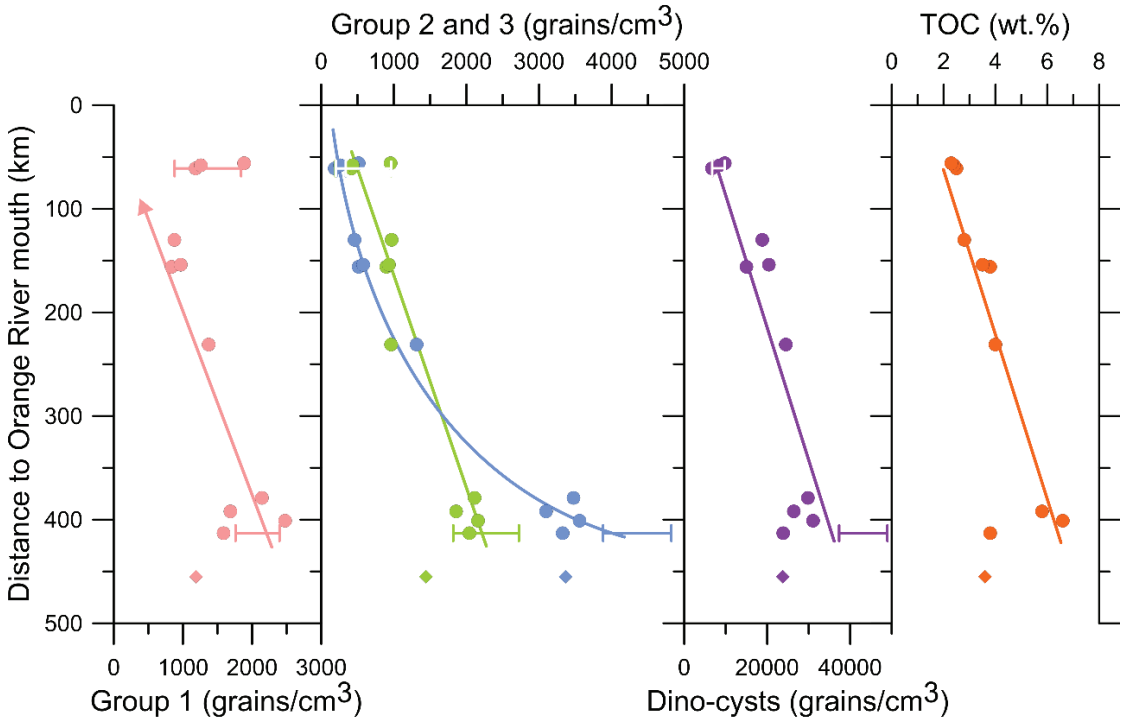


**Figure 2.8** Pollen concentration (X-axes) against distance from the Orange River mouth (Y-axis) for three pollen groups (first panel Group 1 in pink; second panel Groups 2 and 3 in blue and green, respectively), organic-walled dinoflagellate cysts (third panel in purple) and total organic carbon (TOC, fourth panel in orange) after Inthorn et al. (2006). Error bars denote 2 s ranges (mean ± 1 s) of the five uppermost samples from the gravity cores GeoB8331-4 (near Orange

River) and GeoB8323-2 (near Olifants River). Pollen concentration of Group 3 (green, second panel) and cyst concentration (third panel) are positively linearly correlated with distance from the Orange River. With exception of the northernmost samples near the Orange River, pollen concentration of Group 1 (first panel) shows the same trend (arrow). Pollen concentration of Group 2 (blue, second panel) exhibits an exponential correlation with distance. Data of the regression analysis are given in Table 2.2. The southernmost sample (diamonds) is excluded from the regression analysis because of its location on the very edge of the mudbelt.

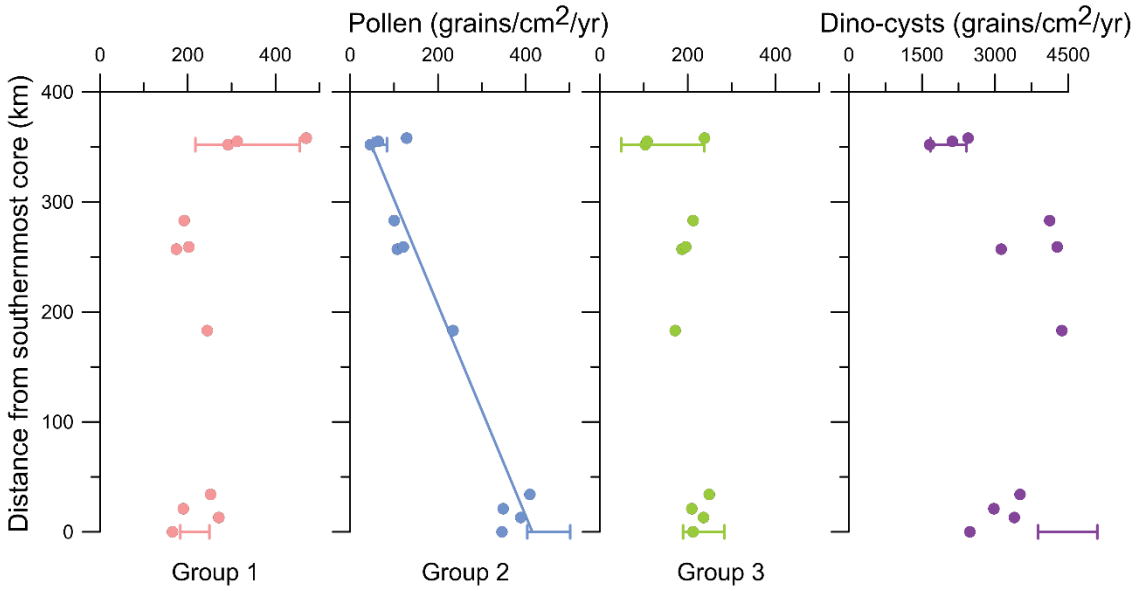


**Figure 2.9** Pollen accumulation rates (calculated with interpolated sedimentation rates) against distance from southernmost core GeoB8323-2 (symbols and colors as in Figure 2.8). Only those of Group 2 decline with increasing distance showing a linear correlation (Table 2.2). Group 1 consists of pollen from Poaceae, Cyperaceae, *Phragmites*-type, *Typha*, *Tribulus*; Group 2 consists of pollen from Restionaceae, Ericaceae, *Anthospermum*, *Stoebe/Elytropappus*-type, *Passerina*, *Cliffortia*, *Artemisia*-type, *Pentzia*-type; Group 3 consists of pollen from Aizoaceae (incl. Mesembryanthemaceae), Cheno/Am (Chenopodiaceae, Amaranthaceae), Asteroideae.

### 2.6.3 Pollen representation in late Holocene marine sediments

The pollen records from GeoB8331-4 and GeoB8323-2 (this study) indicate that the mechanisms of pollen distribution and transportation have not altered substantially during the last 3000 years suggesting that they may be utilized as indicators of the dynamics of adjacent continental vegetation (Figures 2.5 and 2.6, the detailed pollen analysis of both cores see Zhao et al., 2016b). The marked differences in pollen representation between the two cores match the pattern of pollen observed in the

marine surface sediments from the mudbelt. Although it has been proposed that contrasting climate might develop in the SRZ and WRZ during the Holocene, little reliable evidence exists since most of the studies have different sites or proxies which generally lead to contradicted results or make them difficult for comparison (Kristen et al., 2007, 2010; Scott and Woodborne, 2007a, b; Metwally et al., 2014). However, the different sources of pollen in the marine surface sediments provide a mean to interpret the vegetation and climate change of both the SRZ and WRZ in southern Africa using different pollen groups from one marine sediment core in the mudbelt.

The much lower pollen concentrations in GeoB8331-4 during the last 3000 years reflect the consistently higher sediment accumulation rates (average of 1.9 mm/yr) compared to GeoB8323-2 (average of 0.9 mm/yr) (Herbert and Compton, 2007) and results from the high-energy depositional environment which is not conducive to the pollen deposition. Meadows et al. (1997) also found sediment accumulation rates being twice as high (3.7 mm/yr) with laminations in the core off the Orange River mouth compared to the core off the Buffels River mouth (1.8mm/yr) with no laminations. The laminated muds in the core off the Orange River mouth are probably protected from bioturbation due to high sediment accumulation rates (Mabote et al., 1997). This supports our inference that the high-energy depositional environment caused by the dilution effect of the Orange River is the best explanation for the low pollen concentration in the northern mudbelt.

## 2.7 Conclusions

The pollen distribution in marine surface sediments in the mudbelt along the west coast of South Africa has been studied and reflects a good correlation with the extend of the terrestrial biomes.

(1) Pollen concentrations in marine surface sediments show a marked north-south gradient correlated with the latitudinal vegetation biomass changes, but probably more related to the dilution effect of increasing sedimentation by the Orange River.

(2) Pollen distribution in marine surface sediments has the potential to indicate the distribution of the vegetation on the adjacent continent if the effects of relevant pollen transport are taken into account.

(3) Pollen representation patterns of two Holocene marine sediment cores can indicate the dynamics of the vegetation in western South Africa.

In summary, this study of marine surface sediments in the Namaqualand mudbelt offshore of the west coast of South Africa demonstrates conclusively that pollen

records from marine sediment cores in the mudbelt can be utilized as reliable tools to reconstruct palaeovegetation in this region critical for the understanding of late Quaternary climate change.

## 2.8 Acknowledgements

This study was funded by the German Federal Ministry of Education and Research (BMBF). The investigations were conducted within the collaborative project “Regional Archives for Intergrated Investigations” (RAiN) (03G0840A), which is embedded in the international research program SPACES (*Science Partnership for the Assessment of Complex Earth System Processes*). Thanks to the captain, the crew and scientists of the *Meteor* M57-1 cruise for recovering the studied material. We would like to thank Frank H. Neumann and an anonymous reviewer for their useful comments that have helped to improve the manuscript. We also thank Enno Schefuß for critical discussions and valuable suggestions.

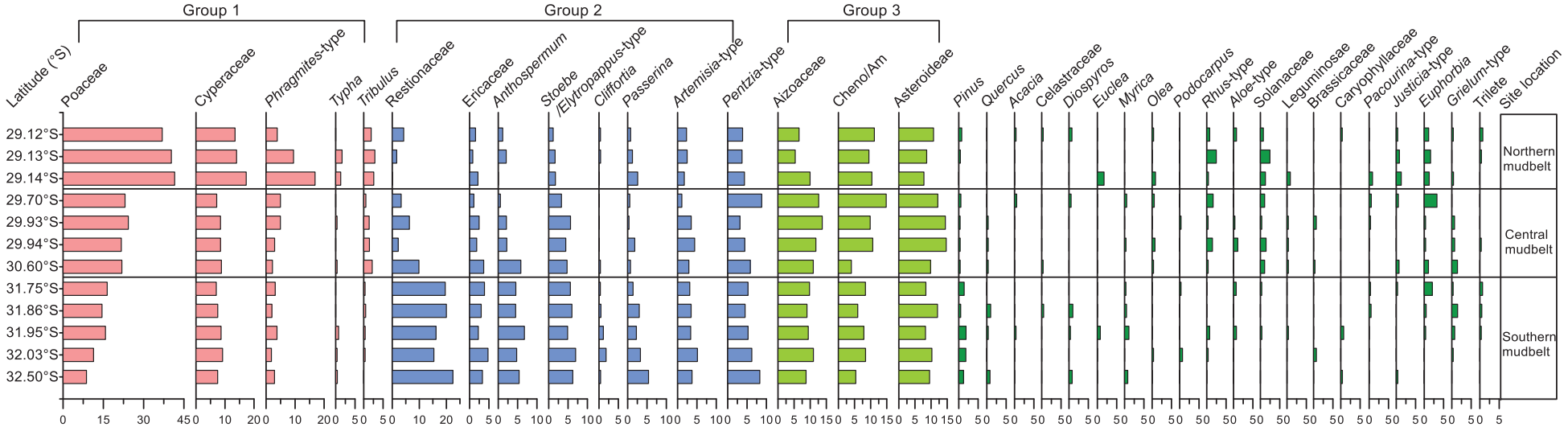


**Supplementary Figure 2.1** Relative abundance of selected pollen taxa in marine surface sediments (multicores) from the Namaqualand mudbelt, plotted against latitude.

# Chapter 3 Holocene vegetation and climate variability in the winter and summer rainfall zones of South Africa

Xueqin Zhao[1], Lydie Dupont[1], Enno Schefuß[1], Michael E. Meadows[2], Annette Hahn[1], Gerold Wefer[1]

[1] MARUM - Center for Marine Environmental Sciences, University of Bremen, P.O. Box 330 440, D-28334, Bremen, Germany

[2] Department of Environmental and Geographical Science, University of Cape Town, Rondebosch 7701, Cape Town, South Africa

**Published as:** Zhao X., Dupont L., Meadows M.E., Hahn A., Wefer G., 2016. The Holocene 26, 843-857.

## 3.1 Abstract

To better understand Holocene vegetation and hydrological changes in South Africa, we analyzed pollen and microcharcoal records of two marine sites GeoB8331 and GeoB8323 from the Namaqualand mudbelt offshore the west coast of South Africa covering the last 9900 and 2200 years, respectively. Our data corroborate findings from literature that climate developments apparently contrast between the summer rainfall zone (SRZ) and winter rainfall zone (WRZ) over the last 9900 years, especially during the early and middle Holocene. During the early Holocene (9900-7800 cal. yr BP), a minimum of grass pollen suggests low summer rainfall in the SRZ, and the initial presence of Renosterveld vegetation indicates relatively wet conditions in the WRZ. Towards the middle Holocene (7800-2400 cal. yr BP), a rather moist savanna/grassland rich in grasses suggests higher summer rainfall in the SRZ resulting from increased austral summer insolation and a decline of Fynbos vegetation accompanied by an increasing Succulent Karoo vegetation in the WRZ possibly suggests a southward shift of the Southern Hemisphere westerlies. During the last 2200 years, a trend towards higher aridity was observed for the SRZ, while the climate in the WRZ remained relatively stable. The Little Ice Age (ca. 700-200 cal. yr BP) was rather cool in both rainfall zones and drier in the SRZ while wetter in the WRZ.

## 3.2 Introduction

South Africa, located at the interface between subtropical and warm-temperate climate zones and between the Indian and Atlantic oceans, is a critical region for Quaternary environmental research and understanding of Holocene climatic history in the Southern Hemisphere (Chase and Meadows, 2007; Scott et al., 2012). The specific atmospheric and oceanic circulation systems across the region (Shannon and Nelson, 1996; Tyson and Preston-Whyte, 2000) shape the precipitation patterns of southern Africa where three rainfall zones are identified (Figure 3.1): a summer rainfall zone (SRZ) in the north and east of southern Africa, a winter rainfall zone (WRZ) at the south-western tip of the continent extending northward from the Cape Peninsula along the west coast to about 28°S and a transitional year-round rainfall zone (YRZ) between these two regions (Chase and Meadows, 2007; Tyson and Preston-Whyte, 2000). The change in vegetation from the northeastern SRZ to southwestern WRZ along the gradient of rainfall seasonality is expected to be very sensitive to climate change.

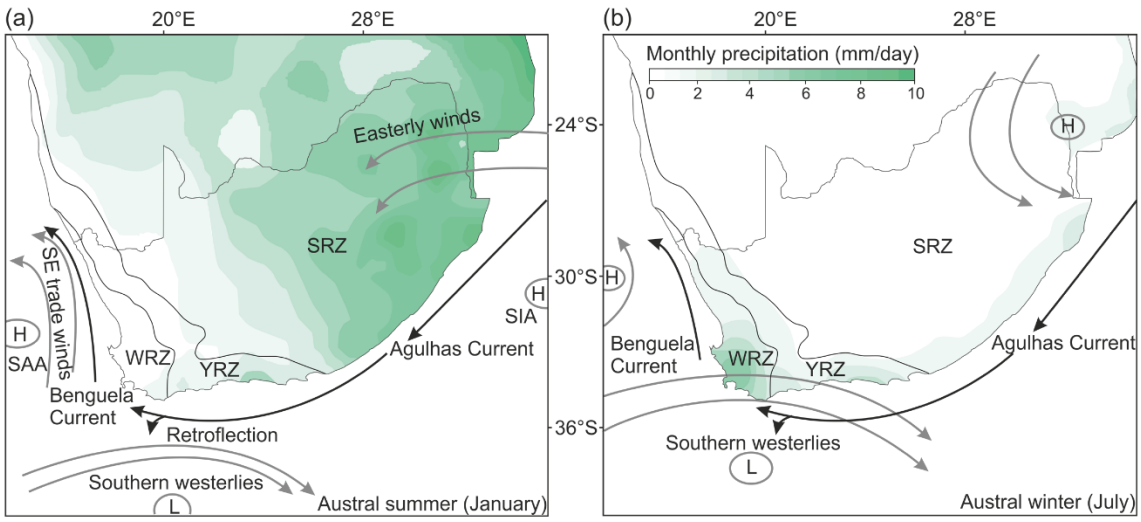


**Figure 3.1** Modern atmospheric and oceanic circulation systems, monthly precipitation for the period 1981–2010 (http://www.esrl.noaa.gov/psd/data/gridded/tables/precipitation.html) over southern Africa during austral (a) summer and (b) winter. Major representations of atmospheric and oceanic circulation, South Atlantic Anticyclone (SAA), South Indian Anticyclone (SIA), Benguela Current (BC), and Agulhas Current (AgC) are shown (Tyson and Preston-Whyte, 2000). Three rainfall zones of southern Africa are indicated: summer rainfall zone (SRZ), year-round rainfall zone (YRZ), and winter rainfall zone (WRZ).

Although South Africa is known to have experienced phases of significant climate change during the Quaternary, palaeoenvironmental evidence based on terrestrial records is often difficult to obtain due to the paucity of lake or swamp archives in which sedimentation is often discontinuous (Neumann et al., 2008, 2011), having weak age models and/or poor temporal resolution (Meadows et al., 2010) or only covering short time periods (Ekblom et al., 2012; Meadows et al., 1996). Longer, more continuous records (Figures 3.2 and 3.3) are widely spaced over South Africa and have been recovered from distinct local environments, which sometimes leads to contradictory results whereby the use of different proxies impede comparison between them (Baker et al., 2014; Kristen et al., 2007; Norström et al., 2014). Nevertheless, a compilation of results from literature clearly indicates different developments in different regions during the Holocene.

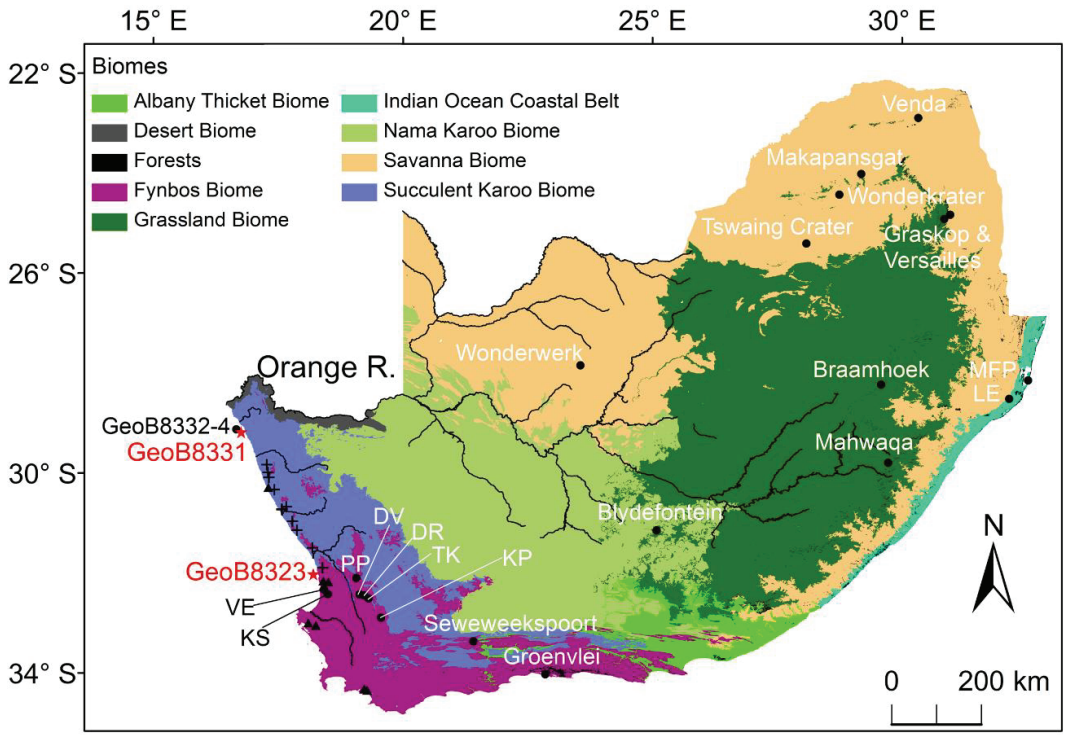


**Figure 3.2** Map of southern Africa showing the location of study sites GeoB8331 (gravity core GeoB8331-4 and multicore GeoB8331-2) and GeoB8323 (gravity core GeoB8323-2 and multicore GeoB8323-1) (red stars), as well as gravity core GeoB8332-4 (dot) (Weldeab et al., 2013). Other terrestrial records mentioned in the text (crosses, triangles, and dots) are shown. The crosses denote the sites from Chase and Thomas (2006), the triangles denote the sites from Klein (1991), and the dots denote the sites from a wider area over South Africa (MFP = Mfabeni peatland, LE = Lake Eteza, VE = Verlorenvlei, KS = Klaarfontein Springs, PP = Pakhuis Pass, DV = Driehoek Vlei, DR = De Rif, TK = Truitjes Kraal, KP = Katbakkies Pass). The major biomes of South Africa (Mucina and Rutherford, 2006) are shown.

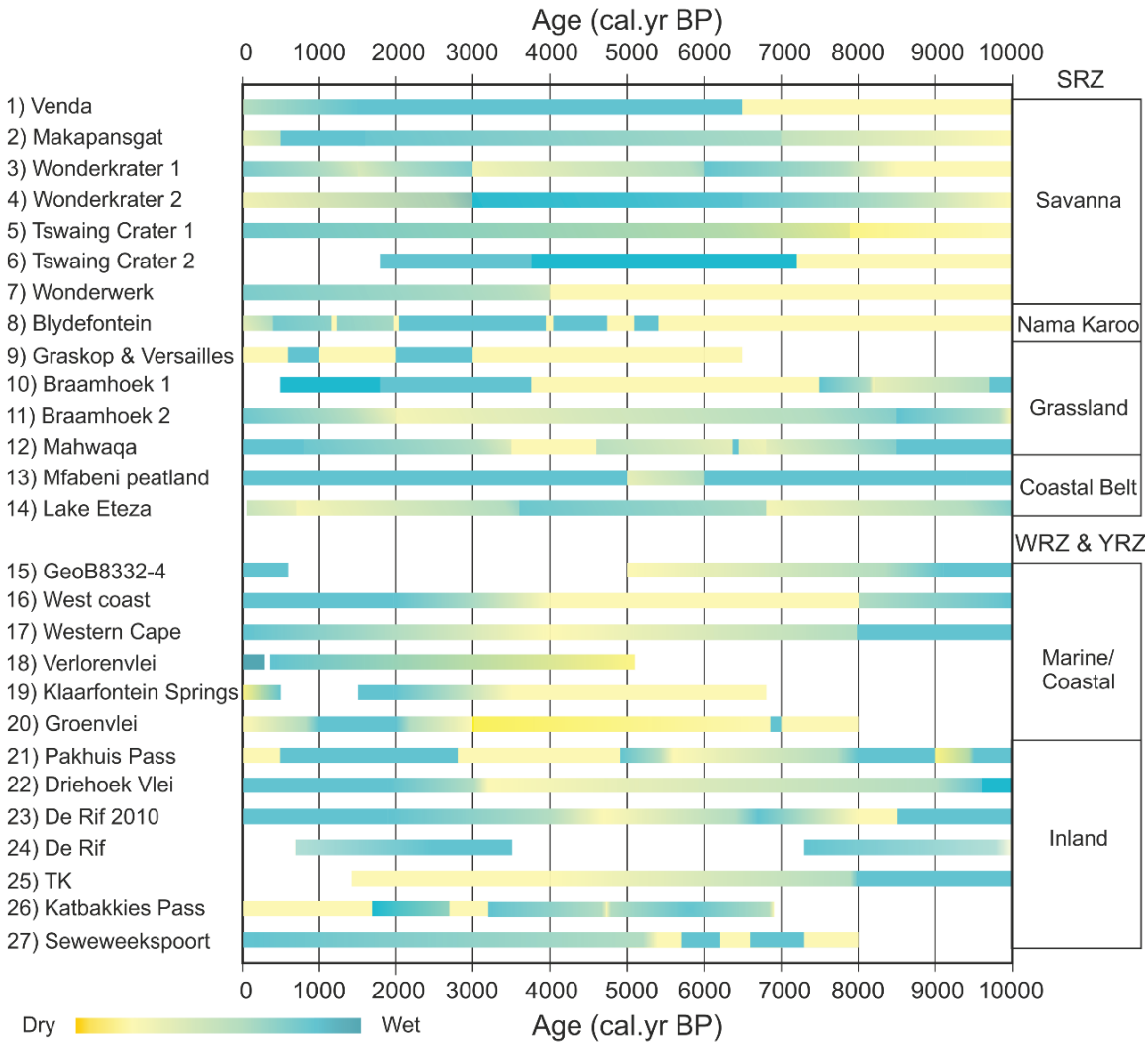


**Figure 3.3** Holocene hydrological records from South Africa discussed in the text. This is not an exhaustive data set but includes records covering the whole or at least most period of Holocene. SRZ: (1) Venda (Scott, 1987); (2) Makapansgat (Holmgren et al., 2003); (3) Wonderkrater 1 (Scott et al., 2012); (4) Wonderkrater 2 (Truc et al., 2013); (5) Tswaing Crater 1 (Kristen et al., 2007); (6) Tswaing Crater 2 (Metwally et al., 2014); (7) Wonderwerk (Brook et al., 2010); (8) Blydefontein (Scott et al., 2005); (9) Graskop & Versailles (Breman et al., 2012); (10) Braamhoek 1 (Norström et al., 2009); (11) Braamhoek 2 (Norström et al., 2014); (12) Mahwaqa (Neumann et al., 2014); (13) Mfabeni peatland (Baker et al., 2014); (14) Lake Eteza (Neumann et al., 2010). WRZ: (15) GeoB 8332-4 (Weldeab et al., 2013); (16) West coast (Chase and Thomas, 2006); (17) Western Cape (Klein, 1991); (18) Verlorenvlei (Meadows et al., 1994, 1996); (19) Klaarfontein Springs (Meadows and Baxter, 2001); (21) Pakhuis Pass (Scott and Woodborne, 2007b); (22) Driehoek Vlei (Meadows and Sugden, 1991); (23) De Rif 2010 (Valsecchi et al., 2013); (24) De Rif (Quick et al., 2011); (25) TK (Truitjes Kraal) (Meadows et al., 2010); (26) Katbakkies Pass (Chase et al., 2015). YRZ: (20) Groenvlei (Martin, 1968); (27) Seweweekspoort (Chase et al., 2013).

Within the WRZ, the palaeoenvironmental records are relatively consistent (Figure 3.3). Climate of the WRZ is characterized by moist conditions during the early Holocene (ca. 10,000-8000 cal. yr BP) (Chase and Thomas, 2006; Klein, 1991; Meadows and Sugden, 1991; Meadows et al., 2010; Quick et al., 2011; Weldeab et al., 2013), except for an arid period between 10,000-9000 cal. yr BP recorded at Pakhuis Pass turning to moist conditions after 9000 cal. yr BP and a brief dry period between 8500-8000 cal. yr BP recorded at De Rif 2010 (Valsecchi et al., 2013). Most studies found conditions gradually becoming drier during the middle Holocene (ca. 8000-3000 cal. yr BP) (Chase and Thomas, 2006; Martin, 1968; Meadows and Sugden, 1991; Meadows and Baxter, 2001; Meadows et al., 2010; Scott and Woodborne, 2007a, 2007b; Weldeab et al., 2013), while generally moist conditions were recorded in Seweweekspoort and Katbakkies Pass between 8000-1700 cal. yr BP interrupted by drier periods (8000-7300, 6600-6200 cal. yr BP, 5700-5200 cal. yr BP and 3200-2700 cal. yr BP). Valsecchi et al. (2013) also found a brief moist period at De Rif 2010 between 7100-6700 cal. yr BP. During the late Holocene (3000 cal. yr BP - present), variable conditions were recorded: increasing humidity such as at Driehoek Vlei, Klaarfontein Spring, De Rif, Pakhuis Pass and Seweweekspoort (Chase et al., 2013; Chase and Thomas, 2006; Klein, 1991; Meadows and Sugden, 1991; Meadows and Baxter, 2001; Scott and Woodborne, 2007b; Valsecchi et al., 2013) but aridity at Katbakkies Pass (Chase et al., 2015).

In the SRZ (Figure 3.3), two different palaeoenvironments developed from northeast to southeast of South Africa especially during the early Holocene (10,000-8000 cal. yr BP). Generally dry conditions characterized the northeast (savanna) region as recorded at Venda, Wonderkrater, Makapansgat and Tswaing Crater (Holmgren et al., 2003; Kristen et al., 2007; Metwally et al., 2014; Scott, 1987; Scott et al., 2012; Truc et al., 2013). To the south, in central South Africa, studies from Wonderwerk and Blydefontein also indicate aridity (Brook et al., 2010; Scott et al., 2005), while at Braamhoek the early Holocene started relatively moist turning more arid later (ca. after 9000 cal. yr BP) (Norström et al., 2009, 2014) compared to northeast South Africa. Along the east coast moist conditions were recorded at Lake Eteza, Mahwaqa and Mfabeni peatland between 10,000-8000 cal. yr BP (Baker et al., 2014; Neumann et al., 2010, 2014). During the middle Holocene climate became variable in particular along the east coast and records of the same region such as Wonderkrater (Scott et al., 2012; Truc et al., 2013) and Tswaing Crater (Kristen et al., 2007; Metwally et al., 2014) show inconsistent results. However, generally an increase in humidity after 8000 cal. yr BP is indicated for the northeast region, whereas to the central South Africa, dry conditions persisted until ca. 4000 cal. yr BP. The different climate conditions in the two regions

were also observed by Chevalier and Chase (2015), which was interpreted to be attributable to different modes of variability with the SRZ. The climate was variable and relatively moist during the late Holocene in both northeastern and southeastern South Africa except at Wonderkrater (Truc et al., 2013), Lake Eteza (Neumann et al., 2010), and Graskop and Versailles (Breman et al., 2012), where gradually drier conditions were recorded.

Comparing the Holocene terrestrial records, it becomes clear that the climate developed differently in the SRZ and WRZ. Hahn et al. (2016) found anti-phased climate variations during the last ca. 3000 years between the SRZ and WRZ which were already proposed by Tyson (1986) and Cockcroft et al. (1987) based on contemporary climatic patterns. To better understand millennial to centennial mechanisms of regional vegetation and climate change in South Africa, more continuous and high-resolution environmental records are required. Here, marine sediments can offer continuous and well-dated archives. Sediment cores from the continental shelf with terrigenous material mainly from the adjacent continent areas have the potential of providing high-resolution Holocene records. Although the interpretation of marine pollen records is complex due to potentially extensive source areas and different modes of transportation and preservation, the pollen distribution in modern marine sediments of the Namaqualand mudbelt along the west coast of South Africa (Zhao et al., 2016a) indicates distinctive pollen spectra reflecting vegetation communities on the adjacent continent and demonstrates that pollen records from marine sediment cores of the Namaqualand mudbelt have the potential to be a tool to reconstruct vegetation development in this region and better understand late Quaternary climate change.

In this study, pollen and microcharcoal records from two marine sites GeoB8331 and GeoB8323 retrieved from the Namaqualand mudbelt (Figure 3.2) offshore of the west coast of South Africa were analyzed for the following objectives: (1) to reconstruct Holocene vegetation and climate changes in the SRZ and WRZ of South Africa; (2) to compare the regional climate developments during the late Holocene based on two marine records; (3) to address the issue as to if and when the climate trends in the two rainfall zones developed in different directions. We aim at a better understanding of the spatial and temporal climate dynamics of South Africa during the Holocene associated to the position and intensity of atmospheric and oceanic circulation systems.

## 3.3 Regional setting

During the austral summer (Figure 3.1a), the rainfall in the SRZ is generated mainly by warm and moist easterly winds associated with the South Indian Anticyclone (SIA) and more than 66% of the annual precipitation falls between October and March. In the WRZ, precipitation is minimized in summer when the westerlies are located south due to alongshore winds resulting from a southern position of the South Atlantic Anticyclone (SAA). In contrast, during the austral winter (Figure 3.1b), dry conditions and high pressure prevail over the SRZ. The southern westerlies are at their northernmost position over the southwestern Cape during austral winter supplying rainfall to the WRZ and more than 66% of the annual precipitation falls between April and September. Between these two regions, the YRZ receives both summer and winter rainfall all the year where the summer rainfall progressively increases eastward along the south coast of South Africa (Tyson and Preston-Whyte, 2000).

There are nine biomes in southern Africa, which reveal a marked east to west gradient driven by rainfall amount and seasonality (Figure 3.2) (Bredenkamp et al., 1996; Cowling et al., 1997; Mucina and Rutherford, 2006; White, 1983). The Savanna Biome, which is the most extensive in southern Africa occupying 46% of its area, is characterized by a grassy ground layer and a distinct upper layer of woody elements associated with mean annual rainfall varying from 235 to 1000 mm/yr. The Grassland Biome, situated on the cooler and higher interior plateau, is dominated by a single layer of grasses and trees are largely absent except in a few localized habitats. It spans a large rainfall gradient from 400 to 1200 mm/yr. The Forest Biome, which is restricted to areas with mean annual rainfall of more than 725 mm in the SRZ and more than 525 mm in the WRZ (Mucina and Rutherford, 2006) comprises mostly of evergreen trees in multi-layered canopies, while the ground layer is often poorly developed due to the dense shade. The Nama Karoo Biome is semi-desert grassy and dwarf shrubland on the central plateau and is dominated by members of the Asteraceae, Poaceae, Aizoaceae, Liliaceae and Scrophulariaceae families. The rain in this biome falls mainly during austral summer varying between 100 and 520 mm/yr. The Succulent Karoo Biome, located in a narrow strip along the west coast and south of the escarpment, is characterized by dwarf leaf-succulents of which Aizoaceae (including Mesembryanthemaceae) and Crassulaceae are particularly prominent, where Asteraceae, Amaranthaceae, Euphorbiaceae (*Euphorbia*) and Zygophyllaceae (*Zygophyllum*) (Wheeler, 2010) are relatively common. Grasses are rare except in some sandy areas. This biome is primarily determined by low winter rainfall and extreme summer aridity with rainfall varying between 20 and 290 mm/yr. The Desert

Biome, found under very harsh environmental conditions, is characterized by dominance of annual plants (often annual grasses like *Stipagrostis sabulicola*). The climate is characterized by occasional summer rainfall, but high levels of summer aridity with mean annual rainfall from approximately 10 mm in the west to 70 or 80 mm on the inland margin of the desert. The Fynbos Biome, which is an evergreen shrubland in the southwest Cape, is typified by the presence of Restionaceae, Ericaceae and Proteaceae with rainfall usually varying from 600 to 800 mm/yr. Renosterveld is another type of shrubland occurring within the Fynbos Biome and is dominated by Asteraceae, in particular by one species - renosterbos (*Elytropappus rhinocerotis*), together with other important shrub families including Rubiaceae (*Anthospermum*), Thymelaeaceae (*Passerina*), Rosaceae (*Cliffortia*), Boraginaceae, Fabaceae and Malvaceae (Goldblatt and Manning, 2002). The rainfall in the Renosterveld is between 250 and 600 mm/yr of which at least 30% falls during austral winter. Other two biomes (Albany Thicket Biome and Indian Ocean Coastal Belt) are located in the southeastern South Africa, which are not relevant for this study considering the pollen sources in the Namaqualand mudbelt (Zhao et al., 2016a).

The Namaqualand mudbelt stretches over 500 km on the inner continental shelf along the western coast of southern Africa from 20 km north of the Orange River mouth to south of St Helena Bay (Rogers and Bremner, 1991). Sedimentation, source material and texture of the mudbelt have been extensively discussed in several papers (Compton et al., 2010; Hahn et al., 2016; Mabote et al., 1997; Meadows et al., 1997, 2002; Rogers and Rau, 2006). The pollen distributions in modern marine sediments of the Namaqualand mudbelt along the west coast of South Africa indicate that vegetation communities on the adjacent continent are reflected in the marine pollen assemblages (Zhao et al., 2016a). Three groups can be distinguished: Group 1 (Poaceae, Cyperaceae, *Phragmites*-type, *Typha*, *Tribulus*) consisting of pollen that is mainly contributed by the Orange River to the northern mudbelt; Group 2 (Restionaceae, Ericaceae, *Anthospermum*, *Stoebe/Elytropappus*-type, *Cliffortia*, *Passerina*, *Artemisia*-type, *Pentzia*-type) consisting of typical Fynbos elements and dominating in the southern mudbelt; and Group 3 (Aizoaceae, Cheno/Am, Asteroideae) consisting of pollen contributed mainly from the nearshore Succulent Karoo and Nama Karoo vegetation by so-called berg winds and local ephemeral Namaqualand rivers to the central mudbelt (Mabote et al., 1997).

## 3.4 Materials and methods

The two gravity cores GeoB8331-4 (29°08.12'S, 16°42.99'E, 887 cm long, Figure 3.2) and GeoB8323-2 (32°01.70'S, 18°12.21'E, 285 cm long, Figure 3.2) were retrieved in January-February 2003 during *Meteor* cruise M57/1 (Schneider et al., 2003) at 97 m water depth from the northern Namaqualand mudbelt off the Holgat River (just south of the estuary of the Orange River), and at 92 m water depth from southern Namaqualand mudbelt off the Olifants River, respectively. The GeoB8331-4 sedimentary sequence consists of olive brown mud from 887 to 15 cm and dark laminated layers within olive brown mud above 15 cm. The GeoB8323-2 sedimentary sequence consists of dark greenish gray sandy mud with bilvalve shell fragments, and shell layers from 182 to 178 cm. Additionally, considering the disturbance and compaction of the uppermost parts of the gravity cores during coring, two multicores GeoB8331-2 (10 samples, same site as GeoB8331-4) and GeoB8323-1 (12 samples, same site as GeoB8323-2) were processed to extend the coverage of both records towards the present.

A total of 65 samples were analyzed from GeoB8331-4 and GeoB8331-2, providing a high temporal resolution of ca. 170 years on average (range: 4 - 770 years). 31 samples were analyzed from GeoB8323-2 and GeoB8323-1, providing an average resolution of ca. 110 years (range: 8 - 200 years). The samples were decalcified with diluted HCl (~12%) and two *Lycopodium* spore tablets (each containing 18584 ± 372 markers) were added during the decalcification step. After washing, the samples were treated with HF (~ 40%). The samples were shaken for 2 hours, and then kept standing for two days to remove silicates. Samples were sieved ultrasonically to remove particles smaller than 10-15 µm. Samples were stored in water, mounted in glycerol and identified under a light microscope (magnification 400 and 1000×) for pollen, spores, fresh-water algae, dinoflagellate cysts and microcharcoal. Pollen grains were identified using the African pollen reference collection of the Department of Palynology and Climate Dynamics of the University of Göttingen, African Pollen Database and after Scott (1982), Bonnefille and Riollet (1980). At least 300 pollen grains (including terrestrial pollen taxa, sedges and aquatic taxa but excluding those unidentified and broken) were counted per sample and percentages related to the total number of terrestrial pollen taxa (excluding sedges and aquatic taxa). Pollen diagrams were constructed with TILIA 1.7.16 (Grimm, 2011), using the terrestrial pollen taxa as the pollen sum. Pollen zonation was conducted by Constrained Incremental Sum of Squares Cluster Analysis (CONISS, TILIA 1.7.16) including all counted taxa. 95% confidence intervals were calculated following Maher (1972). Samples volumes were measured using water displacement to calculate concentration values. Pollen

accumulation rates were calculated by multiplying the pollen concentration (grains/$cm^3$) by the sedimentation rate (cm/yr) for each sample. Microcharocal particles (5-150µm) were counted on the same slides for pollen analysis using the 202 touch point-count method (Clark, 1982) to calculate the microcharcoal concentration as $cm^2/cm^3$. At least 225 fields were analyzed to improve the statistical reliability of the results. Pollen counts and microcharcoal concentrations are stored in Pangaea, available from www.pangaea.de.

## 3.5 Results

### 3.5.1 Chronology

Lithology, sediment texture and other physical property data (including reflectance, magnetic susceptibility, porosity and density) indicate an undisturbed and continuous sedimentation of core GeoB8331-4 (Schneider et al., 2003). The age model of GeoB8331-4 is based on small well-preserved *Nassarius vinctus* shells of which seven radiocarbon ages have been publishes by Herbert and Compton (2007) and two new radiocarbon ages are presented in Hahn et al. (2016) (Table 3.1). In this study, a local ΔR of 146±85 $^{14}C$ years (Dewar et al., 2012) and the Marine13 calibration curve (Reimer et al., 2013) was used for age calibration. The age-depth model is established using linear interpolation to describe the relationship between calendars ages and sediment depth, showing a basal age of 9900 cal. yr BP (Hahn et al., 2016). Sedimentation rates vary from 0.09 cm/yr near the base of the core to approximately 0.24 cm/yr near the top of the core (Table 3.1). The chronology of multicore GeoB8331-2 has been established by Leduc et al. (2010) based on $^{210}Pb_{ex}$ measurements suggesting coverage of the period 1940-2000 A.D.

**Table 3.1** Radiocarbon ages for gravity cores GeoB8331-4 and GeoB8323-2.

| Core site | Depth (cm) | Material | Uncalibrated $^{14}C$ age | Calibrated $^{14}C$ age 95.4%(2 δ) | median | Rate (cm/yr) | Source |
|---|---|---|---|---|---|---|---|
| GeoB8331-4 | 37.5 | Gastropod | 675±30 | 320- | 159 | 0.24 | Hahn et al., 2016 |
| GeoB8331-4 | 195 | Gastropod | 1420±35 | 999-650 | 819 | 0.24 | Herbert and Compton, 2007 |
| GeoB8331-4 | 211.5 | Gastropod | 1535±30 | 1146-736 | 937 | 0.14 | Hahn et al., 2016 |
| GeoB8331-4 | 271 | Gastropod | 1870±35 | 1484-1073 | 1277 | 0.18 | Herbert and Compton, 2007 |
| GeoB8331-4 | 475 | Gastropod | 3145±35 | 3005-2509 | 2780 | 0.14 | Herbert and Compton, 2007 |
| GeoB8331-4 | 615 | Gastropod | 5020±35 | 5430-4909 | 5166 | 0.06 | Herbert and Compton, 2007 |
| GeoB8331-4 | 704 | Gastropod | 6215±35 | 6696-6290 | 6495 | 0.07 | Herbert and Compton, 2007 |
| GeoB8331-4 | 775 | Gastropod | 8410±35 | 9027-8536 | 8798 | 0.03 | Herbert and Compton, 2007 |

| | | | | | | | |
|---|---|---|---|---|---|---|---|
| GeoB8331-4 | 858 | Gastropod | 9130±40 | 9996-9547 | 9675 | 0.09 | Herbert and Compton, 2007 |
| GeoB8323-2 | 39.5 | Gastropod | 740±70 | 421- | 222 | 0.18 | Hahn et al., 2016 |
| GeoB8323-2 | 111 | Gastropod | 1700±30 | 1276-925 | 1108 | 0.08 | Hahn et al., 2016 |
| GeoB8323-2 | 124 | Gastropod | 1790±35 | 1369-981 | 1195 | 0.15 | Herbert and Compton, 2007 |
| GeoB8323-2 | 227 | Gastropod | 2730±35 | 2514-1992 | 2254 | 0.10 | Herbert and Compton, 2007 |

The sandy basal sediment of core GeoB8323-2 was interpreted to be a high-energy lag deposit formed by sea level rise during the last deglaciation, resulting in a hiatus between 285 and 234 cm (Herbert and Compton, 2007). Therefore, in this study, only the material above 227 cm was analyzed and the age model is based on small well-preserved *Nassarius vinctus* shells of which two radiocarbon ages have been published by Herbert and Compton (2007) and two new radiocarbon ages are presented in Hahn et al. (2016) (Table 3.1). The age-depth model shows a basal age of 2,254 cal. yr BP. Sedimentation rates vary markedly: ca. 0.09 cm/yr around 227-124 cm and 111-39.5 cm, and higher values at 124-111 cm (ca. 0.15 cm/yr) and 39.5-0 cm (ca. 0.18 cm/yr) (Table 3.1). $^{210}Pb_{ex}$ measurements of 69, 67, 82, 77, 62, 69 and 39 Bq/kg were performed on multicore GeoB8323-1 at depths of 3, 4, 5, 8, 9 and 12 cm respectively. The calculated mean sedimentation rate for this core is 0.31 cm/yr assuming a constant initial 210Pbex concentration and a constant sedimentation rate. Hence the multicore covers the period of 1870-2003 A.D.

### 3.5.2 Pollen and microcharcoal

Pollen appears to be well preserved within sites GeoB8331 (including GeoB8331-4 and GeoB8331-2) and GeoB8323 (including GeoB8323-2 and GeoB8323-1) and pollen concentrations vary from 1400-15000 grains/cm$^3$ and 6100-14000 grains/cm$^3$, respectively. The following two subsections describe the pollen and microcharcoal data from the two sites.

#### *3.5.2.1 Site GeoB8331*

The frequency distribution of selected pollen taxa over the last 9900 years is provided in Figure 3.4 (see Appendix 3.1 for the list of identified pollen taxa). The record has been divided into three pollen assemblage zones (PZ) using the CONISS calculation (Grimm, 2011).

Zone PZ GeoB8331a (ca. 9900-7800 cal. yr BP, 878-745 cm of GeoB8331-4) is characterized by pollen percentage maxima of Fynbos elements such as

*Stoebe/Elytropappus*-type (4%), Restionaceae (7%) and *Anthospermum* (4%) at the base of the zone. These percentages decline gradually towards the top of the zone, as do the pollen percentages of Asteroideae (from 15 to 9%). The decline is accompanied by an increase in Cheno/Am (Chenopodiaceae and Amaranthaceae), and a maximum in Aizoaceae pollen percentages characteristic of Succulent Karoo between 847 and 823 cm, which thereafter decrease towards the end of the zone. The microcharcoal concentration increases from 0.1 $cm^2/cm^3$ to a maximum value of 0.3 $cm^2/cm^3$ at 823 cm and then decreases again towards the end of the zone. Fluctuations in microcharcoal concentration are matched by those in pollen concentrations and accumulation rates, which also have maxima at 823 cm and then decrease towards the end of the zone.

Zone PZ GeoB8331b (ca. 7800-2400 cal. yr BP, 745-418 cm of GeoB8331-4) begins with a pollen percentage increase of Poaceae and *Phragmites*-type (grass pollen <25 µm; Bonnefille and Riollet, 1980). Poaceae values increase from 35% at the beginning of this zone to 52% at 589 cm, and then fluctuate around 47% decreasing towards the end of the zone. Pollen percentages of Fynbos elements, *Stoebe/Elytropappus*-type in particular, decline compared to PZ GeoB8331a, with the exception of Restionaceae. The tree and shrub elements of *Acacia*, Celastraceae, *Diospyros*, *Lannea*-type and *Rhus*-type are more prominently represented here than PZ GeoB8331 a. Aizoaceae pollen percentages increase to a maximum value (7%) at 464 cm and decrease afterwards. Neuradaceae pollen percentages reach the highest value (2%) of the record between 614 and 588 cm, corresponding with the maximum value of Cyperaceae (41%) and the presence of other aquatics and swamp elements (*Gunnera*, *Typha*). The spores including Trilete, *Ophioglossum*, *Phaeoceros* and *Polypodium* occur more often than in PZ GeoB8331a. *Concentricystes* (possibly a fresh-water algae) (Rossignol, 1962), increases to a maximum value (4%) at the beginning of PZ GeoB8331b and fluctuates around 2% for the rest of the zone. The microcharcoal concentrations in this zone are initially at a low value (0.1 $cm^2/cm^3$) in comparison to the previous zone and generally increase with two peaks at 538 and 457 cm. The similar trend is observed in the pollen concentrations and pollen accumulation rates.

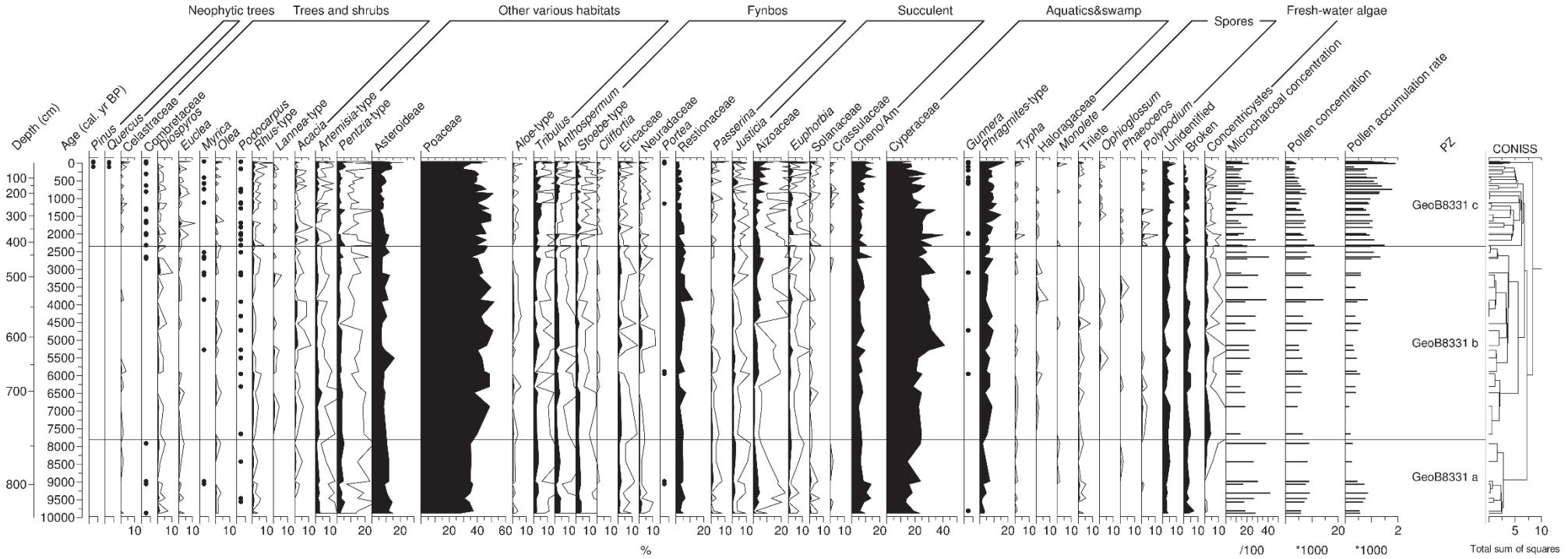


**Figure 3.4** Pollen percentages of selected taxa, microcharcoal concentration ($cm^2/cm^3$), pollen concentration ($grains/cm^3$), and accumulation rates ($grains/cm^2/yr$) from gravity core GeoB8331-4 and multicore GeoB8331-2 (upper 10 samples covering the period 1940–2000 AD). Lines denote five times exaggeration of percentage curves with low values, and the dots denote presence of taxa with percentage values less than 1%. Pollen assemblage zones (PZ) were conducted using the CONISS calculation. For the identified pollen taxa of each group, see Appendix 3.1.

Zone PZ GeoB8331c (ca. 2400 cal. yr BP-2003 A.D., 418-0 cm of GeoB8331-4 and all samples (30-0 cm) of GeoB8331-2) is characterized by the increased presence of arboreal pollen such as Celastraceae, Combretaceae and *Euclea*. *Rhus*-type and *Acacia* percentages also increase in this zone, together with the presence of neophytic trees (*Pinus* and *Quercus*). Grass pollen percentages are relatively stable in comparison to PZ GeoB8331b between 418 and 199 cm and then decline from 51% to 30% followed by a sharp increase in the uppermost sample. The percentages of Restionaceae pollen decline towards the end of the zone and also the other Fynbos elements are less represented. The pollen percentages of Cheno/Am and Aizoaceae both reach maximum values at the top of the zone with increased representation of Crassulaceae, Solanaceae and *Euphorbia*. The percentages of Asteroideae and *Pentzia*-type first fluctuate around 8% and 3%, respectively, and increase abruptly from 49 cm to the top of the sequence. Percentages of *Phragmites*-type pollen increase to a maximum at the middle of the zone corresponding to a decline in Asteroideae percentages, and again rise to another maximum at the end of the zone parallel to the decline in grass pollen. *Ophioglossum*, *Phaeoceros* and *Polypodium* spores are much more prominent than in PZ GeoB8331b, while *Concentricystes* decreases to low values. The microcharcoal concentration fluctuates around 0.1 $cm^2/cm^3$ with maxima at 392 cm and 200 cm, in parallel with the pollen concentration. Pollen accumulation rates increase to higher values in comparison to PZ GeoB8331a and PZ GeoB8331b.

#### *3.5.2.2 Site GeoB8323*

The frequency distribution of selected pollen taxa over the last 2300 years is presented in Figure 3.5 (see Appendix 3.1 for the list of identified pollen taxa). Although the record has been divided into three pollen assemblage zones (PZ) using the CONISS calculation, the overall pollen assemblage shows little variability except for the upper zone (PZ GeoB8323c). The pollen sequence is dominated by typical Fynbos elements such as Restionaceae, *Anthospermum*, *Stoebe/Elytropappus*-type and Ericaceae. Restionaceae pollen percentages show small fluctuations except for two maxima at 137 cm and 65 cm. *Stoebe/Elytropappus*-type and *Passerina* values remain constant and increase to the maximum values only at the end of the record when the representation of *Anthospermum* declines. The succulent elements (Aizoaceae and Cheno/Am) also contribute a large proportion to the assemblage, as well as other Asteraceae pollen (Asteroideae, *Artemisia*-type and *Pentzia*-type) whose percentages are comparable to those of site GeoB8331 but show very little variation throughout the record. Poaceae pollen also represents a significant proportion of the assemblage slightly decreasing towards the end of the record. However, Poaceae pollen

percentages are much lower (9-22%) than in site GeoB8331 (28-52%) where they dominate the record. Tree and shrub elements such as *Diospyros*, *Euclea*, *Myrica*, *Podocarpus* and *Rhus*-type are little represented throughout the record. The neophytic pollen, *Pinus* and *Quercus* are present in the upper 17 cm of core GeoB8323-2 and throughout core GeoB8323-1 (35-0 cm). Aquatics and swamp elements such as Cyperaceae and *Phragmites*-type are also well represented with percentage values between 6-13% and 1-7%, respectively. *Monolete* spores occur mainly in PZ GeoB8323b, while the other spores (Trilete and *Ophioglossum*) are not continuously present. Pollen concentrations are relatively stable around 9800 grains/cm$^3$, while microcharcoal concentration varies showing maxima, at 209 cm and 145 cm. Pollen accumulation rates remain constant between 227-49 cm, and then increase to higher values towards the end of the record probably due to the effect of high sedimentation rates of the multicore GeoB8323-1 (0.31 cm/yr) compared to the gravity core GeoB8323-2 (0.18 cm/yr).

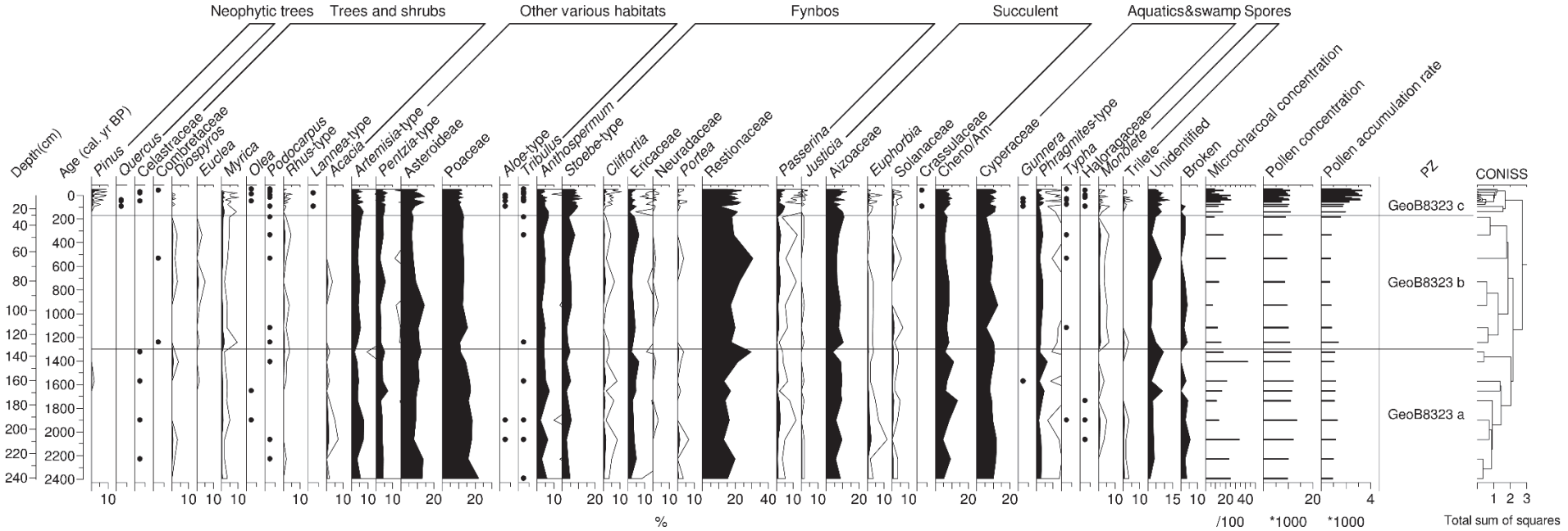


**Figure 3.5** Pollen percentages of selected taxa, microcharcoal concentration ($cm^2/cm^3$), pollen concentration ($grains/cm^3$), and accumulation rates ($grains/cm^2/yr$) from gravity core GeoB8323-2 and multicore GeoB8323-1 (upper 12 samples covering the period 1870–2003 AD). Lines denote five times exaggeration of percentage curves with low values, and the dots denote presence of taxa with percentage values less than 1%. Pollen assemblage zones (PZ) were conducted using the CONISS calculation. For the identified pollen taxa of each group, see Appendix 3.1.

## 3.6 Discussion

### 3.6.1 Interpretation of the pollen record

Interpretation of pollen and spore records (as those of other particles in the marine sediments) should take into account the wide and complex source area, transport and sedimentation processes (Dupont, 1999). Many studies of the pollen distribution in marine surface sediments around Africa and elsewhere have shown that the lateral displacement of pollen by ocean currents is relatively small, even in deep-sea sediments (e.g. Hooghiemstra et al., 2006). The sediments used in our study are far shallower being all retrieved on the inner-shelf with water depths not exceeding 120 m further limiting the effect of ocean currents. Moreover, Mabote et al. (1997) showed that the poleward countercurrent is not competent to transport medium to fine silt as far south as the Buffels River mouth. Absolute dating of several multicores and gravity cores from the mudbelt (Herbert and Compton, 2007; Leduc et al., 2010; Taylor, 2004) asserted that vertical mixing within the Holocene sediment is not prominent.

Site GeoB8331 from the northern mudbelt, is located approximately 17 and 60 km away from the mouths of the Holgat and Orange Rivers, respectively. Comparing this record with the pollen distribution of the mudbelt indicates that the pollen in site GeoB8331 is mainly fluvially transported and probably originates mostly from the karroid vegetation in the middle catchment area of the Orange River (Zhao et al., 2016a). We do not exclude that single pollen grains may have been transported over long distances, even as far as the Drakensberg region, as is the case for much of the Orange River sediment load (Hahn et al., 2016). However, the pollen sources lying between the Drakensberg and the Orange River mouth would have overwhelmed any signal from eastern South Africa being so much closer to deposition in front of the Orange River. Also the sparse occurrences of *Podocarpus* and *Pinus* pollen, which highly productive sources grow far from the western coast, argue that long-distance transport of pollen is only of minor importance.

The pollen of grasses (Poaceae, dominant taxa in Group 1; see 3.2 Regional setting) probably having its main origin in the savanna, grassland and Nama Karoo vegetation, dominate the entire record of GeoB8331 (28-52%). Our Poaceae pollen percentages compare well with the records of Blydefontein (Scott et al., 2005) and Braamhoek wetland (Norström et al., 2009) situated in the Orange River basin. Other abundant pollen types belonging to Group 1 originate from Cyperaceae species (sedges etc.) (8-41%) and *Phragmites*-type (1-18%) probably growing in the Orange River riparian zone

and swamps (e.g. halophytic swamps in the savanna biome). Arboreal pollen originates from trees and shrubs such as *Acacia*, *Olea*, *Diospyros*, *Euclea*, *Myrica* and *Rhus*-type growing in diverse habitats of savanna, woodland and dry forest. Pollen of the Fynbos elements (Group 2) is present throughout the record of GeoB8331 with low percentages indicating a small but continuous pollen supply from the Cape region. In contrast, the pollen assemblage of site GeoB8323 is dominated by Group 2 and has a relatively poor representation of Group 1, while the proportion of Group 3 shows no significant differences with that of site GeoB8331.

In summary, the pollen in site GeoB8331 mainly originates from fluvial transport by the Orange River, as well as local runoff and berg winds (pollen from Succulent Karoo, Nama Karoo, possibly Namib Desert) and Fynbos elements from the Cape region, while the pollen in site GeoB8323 are dominated by Fynbos elements from the Cape region with much less contribution by the Orange River. Therefore, we use the record of pollen types mainly coming from the Orange River catchment area (Group 1, including Poaceae, Cyperaceae, *Phragmites*-type and *Typha*) to infer vegetation change in the SRZ and pollen types from the Fynbos elements (Group 2, including Restionaceae, *Anthospermum*, Ericaceae, *Cliffortia*, *Stoebe/Elytropappus*-type, *Passerina*, *Artemisia*-type and *Pentz*ia-type) for interpretation of vegetation change in the WRZ. *Tribulus* was excluded from Group 1 to avoid the possible effect of pioneer vegetation from disturbance areas.

Grass pollen are mainly derived from grassland, savanna and Nama Karoo which are vegetation types strongly associated with predominantly summer rainfall regions, while Asteraceae (excluding *Stoebe/Elytropappus*-type) pollen mainly originating from the Nama Karoo is favored by weaker rainfall seasonality or drier and cooler summers (Cooremans, 1989; O'Connor and Bredenkamp, 1997). Thus, the Poaceae/Asteraceae ratio (Poac/Ast) can be used to offer a perspective on total rainfall and degree of seasonality (Norström et al., 2009; Scott et al., 2005). Additionally, pollen taxa growing along the Orange River and swamps (Cyperaceae, *Phragmites*-type, *Typha*) may provide some indication of a high water availability in the Orange River floodplain.

The microcharcoal concentration is expressed as area of fragments per $cm^3$. It is difficult to distinguish between the microcharcoal sources from the SRZ and WRZ. Therefore, in this study, the microcharcoal concentration was interpreted based on the vegetation change in the SRZ and WRZ inferred from the pollen record.

### 3.6.2 Holocene climate history and regional comparison

Analysis of sites GeoB8331 yields a high-resolution record of Holocene climate and vegetation change of South Africa. In order to test the contention that the climate variability in the SRZ and WRZ are contrasted, our data are compared in Figure 3.6 with the pollen record of Wonderkrater (Figure 3.6e) (Scott et al., 2012) and the $\delta^{13}C$ record of the Makapansgat stalagmite (Figure 3.6d) (Holmgren et al., 2003) from the SRZ, the pollen record of Pakhuis Pass (Figure 3.6h) (Scott et al., 2012) from the WRZ and the alkenone-derived sea surface temperature record from the same core GeoB8331-4 (Figure 3.6i) (Leduc et al., 2010). We also compare our results with iron concentrations from the Chilean continental margin at 41°S (Figure 3.6j) (Lamy et al., 2001) which might provide a record of the global latitudinal position of the southern westerlies as its position is mainly determined by the global temperature gradient.

#### *3.6.2.1 Early Holocene (9900-7800 cal. yr BP)*

The low representation of Poaceae in the pollen record at the beginning of the sequence indicates a reduced extension of grasslands/savanna and less summer rainfall in the interior of South Africa (SRZ) during the early Holocene, which is also reflected in the low Poac/Ast ratio (Figure 3.6c). Many shrubs and trees such as *Rhus*-type, *Diospyros* and *Euclea* are represented with few pollen grains only, although *Acacia* does appear and sustains its contribution to the pollen sum. Both the Makapansgat $\delta^{13}C$ record and the Wonderkrater pollen record indicate a decreased $C_4$ grass cover and considerably drier environments between 10,200-8400 cal. yr BP. After 8500 cal. yr BP, aridity persisted at Wonderkrater as indicated by the increased grass pollen record, while no clear trend was found at Makapansgat. Drier conditions with low summer rainfall in the SRZ before 7800 cal. yr BP are corroborated by the pollen and geochemistry records from the Tswaing Crater (Kristen et al., 2007; Metwally et al., 2014). Early Holocene aridity concurs with a minimum for the austral summer insolation (Figure 3.6a) (Berger and Loutre, 1991).

Maximum percentages of *Stoebe/Elytropappus*-type pollen in combination with high relative abundance of *Anthospermum* pollen during the earliest Holocene indicate the presence of Renosterveld vegetation, which is part of the Fynbos biome. However, the declining trend in Fynbos elements accompanied by a brief expansion of Aizoaceae and Cheno/Am between 9600-9300 cal. yr BP suggests a short period of warmer and drier climate with the expansion of Succulent Karoo in the WRZ. This is supported by the pollen record of Pakhuis Pass indicating a brief phase of humid conditions prior to 9500 cal. yr BP and followed by a marked shift to drier conditions favoring succulent

and scrub vegetation between 9500-9000 cal. yr BP (Scott and Woodborne, 2007a, 2007b). Other records from the WRZ also indicate humid conditions between 10,000-8000 cal. yr BP (Klein, 1991; Meadows and Sugden, 1991; Meadows et al., 2010; Quick et al., 2011; Valsecchi et al., 2013; Weldeab et al., 2013). During this period the high microcharcoal concentrations indicate enhancement of fires, probably attributable to lower summer rainfall in the SRZ and subsequent expansion of Succulent Karoo accompanied by relatively abundant Fynbos vegetation, which is fire-prone (Mucina and Rutherford, 2006).

#### *3.6.2.2 Middle Holocene (7800-2400 cal. yr BP)*

The gradual increase of Poaceae pollen after 7800 cal. yr BP suggests increasing grass cover especially between 6900-3500 cal. yr BP, which might imply increased summer rainfall in the SRZ. Representation of local riparian vegetation (*Phragmites*-type, Cyperaceae and *Typha*) increased somewhat. The presence of pollen of other aquatics and swamp plants as well as spores is suggestive of moister conditions in the Orange River catchment since 7800 cal. yr BP. The middle Holocene trend towards relatively higher $\delta^{13}C$ values at Makapansgat parallels the increase in grass pollen of site GeoB8331 and the Wonderkrater humidity index also indicated wetter conditions. Between 6900-3500 cal. yr BP, the maximum grass cover and high Poac/Ast ratio indicate high summer rainfall corresponding to a humidity maximum at Wonderkrater around 5500 cal. yr BP. A similar conclusion has been drawn from Blydefontein where the transition from dominantly Karoo shrubs to more grassy vegetation after 5400 cal. yr BP has been interpreted as a response to increased summer rainfall (Scott et al., 2005). A rather humid climate during the middle Holocene has been supported by the pollen record of Tswaing Crater showing increased representation of mesic woodland, savanna trees and local swamps (Metwally et al., 2014). The geochemical record of Tswaing Crater also suggests that conditions gradually became wetter after 6000 cal. yr BP (Kristen et al., 2007). The enhanced moisture availability in the SRZ of the middle Holocene appears to be associated with increasing austral summer insolation (Figure 3.6a).

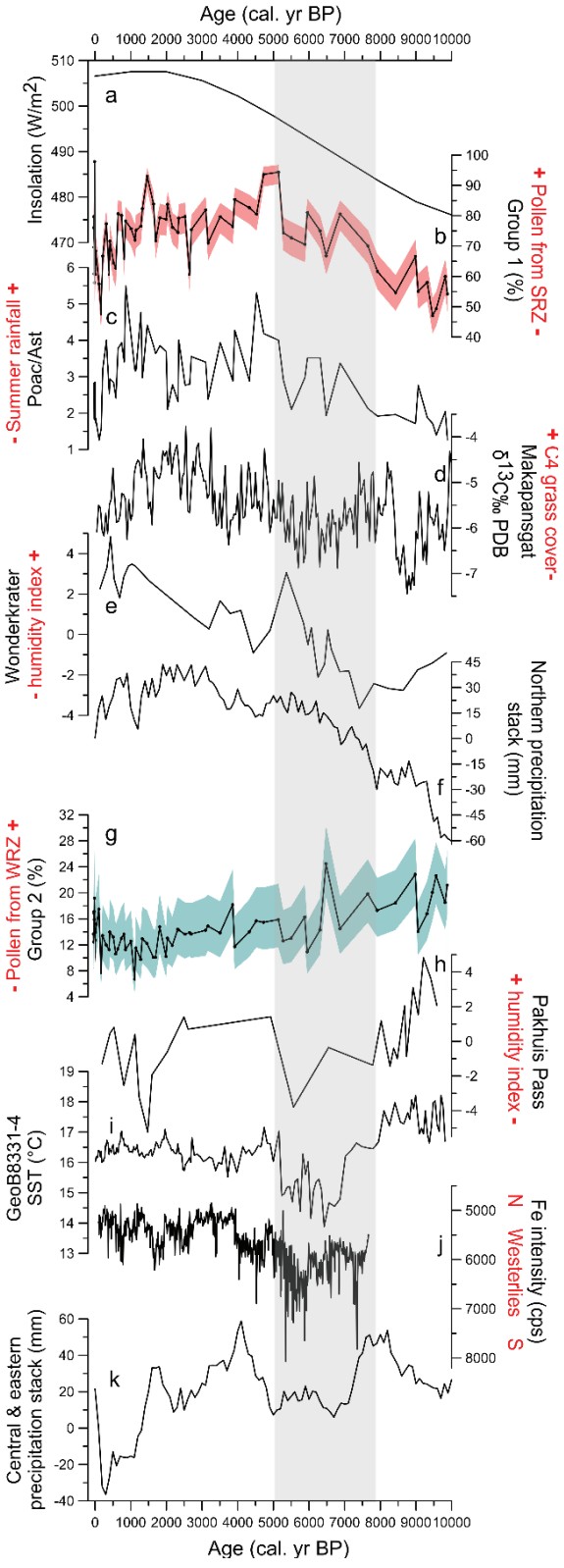


**Figure 3.6** Comparison of the percentage of (b) Group 1, (g) Group 2, and (c) ratio of Poaceae over Asteraceae counts from gravity core GeoB8331-4 and multicore GeoB8331-2 (upper 10 samples) (a) with austral summer (December) insolation at 30°S (Berger and Loutre, 1991), (d) δ13C record from Makapansgat (Holmgren et al., 2003), (e) humidity index based on pollen records from Wonderkrater (Scott et al., 2012), and (h) Pakhuis Pass (Scott et al., 2012), (f) precipitation stack of the wettest quarter in northern South Africa, and (k) central and eastern South Africa (Chevalier and Chase, 2015), (i) alkenone-derived sea surface temperature (SST) records from gravity core GeoB8331-4 (Leduc et al., 2010), and (j) the latitudinal position of the southern westerlies based on iron concentrations from the Chilean continental margin at 41°S (Lamy et al., 2001).

Fynbos elements (Group 2) fluctuate around a very slightly decreasing trend, while the representation of Aizoaceae gradually increase suggesting a warmer and drier climate in the WRZ, which corresponds with a dry period at Pakhuis Pass ca. 8000-5000 cal. yr BP (Scott and Woodborne, 2007a 2007b). Most records from the WRZ (Klein, 1991;

Meadows and Sugden, 1991; Meadows et al., 2010; Quick et al., 2011) indicate relatively dry conditions between 8000-3000 cal. yr BP except that of De Rif 2010, which indicates more variable conditions (Valsecchi et al., 2013). The drier climate during this period might be related to a southward shift of the southern westerlies (Lamy et al., 2001) especially between 8000-5000 cal. yr BP resulting in less winter rainfall in the WRZ. A southward shift of the westerlies would also have resulted in more upwelling in the northern mudbelt area decreasing the SSTs at GeoB8331 (Leduc et al., 2010). Pollen and isotope records of Katbakkies Pass (Chase et al., 2015) indicate increasing moisture ca. 7000-3000 cal. yr BP interpreted to be a result of increased tropical easterly flow, which could explain the variable moisture conditions at Seweweekspoort which is located in the YRZ (Chase et al., 2013). The low values in microcharcoal concentration between 7600-5900 cal. yr BP could be attributed to a moister climate trend in the SRZ leading to less frequent fire. The gradual increase in microcharcoal concentration between 5900-2600 cal. yr BP could be associated with accumulated availability of fuel supplied by the abundant grasses under relatively humid conditions in the SRZ as well as gradually drier climate in the WRZ.

#### *3.6.2.3 Late Holocene (2400 cal. yr BP - modern)*

Expansion and a change in the composition of the savanna since the middle Holocene is indicated by the regular occurrence of tree and shrub pollen, notably that of Combretaceae, in the record after 2400 cal. yr BP. Combretaceae species are mostly constituents of the savanna and are missing in the southern and western parts of South Africa today (Dyer, 1975). Development of savanna woodlands is also recorded at Tswaing Crater between ca. 7200-1800 cal.yr BP (Metwally et al., 2014). The expansion of savanna suggests a southward shift or an intensification of the SRZ. The Poac/Ast ratio increases towards a maximum at about 850 years ago, indicating more summer rainfall in the SRZ corresponding with the austral summer insolation maxima. Gradually increasing representation of *Phragmites*-type until ca. 1500 cal. yr BP indicates the development of a riparian reed belt along the Orange River corresponding with the increase of Cyperaceae and *Typha* pollen in Tswaing Crater (Metwally et al., 2014). The $\delta^{13}C$ record at Makapansgat reaches a maximum between 3000-2000 cal. yr BP indicating a grassy environment that turns to a bushy environment after 2000 cal. yr BP, while the humidity index of Wonderkrater increases to the maximum at about 500 cal. yr BP. The sharp decrease of moisture at Wonderkrater and higher Asteraceae pollen in site GeoB8331 corresponding to the decline in grass pollen since the last 850 years could be a consequence of a drier climate with less summer rainfall in the SRZ. Additionally, grasses could have been reduced at least in part by the

grazing of domestic stock since the arrival of the Iron Age people, which were present in at least some parts of the SRZ as early as ca. 1700 cal. yr BP (Evers, 1975; Klapwijk, 1974).

The continuing low representation of Fynbos elements and strong increase of Succulent Karoo elements (Aizoaceae, Crassulaceae, *Euphorbia* and Cheno/Am) suggest that the climate was becoming more arid in the WRZ. The humidity index of Pakhuis Pass first declines to minimum values and after that rises again with large variations to the middle Holocene level. However, general moist conditions were indicated in other records from the WRZ (Klein, 1991; Meadows and Sugden, 1991; Valsecchi et al., 2013) except at Katbakkies Pass where drier conditions were indicated after 1700 cal. yr BP. The low values in microcharcoal concentration during the late Holocene are difficult to explain. On the one hand, the decline in grasses in turn diminished the fuel supply for fires in the SRZ; on the other hand, the drier climate in the WRZ should have been conducive to fires. Considering the history of Khoikhoi people, which are the native pastoralist people of southwestern Africa since ca. 2300 cal. yr BP, the increase of Asteroideae and Aizoaceae pollen since ca. 1400 cal. yr BP suggesting the occurrence of more shrubby vegetation could indicate drier conditions but also could be (partly) attributable to the activities of Khoikhoi people (Bousman and Scott, 1994; Bousman, 1998).

The neophyte *Pinus* is common and wide-spread in the southwestern mountains of the Cape region for the last ca. 100 years (Shaughnessy, 1986). Pollen of neophytes associated with the arrival of Europeans such as *Pinus* and *Quercus* are found in low percentages (no more than 1%) and only for the last 100 years (which helps to confirm the upper part of the age model). The percentage of neophytes pollen recorded in the modern marine sediments is also very low (no more than 2%, Zhao et al., 2016a). This is supported by most records in both the WRZ and SRZ where *Pinus* pollen is only present in low frequencies (in percentages of less than 5%) during the last 300 years, such as in Driehoek Vlei, Pakhuis Pass, De Rif, Klaarfontein springs, Verlorenvlei and Spring Cave Shelter in the WRZ (Baxter, 1996; Meadows and Sugden, 1991; Meadows and Baxter, 2001; Meadows et al., 1996; Quick et al., 2011; Scott and Woodborne, 2007a), and Wonderkrater, Tswaing Crater, Braamhoek, Blydefontein, and Mahwaqa in the SRZ (Metwally et al., 2014; Neumann et al., 2014; Norström et al.,, 2014; Scott et al., 2005, 2012). Only Neumann et al. found high representation (percentages of up to 60%) of *Pinus* pollen in Princess Vlei of the WRZ (Neumann et al., 2011), Lake Eteza and Lake Sibaya in the SRZ (Neumann et al., 2008, 2010). The low percentages of *Pinus* in our samples indicate that long-distance transport of pollen is not an issue,

otherwise high percentages of *Pinus* pollen would have been found in the upper sediments dated after pine trees have been planted along the south coast etc.

### 3.6.3 Climate variations as deduced from two sites for the last 2200 years

A comparison between the pollen and microcharcoal records of the two sites GeoB8331 and GeoB8323 has been carried out for the last 2200 years. To facilitate the comparison, we have interpolated the pollen and microcharcoal values at regular time intervals of 100 years between 2200 and 100 cal. yr BP and of 10 years between 100 cal. yr BP and modern (Figure 3.7).

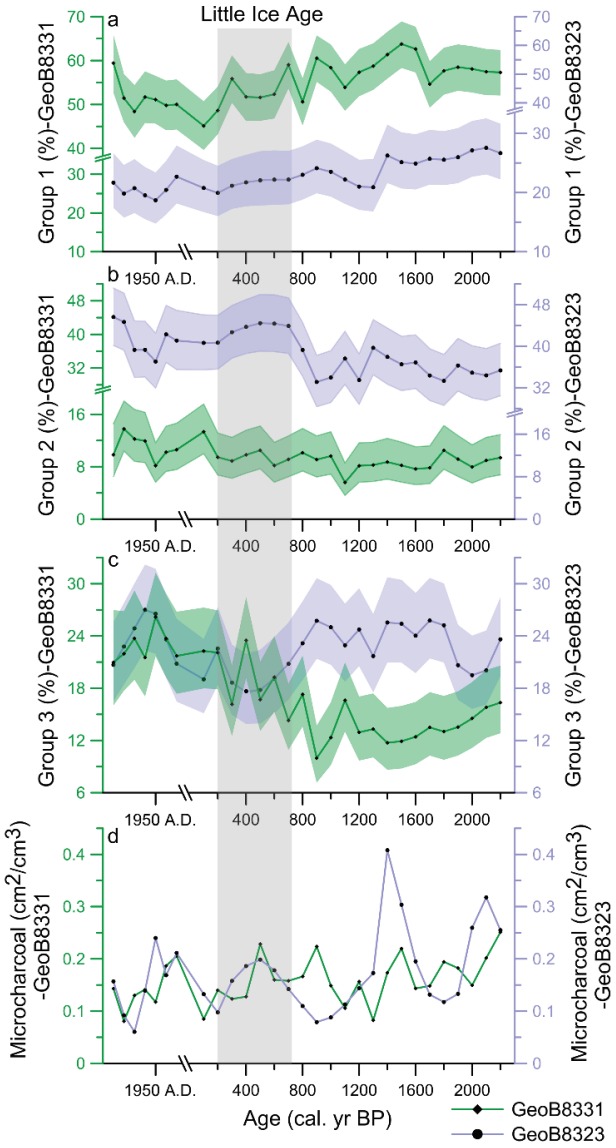


**Figure 3.7** Comparison of the percentages of (a) Group 1, (b) Group 2, (c) Group 3, and (d) microcharcoal concentrations from the sites GeoB8331 (including gravity core GeoB8331-4 and multicore GeoB8331-2 in green) and GeoB8323 (including gravity core GeoB8323-2 and

multicore GeoB8323-1 in blue) during the last 2200 years. Samples dated between 2200 and 100 cal. yr BP have been interpolated every 100 years and those dated thereafter have been interpolated every 10 years.

The same pollen groups are present in both cores but vary in percentage, especially Groups 1 and 2 (Figures 3.7a and 3.7b). These percentage variations are most likely the consequence of different pollen sources for the two sites GeoB8331 and GeoB8323 i.e. being drawn largely from the SRZ and WRZ, respectively. This pattern is consistent with the pollen distribution in modern marine sediments from the mudbelt (Zhao et al., 2016a). The contrasting temporal trends between the two sites in Group 1 pollen types emphasizes the different source areas contributing to the pollen assemblage at each site. Pollen of Group 1 at GeoB8323 may be mainly locally derived from the west coast rather than from the SRZ, while transport via the Orange River might be the case at GeoB8331. The recovery of grasses at GeoB8331 during the last 150 years might be attributed to human control of grazing intensity in the SRZ. Additionally, the greater fluctuations of Group 2 at GeoB8323 (Figure 3.7b) suggest that it more likely reflects climate changes in the WRZ. On the other hand, the obvious increase of Group 3 accompanied by the decline of Group 1 at GeoB8331 after 1400 cal. yr BP (Figure 3.7a) suggests drier conditions with less summer rainfall in the SRZ. The drier conditions may be associated with the event of LIA in the SRZ during which the cold and dry climate is not conducive to the growth of grasses which are more favored under the warm and moist conditions. This is supported by the $\delta^{18}O$ records from Makapansgat stalagmite in which the Little Ice Age (LIA) is expressed as around the last 700-200 years (Tyson et al., 2000). Huffman (1996) reported that it was colder in northeastern South Africa for the last 650-150 years. The maximum percentages of Group 2 and minimum percentages of Group 3 (Figures 3.7b and 3.7c) at GeoB8323 between 700-200 cal. yr BP, however, suggest a wetter climate for the LIA in the WRZ. Wet conditions during the LIA would corroborate the interpretation of the sediment record of core GeoB8332-4 (located near the Orange River, Figure 3.2) as a wet phase in the WRZ during the LIA (Weldeab et al., 2013). The contrasting climate conditions during the LIA between the SRZ and WRZ were also detected based on the geochemical and isotopic records from the same gravity cores GeoB8331-4 and GeoB8323-2 (Hahn et al., 2016). On the other hand, the obvious increase of Group 3 accompanied by the decline of Group 1 suggests an increased pollen contribution from the lower Orange River catchment resulting in less input of grass pollen from the middle catchment. The source shift to the lower catchment is supported by the distinctive Sr and Nd isotopic compositions of gravity core GeoB8331-4 (Hahn et al.,

2016). The greater contribution of Group 3 at GeoB8331 appears also be recorded in the microcharcoal concentrations (Figure 3.7d) which show a comparable variation between two cores following the decline of Group 1 and increase of Group 3 after 1400 cal. yr BP. The vegetation characterized by Group 3 is mainly Nama Karoo and Succulent Karoo, which are distributed in the areas acting as pollen sources for site GeoB8323.

### 3.6.4 Holocene vegetation and climate dynamics of South Africa

The high-resolution pollen record of site GeoB8331 corroborates contrasting climate developments between the SRZ and WRZ during the early and middle Holocene (see 3.1 Introduction, Figure 3.3). For the SRZ, reduced grass cover indicates low summer rainfall during the early Holocene and the expansion of grasses towards the middle Holocene suggests increasing levels of moisture that are associated with higher summer rainfall. The opposite climate trend is found for the WRZ, where a greater prominence of Renosterveld vegetation suggests relatively humid conditions during the earliest Holocene followed by gradually drier conditions towards the middle Holocene accompanied by the expansion of Succulent Karoo and the decline of Fynbos vegetation. The late Holocene comparison between the two sites of GeoB8331 and GeoB8323 also reflects different climate conditions during the LIA being drier in the SRZ but wetter in the WRZ.

What mechanisms can be considered to explain the emerging pattern? The driving forces of continental vegetation and hydrology during the Holocene are debated and four different main drivers of regional climate changes have been proposed: 1) strength and latitudinal position of the southern westerlies; 2) effects of sea surface temperature on continental hydrology associated with the subtropical anticyclones over the southeast Atlantic Ocean; 3) insolation forcing; 4) intensification of human activities.

The latitudinal position of the southern westerlies directly influences the continental hydrology of the Southern Hemisphere (Reason and Rouault, 2005). At present, only the southwestern tip of South Africa is affected by the southern westerlies when they shift equatorward during austral winter (Figure 3.1b) resulting in winter rainfall in the Cape region. Further north, a strengthened South Atlantic Anticyclone would lead to intensified southeast trade winds, intensification of Benguela upwelling and decrease of sea surface temperature along the southwestern coast causing aridification of the coastal region (Shannon and Nelson, 1996). The initial presence of Renosterveld vegetation and the subsequent declining trend of Fynbos elements accompanied by the expansion of Succulent Karoo in the WRZ could be explained by two different

hypotheses. One is a northward shift of the southeast trade winds during the course of the Holocene which would lower the effectivity of wind transport and to bring Fynbos pollen to site GeoB8331. However, a northward shift of the southeast trade winds would be expected if the westerlies are located further north allowing more humidity to penetrate into the continent, which is inconsistent with other records from the WRZ (Meadows et al., 2010; Quick et al., 2011; Scott and Woodborne, 2007a, 2007b). Also the low SSTs between 8000-5000 cal. yr BP (Leduc et al., 2010) indicate rather more upwelling in the northern mudbelt area suggesting trade winds affected the southern Benguela Upwelling system. Another hypothesis is the southward shifting of the southern westerlies towards the middle Holocene which would have arrived its southernmost position between 8000-5000 cal. yr BP (Lamy et al., 2001) resulting in less winter rainfall in the WRZ and drier climate during this period. Reduced winter rainfall negatively impacts Fynbos but induces an expansion of the Succulent Karoo. Therefore, we interpret that the decrease in Fynbos pollen at site GeoB8331 is probably an effect of retreat of the WRZ resulting from a poleward shift of the southern westerlies.

Fluctuations in orbital variation may have a strong influence on glacial-interglacial climate variability (Hopley et al., 2007; Partridge et al., 1997), while Chevalier and Chase (2015) demonstrated that it was not the primary driver of climate variability in northeastern South Africa except during the Holocene when insolation forcing became significant (Figure 6(f)). The insolation forcing on shorter time scales during the Holocene has been also proposed by other studies (Chase et al., 2009, 2010; Schefuß et al., 2011). Higher insolation intensifies atmospheric convection, leading to high rainfall and *vice versa* (Partridge et al., 1997). The trend in the Poac/Ast ratio (Figure 3.6c) which is interpreted as the result of increasing summer rainfall corresponds well with the early Holocene increase in Southern Hemisphere summer insolation (Figure 3.6a) (Berger and Loutre, 1991). The drier conditions with low summer rainfall in the SRZ during the early Holocene concur with a minimum for the austral summer insolation. The middle Holocene period with enhanced moisture availability in the SRZ appears to be associated with increasing austral summer insolation, and the maximum Poac/Ast ratio at about 850 years ago indicates more summer rainfall in the SRZ corresponding with the austral summer insolation maximum. The marine sedimentary leaf wax $\delta^{13}C$ records off the coast of Namibia (MD08-3167) suggest increase in $C_4$ vegetation during the austral summer insolation maximum interpreted as the result of increased summer rainfall (Collins et al., 2014; Daniau et al., 2013). On the other hand, a marine pollen record off the coast of Namibia (GeoB1711-4) suggests that strengthened southeast trade winds were coeval with austral summer insolation

maxima (Shi et al., 2001). This is supported by the hyrax midden records from the Namib Desert (Chase et al., 2009) suggesting aridification towards the middle and late Holocene during austral summer insolation maxima. The results of Shi et al. (2001) and Chase et al. (2009) seem to be in contradiction with those of Collins et al. (2014), Daniau et al. (2013) and our study. One possible explanation is associated with the source areas of these four records. The core site of MD08-3167 was interpreted to receive terrestrial material from a large source area from the Namib Desert to the east of Kalahari Desert stretching far into the interior of the SRZ (Collins et al., 2014). The pollen taxa of Poaceae and Asteraceae which are used to interpret the summer rainfall variability in our record also mainly come from the middle Orange River catchment (interior of the SRZ). However, the pollen source areas of GeoB1711-4 were interpreted to be restricted to the zone west of the Kalahari region (Shi et al., 2001), which is also the case for the hyrax midden record receiving pollen from local to regional sources in the Namib Desert (Chase et al., 2009). On the other hand, changes in seasonality, which is controlled by the precession, might offer another but not excluding explanation. High summer rainfall in the interior of the SRZ related to the austral summer insolation could be coeval with strong southeast trade winds along the west coast of southern Africa during weaker austral winter insolation. Therefore, as Collins et al. (2014) proposed, the inconsistency seems to indicate that the Namib Desert might be more controlled by the southeast trade winds which induce strong upwelling and cause aridity along the coast, while the rainfall into the interior of the SRZ is mainly brought by easterly winds which are associated to austral summer insolation. Overall, the consistence between the rainfall seasonality of the SRZ and the austral summer insolation suggests that insolation forcing on short time scales is a dominant driver of Holocene rainfall variations in the SRZ but does not extend as far as the west coast of southern Africa.

The influence of the latitudinal position of the southern westerlies might have reached no further than the WRZ. Chevalier and Chase (2015) proposed that precipitation variability in central and southeastern South Africa (Figure 3.6k) might be linked to the latitudinal position of the southern westerlies rather than the role of insolation forcing. Low precipitation was indeed recorded between ca. 7500-5000 cal. yr BP in central and southeastern South Africa (Figure 3.6k) corresponding to a southward shift of the southern westerlies. No such evidence from the SRZ is found in our records probably because the pollen sources in our records do not grow as far as southeastern South Africa. However, the strong declining trend in precipitation of central and southeastern South Africa after ca. 4000 cal. yr BP (Figure 3.6k) would not be in line with a relatively stable position of the global southern westerlies (Lamy et al., 2001), suggesting that the

complexities and evolution of this driver remain to be further investigated as proposed by Chevalier and Chase (2015).

The effects of human activities such as deforestation, soil erosion, enhanced burning and overgrazing are not apparent during the Holocene, except for the last 850 years. The decline in grass pollen at site GeoB8331 over the last 850 years could have been partly affected by the grazing of domestic stock, while the recovery of grasses during the last 150 years could possibly be attributed to human control of grazing intensity in the SRZ.

## 3.7 Conclusions

In this study, we reconstructed contrasting vegetation and climate histories in the SRZ and WRZ of South Africa covering the last 9900 years based on continuous high-resolution pollen and microcharcoal records of site GeoB8331 retrieved from the northern mudbelt offshore the west coast of South Africa. Different pollen types were grouped to infer vegetation and climate change in both the SRZ and WRZ based on the distinctive pollen sources and transport processes. Contrasting climate patterns are evident in the SRZ and WRZ corroborating results from literature, especially during the early and middle Holocene. Relatively humid conditions in the WRZ are suggested by the presence of Renosterveld vegetation during the earliest Holocene, which then gave way to gradually warmer and drier conditions inferred from the decline of Fynbos vegetation and expansion of Succulent Karoo. Opposing climate developments are observed for the SRZ, where a rather moist savanna/grassland expanded during the middle Holocene implying increased summer rainfall. The drier conditions towards the middle Holocene in the WRZ are attributable to a southward shift of the southern westerlies, bringing less rainfall during the austral winter, while the increase in austral summer insolation during the middle Holocene might present a dominant driver of higher summer rainfall in the SRZ.

Comparing the results of site GeoB8331 from the northern mudbelt with the pollen and microcharcoal records of site GeoB8323 retrieved from the southern mudbelt allowed a more detailed interpretation for the last 2200 years. Pollen composition of the two sites show marked differences in the proportions of the three pollen groups with distinctive source areas. The climate in the WRZ during the last 2200 years appears to have been more stable in comparison to that of the SRZ. Effects of the Little Ice Age were detected around the last 700-200 years with colder and drier conditions in the SRZ suggested by a decline of grasses and an increase of Succulent Karoo, while in the

WRZ colder and wetter conditions were indicated by the increased presence of Fynbos vegetation and decreased representation of Succulent Karoo.

## 3.8 Acknowledgements

This study was funded by the German Federal Ministry of Education and Research (BMBF). The investigations were conducted within the collaborative project “Regional Archives for Intergrated Investigations” (RAiN), which is embedded in the international research program SPACES (Science Partnership for the Assessment of Complex Earth System Process). Thanks to the captain, the crew and scientists of the Meteor M57-1 cruise for recovering the studied material. $^{210}Pb_{ex}$ measurements were processed at Bremen State Radioactivity Measurements Laboratory, Institute of Environmental Physiks, University of Bremen with the kind help of Helmut Fischer, Dana Pittauer and Manuel Pérez Mayo. We also thank Gesine Mollenhauer, Matthias Zabel, and three anonymous reviewers for critical discussion and helpful advice.

## *Appendix 3.1. Identified pollen taxa from sites GeoB8331 and GeoB8323*

**Neophytic trees**

*Pinus* (Pinaceae)

*Quercus* (Fagaceae)

**Trees and shrubs**

Celastraceae

Combretaceae

*Diospyros* (Ebenaceae)

*Dodonaea* (Sapinadaceae)

*Euclea* (Ebenaceae)

*Ilex* (Aquifoliaceae)

*Myrica* (Myricaceae)

*Olea* (Oleaceae)

*Podocarpus* (Podocarpaceae)

Rhamnaceae

*Salix* (Salicaceae)

*Rhus* (Anacardiaceae)

*Lannea* (Anacardiaceae)

*Tilia* (Tiliaceae)

*Acacia* (Mimosaceae)

Capparaceae

**Other various habitats**

*Artemisia* (Asteraceae)

*Pentzia* (Asteraceae)

Asteroideae (tubulifloreous Asteraceae)

*Gazania* (Asteraceae)

*Gerbera* (Asteraceae)

*Pacourina* (Asteraceae)

*Vernonia* (Asteraceae)

Poaceae

**Spores**

*Monolete*

Trilete

*Ophioglossum* (Ophioglossaceae)

*Phaeceros* (Notothyladaceae)

*Polypodium* (Polypodiaceae)

**Fynbos**

*Anthospermum* (Rubiaceae)

*Stoebe/Elytropappus* (Asteraceae)

*Cliffortia* (Rosaceae)

Ericaceae

Neuradaceae

*Protea* (Proteaceae)

Restionaceae

*Passerina* (Thymelaeaceae)

**Succulent**

*Justicia/Monechma* (Acanthaceae)

Aizoaceae

*Euphorbia* (Euphorbiaceae)

Solanaceae

Crassulaceae

Chenopodiaceae/Amaranthaceae

**Aquatics & swamp**

Cyperaceae

*Gunnera* (Gunneraceae)

*Phragmites* (Poaceae)

*Juncus* (Juncaceae)

*Typha* (Typhaceae)

Haloragaceae

**Other vegetation**

*Alchornea* (Euphorbiaceae)

Alismataceae

*Aloe* (Asparagaceae)

*Balanties* (Zygophyllaceae)

Bignoniaceae

Campanulaceae

Caryophyllaceae

*Canthium* (Rubiaceae)

*Celtis* (Ulmaceae)

*Cheilanthes* (Adianthaceae)

*Coccinia* (Cucurbitaceae)

Convolunaceae

*Cucumis* (Cucurbitaceae)

*Detarium* (Fabaceae)

*Dichrostoehy* (Fabaceae)

Elaeagnaceae

*Geranium* (Geraniaceae)

*Hypoestes* (Acanthaceae)

Icancinaceae

*Indigofera* (Fabaceae)

*Kirkia* (Kirkiaceae)

Labiateae

*Lankesteria* (Acanthaceae)

Leguminosae

Malvaceae

*Myrsine* (Myrsinaceae)

*Parkinsonis* (Fabaceae)

*Pelargonium* (Geraniaceae)

*Persicaria* (Polygonaceae)

*Petalidium* (Acanthaceae)

*Phyllanthus* (Phyllanthaceae)

*Plantago* (Plantaginaceae)

Portulaceae

*Pterocarpus* (Fabaceae)

Polygalaceae

Rannulaceae

Rutaceae

Scrophulariaceae

*Tapiranthus* (Loranthaceae)

*Tetrapterum* (Pottiaceae)

*Tribulus* (Zygophylaceae)

Verbenaceae

**Group 1**

Poaceae

Cyperaceae

*Phragmites-type*

*Typha*

**Group 2**

Restionaceae

*Anthospermum*

Ericaceae

*Cliffortia*

*Stoebe/Elytropappus*-type

*Passerina*

*Artemisia*-type

*Pentzia*-type

**Group 3**

Aizoaceae

Cheno/Am

Asteroideae

# Chapter 4 Palynological evidence for Holocene climatic and oceanographic changes off western South Africa

Xueqin Zhao, Lydie Dupont, Enno Schefuß, Ilham Bouimetarhan and Gerold Wefer

MARUM - Center for Marine Environmental Sciences, University of Bremen, P.O. Box 330 440, D-28334, Bremen, Germany

**Published as:** Zhao X., Dupont L., Schefuß E., Bouimetarhan I., Wefer G., 2017. Quaternary Science Reviews 165, 88-101.

## 4.1 Abstract

Atmospheric and oceanographic interactions between the Atlantic and Indian Oceans influence upwelling in the southern Benguela upwelling system. In order to obtain a better knowledge of paleoceanographic and paleoenvironmental changes in the southern Benguela region during the Holocene, 12 marine surface sediment samples and one gravity core GeoB8331-4 from the Namaqualand mudbelt off the west coast of South Africa have been studied for organic-walled dinoflagellate cysts in high temporal resolution. The results are compared with pollen and geochemical records from the same samples. Our study emphasizes significantly distinct histories in upwelling intensity as well as the influence of fluvial input during the Holocene. Three main phases were identified for the Holocene. High percentages of cysts produced by autotrophic taxa like *Operculodinium centrocarpum* and *Spiniferites* spp. indicate warmer and stratified conditions during the early Holocene (9900-8400 cal. yr BP), suggesting reduced upwelling likely due to a northward shift of the southern westerlies. In contrast, the middle Holocene (8400-3100 cal. yr BP) is characterized by a strong increase in heterotrophic taxa in particular *Lejeunecysta paratenella* and *Echinidinium* spp. at the expense of autotrophic taxa. This indicates cool and nutrient-rich waters with active upwelling probably caused by a southward shift of the southern westerlies. During the late Holocene (3100 cal. yr BP to modern), *Brigantedinium* spp. and other abundant taxa interpreted to indicate fluvial nutrient input such as cyst of *Protoperidinium americanum* and *Lejeunecysta oliva* imply strong river discharge with high nutrient supply between 3100-640 cal. yr BP.

## 4.2 Introduction

The Benguela upwelling system along the west coast of southern Africa is one of four major upwelling systems in the world characterized by the transport of cold and nutrient-rich waters to the surface ocean (Nelson and Hutchings, 1983). The oceanography in the southern Benguela region extending along the west coast of South Africa from the Orange River mouth in the north to the south of the Cape of Good Hope is mainly controlled by the interaction of atmospheric and oceanic circulation (upwelling of sub-surface waters, entrainment of cold Antarctic waters, southeast trade winds, southern westerlies, and influences by the Agulhas Current). Water masses of the Benguela upwelling region are mainly from three different sources (Gordon et al., 1992): (1) cold and nutrient-rich South Atlantic central waters; (2) cold waters of the Antarctic Circumpolar Current; (3) warm and saline Indian Ocean waters derived from the Agulhas Current. The Agulhas leakage plays a crucial role in the global oceanic circulation by supplying warm and salty waters from Indian Ocean to the Atlantic Ocean along the southern tip of Africa, which may affect the intensity of the Atlantic meridional overturning circulation (Peeters et al., 2004; Weijer et al., 1999).

Investigations of the paleoceanographic conditions in this region are therefore crucial to provide information on past variability and mechanisms of the climate systems in South Africa. The variability of Agulhas leakage has been studied on different timescales in the Cape Basin and the Agulhas Bank (Caley et al., 2014; Dyez et al., 2014; Esper et al., 2004; Franzese et al., 2006; Petrick et al., 2015; Rau et al., 2002; Winter and Martin, 1990), however, the extent to which the Agulhas leakage did affect the southern Benguela region during the Holocene remains unclear. We focus in this study on the Namaqualand mudbelt off the west coast of South Africa which is located in the southern Benguela upwelling system (Figure 4.1). Information about the paleoceanographic conditions will allow to better understand the Holocene climate variability in South Africa and to investigate the signature of the Agulhas leakage to the southern Benguela upwelling system during the Holocene.

Unlike calcareous or siliceous biological remains which can be affected by dissolution, organic-walled dinoflagellate cysts (“dinocysts” here after) are composed of resistant organic matter and are generally well preserved in most sediments (Dale, 1996). Additionally, dinocyst species have different environmental preferences and their distribution in surface sediments has been shown to correlate well with sea surface conditions such as temperature, salinity, nutrient levels and productivity (e.g., Dale, 1996; Dale et al., 2002; de Vernal et al., 1994; Marret and Zonneveld, 2003; Zonneveld et al., 2013). Dinocysts, therefore, have become a valuable tool to reconstruct paleoenvironmental and paleoceanographic conditions especially in neritic (shallow marine environment on the continental shelf) highly productive environments (e.g., de Vernal et al., 1997; Pospelova et al., 2006, 2015; Verleye and Louwye,

2010). The modern dinocyst distribution off the west coast of South Africa has been studied by several authors (Davey, 1971; Davey and Rogers, 1975; Holzwarth et al., 2007; Wall et al., 1977; Zonneveld et al., 2001a). However, paleostudies of dinocysts in the southern Benguela upwelling region are mostly limited to Miocene, Pliocene and Pleistocene times (Esper et al., 2004; Petrick et al., 2015; Udeze and Oboh-Ikuenobe, 2005) and Holocene dinocyst records are scarce, even in the entire Benguela upwelling region. The early study of Davey and Rogers (1975) involved the dinocyst distribution of two traverses perpendicular to the west coast of southern Africa (the northern Sylvia Hill traverse and southern Orange River traverse). The dinocyst distribution results, in particular those of the latter traverse, are relevant to our study. The dinocyst assemblages of the Orange River traverse are dominated by *Spiniferites ramosus* and *Operculodinium centrocarpum* showing a trend of more *O. centrocarpum* and less *S. ramosus* further offshore. Davey and Rogers concluded in combination with the more detailed study of Davey (1971) that *O. centrocarpum* characterizes sediments beneath warm water associated with the westward-flowing warm water of the Agulhas rings, while *S. ramosus* is dominant in sediments beneath regions of upwelled cold and nutrient-rich waters. Dinocyst assemblages on the coast of western South Africa (Wall et al., 1977) contain high amounts of *Protoperidinium* species (called "*Peridinium*" by Wall et al.) inshore but are dominated by *O. centrocarpum* and *Spiniferites bulloideus* on the outer shelf and slope. Based on the surface sediments off the western coast of southern Africa, Zonneveld et al. (2001a) and Holzwarth et al. (2007) obtained datasets about the spatial distribution of dinocysts and their relationship with the local environmental conditions, which can be used for paleoceanographic reconstructions. At longer time scales, Esper et al. (2004) reconstructed variations in the Late Quaternary Agulhas retroflection on the basis of records of organic-walled and calcareous-walled dinoflagellate cysts, pollen and spores offshore of southwestern South Africa reflecting dynamic environmental changes driven by orbital forcing. Petrick et al. (2015) using a multiproxy approach demonstrated a complex interaction between influences of the Benguela upwelling and the Agulhas leakage. They also showed that there was no period in the late Pleistocene in which Agulhas leakage had been completely cut off.

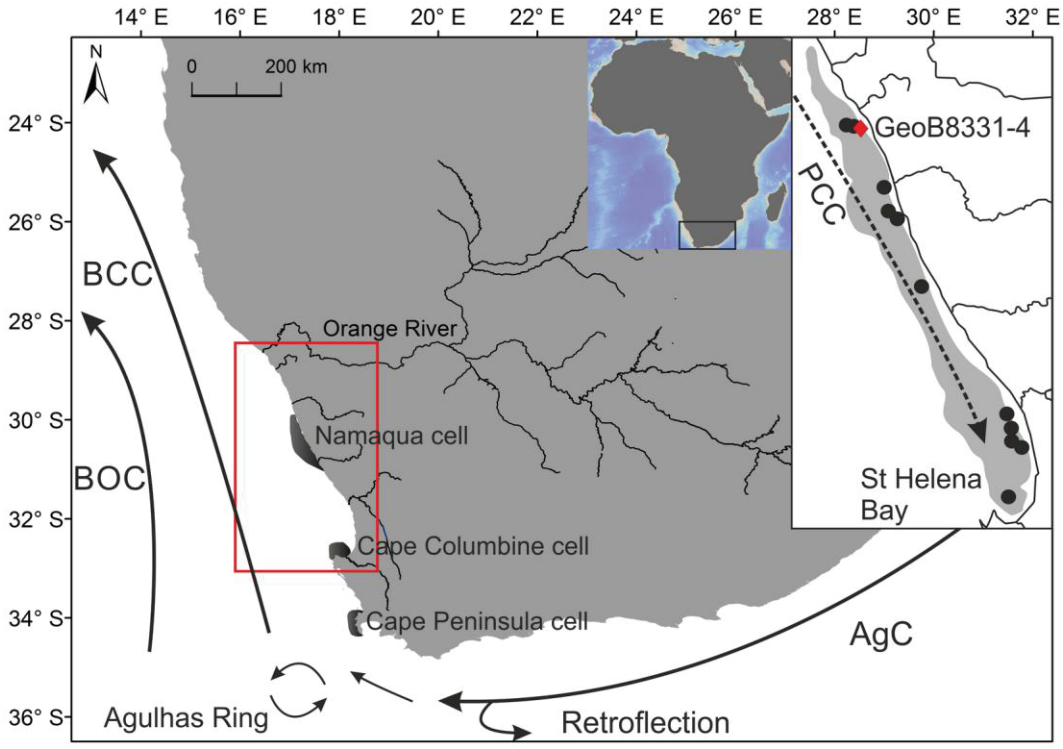


**Figure 4.1** Map of the research area showing the locations of 12 multicores (black dots) and the gravity core GeoB8331-4 (red diamond) retrieved from the Namaqualand mudbelt (grey shaded area in the upper right corner) off the west coast of South Africa. The arrows indicate the major oceanic surface current systems: BCC (Benguela Coast Current), BOC (Benguela Ocean Current), AgC (Agulhas Current), PCC (poleward countercurrent). The locations of three main upwelling cells in the southern Benguela region are denoted with black shading: Namaqua cell, Cape Columbine cell and Cape Peninsula cell.

Paleoceanographic reconstructions using dinocysts are often based on their modern geographic distributions and ecological affinities showing that different dinocyst associations characterize different systems (Bouimetarhan et al., 2009; Holzwarth et al., 2007, 2010; Lewis et al., 1990; Marret and de Vernal, 1997; Zonneveld et al., 2001a). To obtain reliable interpretations, it is essential to study the modern dinocyst distribution in marine surface sediments and the possible relationships with environmental factors. Therefore, we studied dinocyst distribution in marine surface sediments along the mudbelt to extend the modern dinocyst distribution (Holzwarth et al., 2007; Zonneveld et al., 2001a) to more coastal and shallower sites on the shelf (Figure 4.1). Then we present a dinocyst record at a millennial to centennial resolution from gravity core GeoB8331-4 covering the last 9900 years. This core has been retrieved from the northern Namaqualand mudbelt off the west coast of South Africa under the modern pathway of the cold northward-flowing Benguela Current (Figure 4.1). Additionally, published data such as pollen/spores, element ratio, total organic carbon (TOC), total inorganic carbon (TIC), biogenic silica (BSi) and alkenone-derived SSTs are

used for comparison. Our objectives are: (1) to qualitatively reconstruct Holocene paleoceanogaphic changes at the site; (2) to address the effects and intensity of Agulhas leakage; (3) to determine the possible mechanisms of paleoenvironmental variability in the southern Benguela region and its effects on the climate of South Africa during the Holocene.

## 4.3 Modern climatic and oceanographic systems

Today the climate system of southern Africa is controlled by the position and strength of the South Atlantic anticyclone and the Indian Ocean anticyclone (Shannon, 1985; Shannon and Nelson, 1996) (Figure 4.1). The pressure difference between the South Atlantic anticyclone and the continental pressure field causes alongshore southeast trade winds. The southeast trade winds drive an offshore, surface-drift inducing upwelling causing aridity in western southern Africa north of the Cape region. In the Cape region, moisture is mainly supplied by the southern westerlies during austral winter. Westward to south-westward directed offshore winds (known as Berg winds) are very limited because they are blocked by the southern westerlies and almost no dust plumes can be observed south of 28°S (Eckardt and Kuring, 2005).

The oceanography of the research area has been reviewed in detail by e.g., Nelson and Hutchings (1983), Peterson and Stramma (1991) and Shannon and Nelson (1996), (Figure 4.1). The oceanic circulation in the research area is dominated by the northward flowing Benguela Current (BC) stretching from 34°S to 15°S along the west coast of southern Africa. Two branches of the Benguela Current can be distinguished: the Benguela Coastal Current (BCC), flowing along the coast varying in depth from a few meters nearest to the coast to about 120 m along the outer shelf and the Benguela Oceanic Current (BOC), the north-westward flowing branch diverging from the coast at about 28°S. Below the BCC, there is a weak and seasonal poleward countercurrent. Our study sites are located on the 500 km long Namaqualand mudbelt (a Holocene terrigenous mud deposit) offshore of the west coast of South Africa extending from the Orange River mouth in the north (28°S) to St Helena Bay in the south (33°S). The sites lie under the southern part of the Benguela upwelling system driven by the alongshore trade winds which are controlled by position and intensity of the South Atlantic anticyclone (Schell, 1968). In the southern Benguela upwelling system, main upwelling of cold and nutrient-rich water originating from the body of the South Atlantic Central Water at depths of 150-330 m occurs during austral spring and summer (Shannon, 1985). Three upwelling cells with enhanced productivity can be distinguished: the Namaqua cell (30°S), the Cape Columbine cell (33°S) and the Cape Peninsula cell (34°S). During austral winter, when the South Atlantic anticyclone is far to the north, the southern westerlies are in their northernmost position. This leads to less upwelling in the southern Benguela

region. During austral summer, the poleward retreat of the South Atlantic anticyclone and the southern westerlies allow the influence of the southeast trade winds. They promote upwelling and water mixing processes, which increase productivity (Andrews and Hutchings, 1980; Hutchings et al., 2009).

At the southern boundary of the Benguela upwelling system, the relatively cool and oligotrophic waters of the South Atlantic Current and the cold waters of the Antarctic Circumpolar Current meet the south-westward flowing warm and saline waters of the Agulhas Current (AgC). Most of the AgC waters are retroflected to the south and east forming the Agulhas Return Current, while a small part of the AgC forms eddies and transports relatively warm and saline water from the Indian Ocean into the South Atlantic Ocean. This eddy transport is at a maximum during austral summers when the southern westerlies shift poleward and southeast trade winds coincide with maximal upwelling (Shannon and Nelson, 1996). When the AgC shoals against the Agulhas Bank during austral summers, Agulhas leakage may promote a stronger mixing between deep and surface waters between the Subtropical Front and the Cape of Good Hope (Cortese et al., 2004). This coincides with an increase of southern Benguela upwelling enhancing nutrient entrainment in the thermocline.

According to the World Ocean Atlas 2013 (WOA 2013), sea surface temperatures (SSTs) over the Namaqualand mudbelt range from 12.7 to 20.0°C during austral summers showing three minima at 29-30°S, 31-32°S and 33°S. SSTs during austral winters range from 12.0 to 16.0°C but with only two minima at 29-30°S and at 31-32°S. Similar variations are observed for sea surface salinities (SSSs) which range from 34.7 to 35.5 psu during austral summers with three minima at 29-30°S, 31-32°S and 33°S and from 34.2 to 35.4 psu during austral winters with only two minima at 29-30°S and at 31-32°S. During austral summer lower temperatures and salinities are observed in all three upwelling cells compared to other areas of the mudbelt.

The Orange River basin is the most important drainage system in southern Africa covering an area of about 950,000 $km^2$. The perennial Orange River arises in the Drakensberg Mountains of Lesotho running 2160 km westwards through South Africa to the Atlantic Ocean with a discharge of 11 $km^3/yr$ (Figure 4.1) (Milliman et al., 1995). Several lines of evidence indicate the strong influence of terrigenous input into the marine environment (Hahn et al., 2016; Heinrich et al., 2011; Mabote et al., 1997; Udeze and Oboh-Ikuenobe, 2005; Zhao et al., 2016a).

## 4.4 Materials and Methods

### 4.4.1 Materials

The 12 marine surface samples (Table 4.1, Figure 4.1) investigated in this study are from the upper 3 cm of the multicores which were obtained in January-February of 2003 during the M57/1 *Meteor* cruise (Schneider et al., 2003). The multicores are along a north-south transect of the Namaqualand mudbelt with water depths ranging from 20 to134 m. Dating of five multicores revealed modern ages suggesting that all surface sediments are deposited after the end of the 17$^{th}$ and probably no older than 10 years (Zhao et al., 2016a, 2016b). The gravity core GeoB8331-4 (29°08.12'S, 16°42.99'E, 887 cm long, at water depth of 97 m) was obtained on the same cruise from the northern mudbelt near the Orange River mouth consisting of olive brown mud from 887 to 15 cm and dark laminated layers within olive brown mud above 15 cm. The chronology of GeoB8331-4 has been published by Herbert and Compton (2007) and updated by Hahn et al. (2016), revealing that sediments were deposited since the early Holocene covering the last 9900 years (Figure 4.2).

**Table 4.1** Core sites, water depths and devices of 12 multicores and the gravity core GeoB8331-4. (Core locations are shown in Figure 4.1)

| Core name | Longitude (°E) | Latitude (°S) | Water depth (m) | Device |
|---|---|---|---|---|
| GeoB8333-1 | 16.61 | 29.12 | 20 | Multicore |
| GeoB8332-3 | 16.66 | 29.13 | 116 | Multicore |
| GeoB8331-2 | 16.71 | 29.14 | 88 | Multicore |
| GeoB8327-1 | 17.01 | 29.70 | 88 | Multicore |
| GeoB8329-1 | 17.03 | 29.93 | 111 | Multicore |
| GeoB8328-1 | 17.06 | 29.94 | 112 | Multicore |
| GeoB8325-1 | 17.28 | 30.60 | 39 | Multicore |
| GeoB8324-1 | 18.09 | 31.75 | 100 | Multicore |
| GeoB8321-1 | 18.12 | 31.86 | 104 | Multicore |
| GeoB8322-1 | 18.12 | 31.95 | 105 | Multicore |
| GeoB8323-1 | 18.22 | 32.03 | 90 | Multicore |
| GeoB8319-1 | 18.08 | 32.50 | 69 | Multicore |
| GeoB8331-4 | 16.72 | 29.14 | 97 | Gravity core |

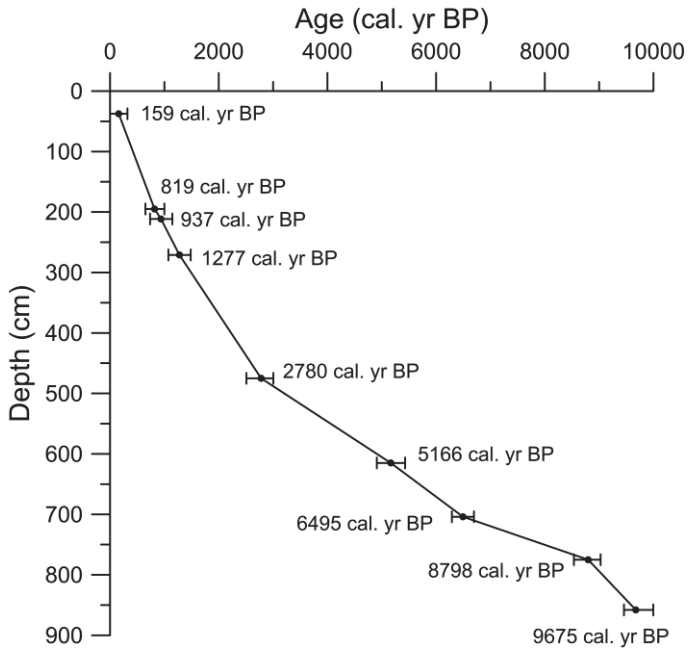


**Figure 4.2** Age-depth curve with calculated uncertainty (2σ) for the gravity core GeoB8331-4 (Herbert and Compton, 2007; Hahn et al., 2016). The median values of calibrated radiocarbon ages are shown in the figure.

### 4.4.2 Organic-walled dinoflagellate cyst analysis

A total of 50 samples were prepared for palynological analysis using the standard laboratory procedures (Faegri and Iversen, 1989), which involves decalcification with diluted HCl (~12%) and removal of silicates with HF (~40%). Two *Lycopodium* spore tablets (each containing 18584±372 markers) were added during the decalcification step. Samples were sieved ultrasonically to remove particles smaller than 10-15 µm. Samples were stored in water, mounted in glycerol and identified under a light microscope (magnification 400× and 1000×) for pollen, spores, dinocysts and fresh-water algae. At least 300 dinocysts were counted per sample; percentages of each taxon were calculated based on the total number of dinocysts. Sample volumes were measured using water displacement, so that concentration values (cysts/$cm^3$) could be calculated. Accumulation rate of dinocysts (cysts/$cm^2$/yr) was calculated by multiplying the dinocyst concentration (cysts/$cm^3$) by the sedimentation rate (cm/yr) for each sample. The percentage values of *Pediastrum*, *concentricystes* and forminiferal organic linings are calculated as the counts relative to total number of dinocysts. Pollen data for comparison are from the same set of samples (Zhao et al., 2016b). All counts of dinocysts are available and stored in the Pangaea database (www.pangaea.de).

The identification for the dinocyst taxa follows Head et al. (2005), Zonneveld (1997), DINOFLAJ3 (Williams et al., 2017), and the online modern dinoflagellate cyst determination

key of Zonneveld and Pospelova (2015). *Brigantedinium* spp. includes all the spherical brown cysts without spines ("round brown cysts"), which are not identified at the species level. This is because too often the orientation of the cysts on the microscope slides is such that species identification is not possible. *O. centrocarpum* includes morphotypes with short and reduced processes. Some specimens referable to the genus *Impagidinium* are grouped within *Impagidinium* spp. because the abundance in the fossil samples is very low and usually associated with open oceanic settings. Other taxa that were not identifiable at species level under the microscope due to unsuitable orientation, adherence of debris or the inability to spot typical taxonomic features were grouped in "spp." like *Spiniferites* spp. and *Echidinium* spp. The *Islandinium* spp. was grouped under *Echinidinium* (and not "spiny browns") to keep consistency with previous studies in the area (Zonneveld et al., 2001a; Holzwarth et al., 2007). "Identification of the *Polykrikos kofoidii* and *Polykrikos schwartzii* was made according to Head et al. (2005). The morphology of *Spiniferites* type 1 identified in this study is similar to that of *Spiniferites mirabilis* with the exception that the crown-like feature is missing. All dinocyst taxa identified in this study are listed in Table 4.2 along with their motile affinities after Williams et al. (2017). Records of dinocyst taxa contributing more than 1.5% at least once to the cyst assemblages are shown in Figures 4.4 and 4.5.

The ratio of autotrophic taxa over heterotrophic taxa (A/H ratio) is calculated as A/(H+A). Heterotrophic and autotrophic groups are more comprehensive and better linked to productivity than gonyaulacaceae and peridinieaceae groups, thus we think the A/H ratio better reflects productivity (e.g. Bringué et al., 2014; Verhoeven and Louwye, 2013). The low values of A/H ratio reflect higher production suggesting more upwelling. The P/D ratio is the ratio of counts of pollen over dinocysts, which can be used as a proxy for terrestrial input over marine primary productivity (e.g., McCarthy and Mudie, 1998). Taxa number that was estimated by the total number of identified taxa in each sample, is used as an estimate for dinocyst diversity.

**Table 4.2** List of dinoflagellate cyst taxa identified in this study (surface sediment samples of 12 multicores and the gravity core GeoB8331-4).

| Cyst name | Motile affinity | Abbreviation | Grouping |
|---|---|---|---|
| **Protoperidiniaceae** | | | |
| *Brigantedinium* spp. | *Protoperidinium* spp. | Bspp | *Brigantedinium* spp. |
| *Dubridinium caperatum* | *Preperidinium meunieri* | Dcap | |
| *Echinidinium aculeatum* | Protoperidiniaceae | Eacu | |
| *Echinidinium delicatum* | Protoperidiniaceae | Edel | |
| *Echinidinium transparantum* | Protoperidiniaceae | Etra | |

| | | | |
|---|---|---|---|
| *Echinidinium* spp. | Protoperidiniaceae | Espp | *Echinidinium* spp. |
| *Islandinium* spp. | *Protoperidinium* spp. | Ispp | *Echinidinium* spp. |
| *Lejeunecysta oliva* | *Protoperidinium* sp. | Loli | |
| *Lejeunecysta sabrina* | ? *Protoperidinium leonis* | Lsab | |
| *Lejeunecysta paratenella* | ? *Protoperidinium* sp. | Lpar | |
| *Cyst of Protoperidinium monospinum* | *Protoperidinium monospinum* | Pmon | *Echinidinium* spp. |
| *Cyst of Protoperidinium americanum* | *Protoperidinium americanum* | Pame | |
| *Protoperidinium* spp. | Peridiniaceae | Pspp | *Brigantedinium* spp. |
| *Quinquecuspis concreta* | ? *Protoperidinium leonis* | Qcon | |
| *Selenopemphix nephroides* | *Protoperidinium subinerme* | Snep | |
| *Selenopemphix quanta* | *Protoperidinium conicum* | Squa | |
| *Stelladinium robustum* | *Protoperidinium* sp. | Srob | |
| *Trinovantedinium applanatum* | *Protoperidinium pentagonum* | Tapp | |
| *Votadinium calvum* | *Protoperidinium oblongum* | Vcal | |
| *Votadinium spinosum* | *Protoperidinium claudicans* | Vspi | |
| *Xandarodinium xanthum* | *Protoperidinium divaricatum* | Xxan | |
| **Polykrikaceae** | | | |
| Cyst of *Polykrikos kofoidii* | *Polykrikos kofoidii* | Pkof | |
| Cyst of *Polykrikos schwartzii* | *Polykrikos schwartzii* | Psch | |
| **Gonyaulacaceae** | | | |
| *Bitectatodinium spongium* | Unknown | Bspo | |
| *Bitectatodinium tepikiense* | *Gonyaulax digitale* | Btep | |
| *Impagidinium aculeatum* | *Gonyaulax* sp. | Iacu | *Impagidinium* spp. |
| *Impagidinium* spp. | *Gonyaulax* spp. | Imsp | *Impagidinium* spp. |
| *Lingulodinium machaerophorum* | *Lingulodinium polyedrum* | Lmac | |
| *Nematosphaeropsis labyrinthus* | *Gonyaulax spinifera* | Nlab | |
| *Nematosphaeropsis rigida* | *Gonyaulax* sp. | Nrig | |
| *Operculodinium centrocarpum* | *Protoceratium reticulatum* | Ocen | |
| *Polysphaeridium zoharyi* | *Pyrodinium bahamense* | Pzoh | |
| *Spiniferites bentorii* | *Gonyaulax* sp. | Sben | |
| *Spiniferites bulloideus* | *Gonyaulax baltica* | Sbul | *Spiniferites* spp. |
| *Spiniferites elongatus* | *Gonyaulax elongata* | Selo | |
| *Spiniferites membranaceus* | *Gonyaulax membranacea* | Smem | |
| *Spiniferites mirabilis* | *Gonyaulax spinifera complex* | Smir | |
| *Spiniferites pachydermus* | *Gonyaulax* sp. | Spac | |

| | | | |
|---|---|---|---|
| *Spiniferites ramosus* | *Gonyaulax spinifera complex* | Sram | |
| *Spiniferites* spp. | *Gonyaulax* spp. | Sspp | *Spiniferites* spp. |

### 4.4.3 Statistical methods

Dinocyst assemblages of gravity core GeoB8331-4 have been statistically analyzed using the CANOCO software (Canonical Community Ordination: version 5) (Ter Braak and Šmilauer, 2012). The percentage data used for statistical analysis were not transformed. A detrended correspondence analysis (DCA) was done first to test the distribution of the dataset (unimodal or linear). The longest gradient of DCA analysis was found to be shorter than 3 standard deviations (1.6), indicating that a linear model is more suitable. Therefore, a Principal Component Analysis (PCA) and a Redundancy analysis (RDA) were performed to distinguish the samples and to determine the relationship between relative abundances of dinocyst taxa and selected paleoenvironmental variables (alkenone SSTs, TOC, TIC, BSi, K/Al and Fe/Ca) in samples from core GeoB8331-4. A Monte Carlo permutation test with 499 unrestricted permutations was used to determine the statistical significance of the variables. Paleoenvironmental variables with a *p*-value less than 0.05 were considered to be significantly related to dinocyst taxa data. The approach used for zonation of core GeoB8331-4 is based on the ordination of samples generated from RDA analysis. Zones defined by cluster analysis (not shown) were identical.

## 4.5 Results

All samples analyzed in this study including multicore surface samples and the samples from gravity core GeoB8331-4, reveal abundant and well-preserved dinocysts and other palynomorphs (e.g., pollen, spores, fresh-water algae, foraminiferal organic linings).

### 4.5.1 Marine surface sediments

Dinocyst concentrations of marine surface samples vary between ~6700 and ~31,000 cysts/cm$^3$ with an average of ~20,000 cysts/cm$^3$ (Figures 4.3 and 4.4). Dinocyst concentrations show a clear pattern increasing southwards, which suggest that the samples can be divided into three groups. In the northern mudbelt (29.12-29.14°S), the dinocyst concentrations remain below ~9800 cysts/cm$^3$ with a slight increase further offshore. In the central mudbelt (29.70-30.60°S), the dinocyst concentrations are much higher ranging from ~15,000-24,500 cysts/cm$^3$ with an average of ~19,700 cysts/cm$^3$. In the southern mudbelt, the dinocyst concentrations reach maximum values, which are never less than 24,000

cysts/cm$^3$ with an average of ~27,000 cysts/cm$^3$. However, the ratio of pollen/dinocyst (Figure 4.3) show high values in the northern (0.21-0.29) and southern (0.22-0.24) mudbelt with lower values in the central mudbelt (0.12-0.15).

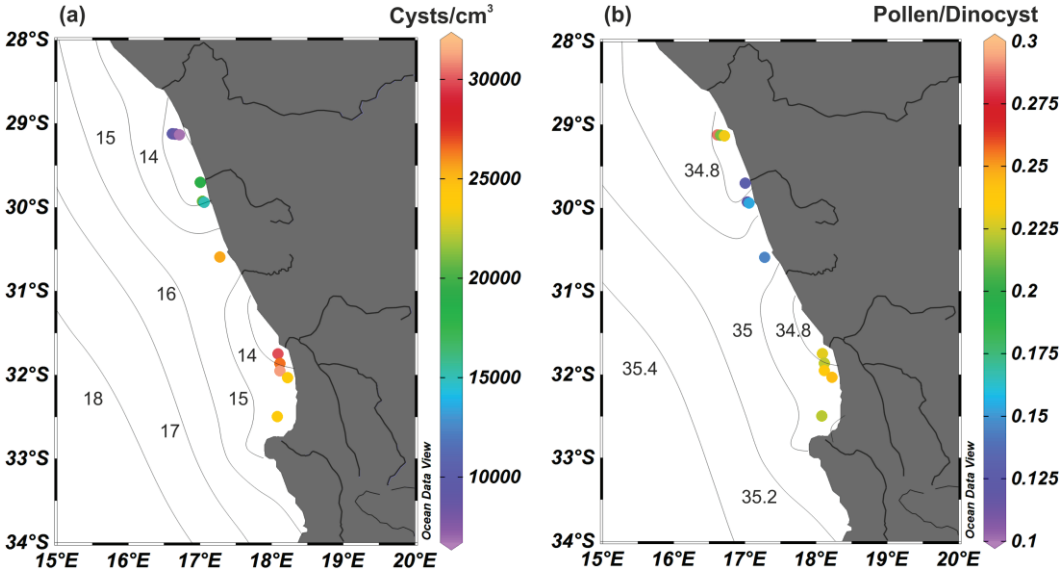


**Figure 4.3** Total dinoflagellate cyst concentration (cysts/cm$^3$) (a) and the ratio of pollen over dinoflagellate cyst (b) in12 multicore surface sediment samples. Annual sea surface temperature (line, °C) and annual sea surface salinity (line, psu) are presented in (a) and (b), respectively (Ocean Data View, U.S. NODC World Ocean Atlas 2013).

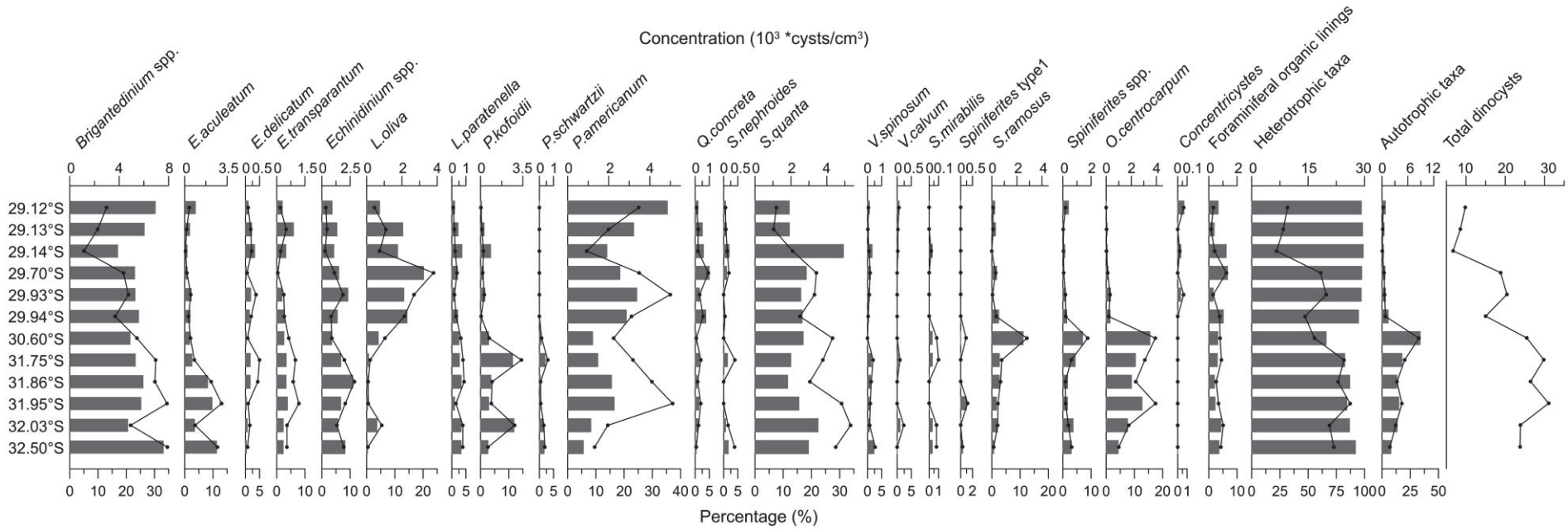


**Figure 4.4** Relative abundance (%, horizontal bars) and concentrations (cysts/cm$^3$, lines) of dinoflagellate cyst taxa in marine surface sediments (multicores) from the Namaqualand mudbelt, plotted against latitude. The percentage values of *concentricystes* and forminiferal organic linings are calculated as the counts relative to total number of dinocysts.

Marine surface samples along the mudbelt are dominated by heterotrophic taxa such as *Brigantedinium* spp., *Selenopemphix quanta* and cyst of *Protoperidinium americanum* with maximum percentages of ~33%, ~31% and ~35%, respectively (Figure 4.4). The central and northern mudbelt samples exhibit high percentages of *Lejeunecysta oliva* (up to 20%) while for the southern mudbelt the percentages of autotrophic taxa like *O. centrocarpum* (~4-15%), *Spiniferites* spp. (~0.6-7%) and *Spiniferites ramosus* (~0.7-11%) are higher. Some heterotrophic taxa, *Echidinium aculeatum* (~3-11%), *Polykrikos kofoidii* (~3-12%) and *Polykrikos schwartzii* (~0.3-2%) are more abundant in the southern mudbelt. However, most of the heterotrophic taxa, in particular *L. oliva*, cyst of *P. americanum* and *Quinquecuspis concreta* occur predominantly in the central and northern mudbelt. Additionally, the percentages and concentrations of *Brigantedinium* spp. and cyst of *P. americanum*, as well as the total dinocyst concentrations, show an increase offshore (for the northernmost three samples). *Concentricystes*, which are probably fresh-water algae (Mudie et al., 2010; Tang et al., 2013), occur mainly in the northern mudbelt and only in one sample of the central mudbelt.

### 4.5.2 Sediment core GeoB8331-4

Dinocysts are the most predominant palynomorphs in core GeoB8331-4 and a total of 61 cyst taxa (including types and morphotypes) were identified (Table 4.2). No reworked dinocyst from older material was observed in the core samples. Maximum dinocyst concentrations were recorded prior to ca. 8400 cal. yr BP (calibrated years before present (1950 AD)) varying from ~16,700 to ~32,400 cysts/cm$^3$ (average of ~24,000 cysts/cm$^3$). Dinocyst concentrations then quickly fell to low values fluctuating around ~11,800 cysts/cm$^3$ after 7600 cal. yr BP. The dinocyst accumulation rates showed high values ranging from ~1100 to 3100 cysts /cm$^2$/yr (average of ~2200 cysts /cm$^2$/yr) prior to ca. 8400 cal. yr BP, relatively low values between 8400 and 2650 cal. yr BP (fluctuating around 730 cysts /cm$^2$/yr), and steadily increased after 2650 cal. yr BP reaching maximum values (~3200 cysts /cm$^2$/yr) at about 500 cal. yr BP declining again to ~1400 cysts /cm$^2$/yr afterwards. Cyst concentrations and accumulation rates show similar trends as found in the percentage record (Figure 4.5).

The number of taxa in each sample ranged from 16 to 29, with an average of 24. The most dominant dinocyst taxa throughout the record were *Brigantedinium* spp. (max of ~41%), *Echinidinium* spp. (max of ~40%) and *S. quanta* (max of ~27%). Other dominant contributors include *O. centrocarpum* (max of ~38%), *Lejeunecysta paratenella* (max of ~39%), *Spiniferites* spp. (max of ~24%), cyst of *P. americanum* (max of ~32%), and *L. oliva* (max of ~19%). Dinocysts produced by Gymnodiniales (*P. kofoidii* and *P. schwartzii*) contribute less

than 9% of the assemblage having slightly higher values in the upper half of the record. Dinocysts produced by heterotrophic dinoflagellates dominate the cyst assemblage especially after 8400 cal. yr BP, while the contribution of dinocysts produced by autotrophic dinoflagellates is much higher before 8400 cal. yr BP representing up to 72% (average of ~58%) of the assemblage (Figure 4.5).

The results of RDA analysis using the percentages of individual dinocyst taxa show the first and second axis accounting for 34% and 12% of the total variance, respectively. The RDA results reveal that the gradients K/Al, Fe/Ca, TIC, SST and TOC significantly relate to more than 9% of the variance in the dinocyst association (Table 4.3, simple effects). However, after correcting for covariance only K/Al, SST and Fe/Ca can explain the cyst taxa variance significantly (Table 4.3, conditional effects). Figure 4.6 shows the ordination of all the samples and the most common cyst taxa with selected paleoenvironmental variables based on the first two axes (RDA1 and RDA2).

**Table 4.3** Percentage of variance explained by paleoenvironmental variables used in RDA analysis. Bold variables are significant at the 5% significance level ($P \leq 0.05$).

| | Simple effects | | Conditional effects | |
|---|---|---|---|---|
| Variable | Variance (uncorrected) | *P*-Value | Variance (corrected) | *P*-Value |
| K/Al | 0.27 | **0.002** | **0.27** | **0.002** |
| Fe/Ca | 0.23 | **0.002** | **0.06** | **0.002** |
| TIC | 0.18 | **0.002** | 0.006 | 0.79 |
| SST | 0.10 | **0.004** | **0.10** | **0.002** |
| TOC | 0.09 | **0.002** | 0.03 | 0.1 |
| BSi | 0.006 | 0.88 | 0.02 | 0.07 |

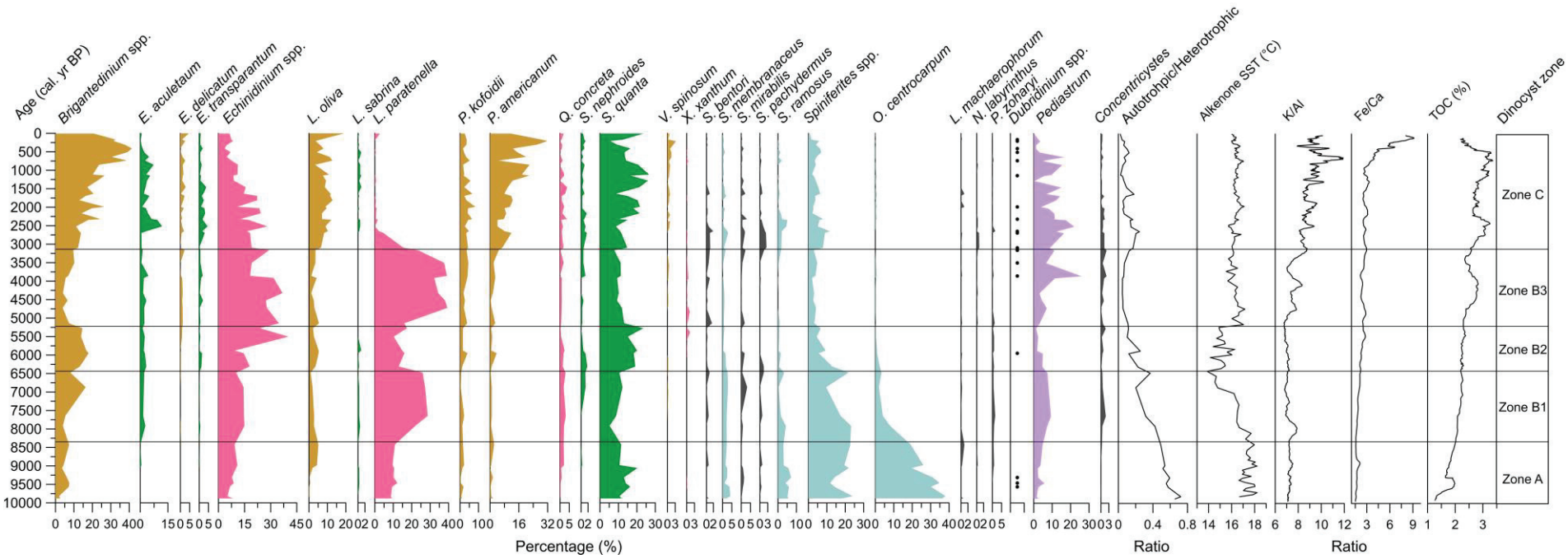


**Figure 4.5** Relative abundance (%) of dinoflagellate cyst taxa (scores >1.5% at least once) in gravity core GeoB8331-4 from the Namaqualand mudbelt. Taxa included in Groups 1, 2, 3 and 4 are filled in blue, brown, green and pink, respectively (see Section 4.2, the color grouping is based on the RDA ), fresh-water algae are filled in purple (the percentage values of *Pediastrum* and *concentricystes* are calculated as the counts relative to total number of dinocysts), other taxa are filled in black. Alkenone-derived sea surface temperature (SST, °C) (Leduc et al., 2010), element ratios of K/Al and Fe/Ca (Hahn et al., 2016) and total organic carbon (TOC, %) (Hahn et al., 2016) from the same core GeoB8331-4 are also shown.

Four different groups for cyst taxa and three dinocyst zones can be distinguished based on the RDA results:

Group 1: *O. centrocarpum*, *Spiniferites* spp., *S. ramosus* and *S. membranaceus*. These taxa are ordinated at the most positive side of axis 2 and negative side of axis 1, and they are most positively correlated to the TIC and SST gradients, and negatively correlated to K/Al and Fe/Ca.

Group 2: *Brigantedinium* spp., cyst of *P. americanum*, *L. oliva*, *V. spinosum*, *E. delicatum* and *P. kofoidii*. These taxa are ordinated at the most positive side of axis 1, which are positively related to the ratios of K/Al and Fe/Ca.

Group 3: *S. quanta*, *L. sabrina*, *E. aculeatum*, *E. transparantum* and *S. nephroides*. These taxa are grouped more or less in the center of axis 1 showing a positive relationship with TOC, and negatively correlated to SST.

Group 4: *Echinidinium* spp., *L. paratenella*, *Q. concreta* and *X. xanthum*, which are ordinated at the negative sides of both axes 1 and 2 showing a positive relationship with BSi and a negative relationship with K/Al and Fe/Ca.

Zone A (ca. 9900-8400 cal. yr BP, 878-763 cm) is characterized by autotrophic taxa accounting for up to 72% of the assemblage including *O. centrocarpum*, *Spiniferites* spp. (~12-24%) and *S. ramosus* (~3-7%). *O. centrocarpum*, reaching maximum values (~38%) at the base of the zone followed by a decline towards the end of the zone (~19%), while *Spiniferites* spp. fluctuates around 18% with the exception of low values (~13%) between 9600 and 9300 cal. yr BP. The high dinocyst concentrations in this zone are mainly attributable to cysts produced by autotrophic dinoflagellates. The heterotrophic taxa such as *S. quanta*, *Brigantedinium* spp., *Echinidinium* spp. and *L. paratenella* are also present with minor variations except for *S. quanta* which has two maxima around 9600 and 9100 cal. yr BP. Fresh-water algae like *Pediastrum* sp. and *Concentricytes* are present with low values (~1-6%, ~0-0.4%, respectively). This zone is marked by the most negative RDA1 and the highest positive RDA2 values (Figure 4.7).

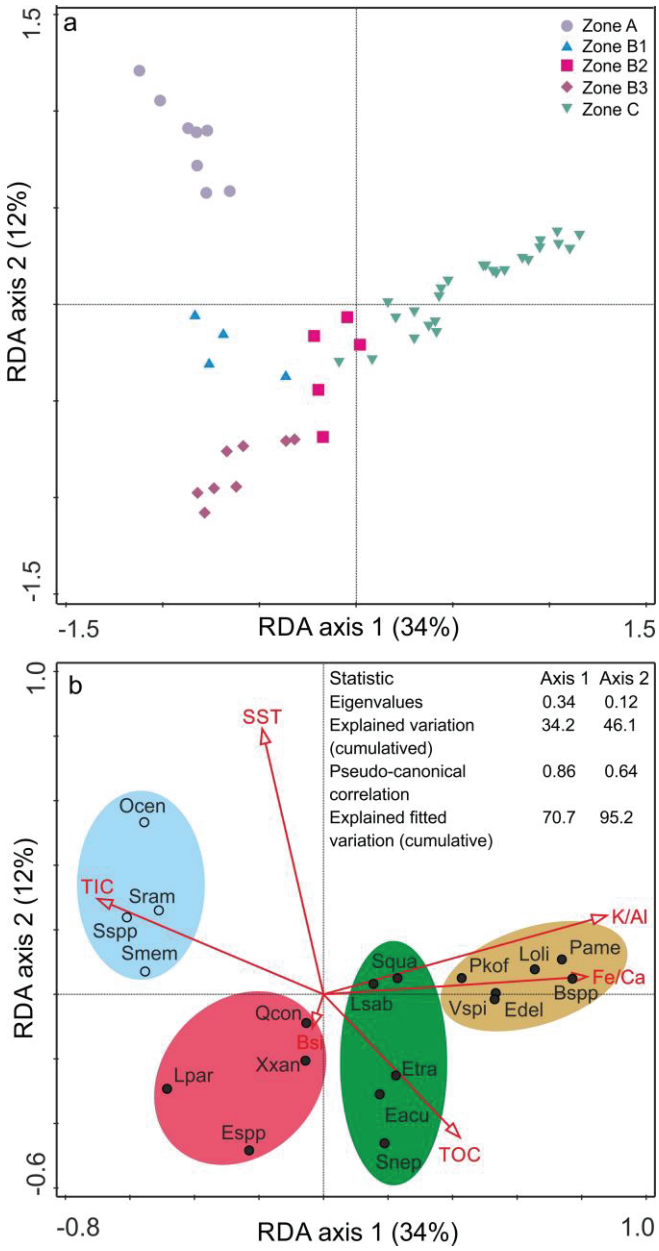


**Figure 4.6** (a) Ordination of samples from gravity core GeoB8331-4 generated from the Redundancy analysis (RDA) performed on dinoflagellate cyst percentages, colored symbols denote different zones. (b) Results of the Redundancy analysis (RDA) illustrating dinoflagellate cyst taxa in relation to palaeoenvironmental variables from gravity core GeoB8331-4. Abbreviations for cyst taxa of Group 1 (blue): Ocen (*Operculodinium centrocarpum*), Sram (*Spiniferites ramosus*), Sspp (*Spiniferites* spp.), Smem (*Spiniferites membranaceus*). Abbreviations for cyst taxa of Group 2 (brown): Pame (cyst of *Protoperidinium americanum*), Bspp (*Brigantedinium* spp.), Loli (*Lejeunecysta oliva*), Edel (*Echinidinium delicatum*), Vspi (*Votadinium spinosum*), Pkof (cyst of *Polykrikos kofoidii*). Abbreviations for cyst taxa of Group 3 (green): Squa (*Selenopemphix quanta*), Lsab (*Lejeunecysta sabrina*), Etra (*Echinidinium transparantum*), Eacu (*Echinidinium aculeatum*), Snep (*Selenopemphix nephroides*). Abbreviations for cyst taxa of Group 4 (pink): Lpar (*Lejeunecysta paratenella*), Espp (*Echinidinium* spp.), Xxan (*Xandarodinium xanthum*), Qcon (*Quinquecuspis concreta*).

Zone B1 (ca. 8400-6500 cal. yr BP, 763-702 cm) is marked by a continuous decline of autotrophic taxa shifting to an association dominated by heterotrophic taxa accounting for up to 80% of the assemblage. *O. centrocarpum* percentages quickly fall from ~19% to marginal occurrence around 6900 cal. yr BP. *Spiniferites* spp. also rapidly reaches low values with the exception of a high value around 6500 cal. yr BP. The noticeable feature of this zone is the accompanying rise of *L. paratenella* from an average of ~10% to ~26% and a slight increase of *Echinidinium* spp. from ~11% to ~15%, as well as high representations of *Pediastrum* sp. and *Concentricystes*. Zone B1 is characterized by a less negative RDA1 with a sharp shift of RDA2 to the negative values.

Zone B2 (ca. 6500-5300 cal. yr BP, 702-621 cm) is characterized by a quick decline of *L. paratenella* to an average of ~15% and relatively higher values of *Brigantedinium* spp. (average of ~15%) and *S. quanta* (average of ~19%). *Echinidinium* spp. values continue to increase from an average of ~14% to ~21% together with a decline in *Pediastrum* sp. Zone B2 is generally characterized by increasing RDA1 to almost zero and increasingly negative RDA2.

Zone B3 (ca. 5300-3100 cal. yr BP, 621-496 cm) is characterized by a second rise of *L. paratenella* to maximum values of ~39% accompanied by higher percentages of *Echinidinium* spp. (average of ~27%), while *Brigantedinium* spp. (average of ~7%) and *S. quanta* (average of ~10%) decrease to lower values. *Pediastrum* sp. and *Concentricystes* are much more prominent than in Zone B2. RDA1 falls to minimum values again and RDA2 reaches the most negative values in this zone.

Zone C (ca. 3100-present, 496-0 cm) is continuously dominated by heterotrophic taxa, however, the main feature of this period is a marked shift from the dominace of *L. paratenella* and *Echinidinium* spp. to other heterotrophic taxa including *Brigantedinium* spp. (~11-41%), *L. oliva* (~3-19%), cyst of *P. americanum* (~4-32%) and *S. quanta* (~5-27%) as well as *E. aculeatum* (~0.3-12%), *E. delicatum* (~0-4%), *E. transparantum* (~0.3-4%), *L. sabrina* (~0-1%) and *V. spinosum* (~0-3%). *Pediastrum* sp. show strong fluctuations and decline to low values after 640 cal. yr BP, while the representation of *Concentricystes* is lower relatively to Zone B3. This zone has the highest positive RDA1 values and generally increasing RDA2 values with minor fluctuations at the first half of the zone.

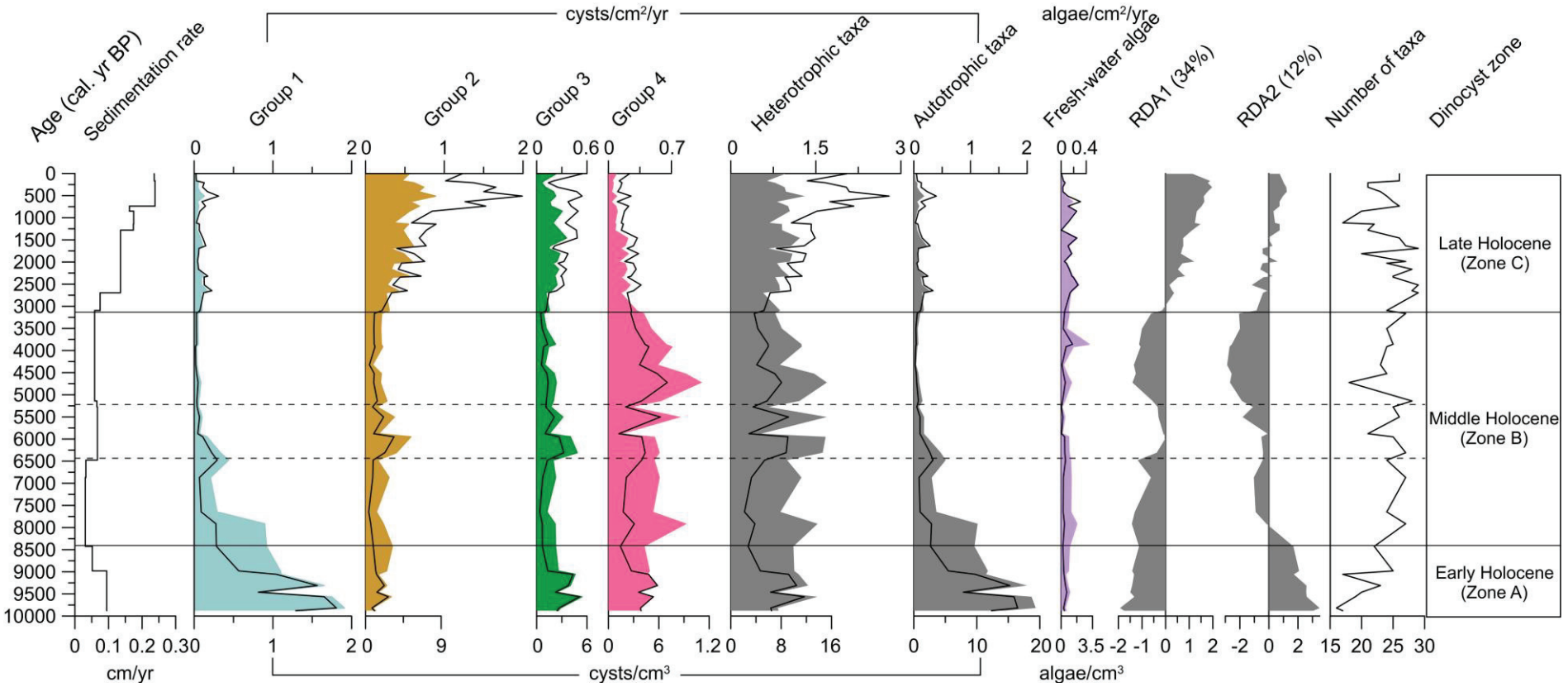


**Figure 4.7** GeoB8331-4: sedimentation rate (cm/yr), concentrations (cysts/cm$^3$, shadings) and accumulation rates (cysts/cm$^2$/yr, lines) of dinocyst Group 1 (*Operculodinium centrocarpum*, *Spiniferites ramosus*, *Spiniferites* spp., *Spiniferites membranaceus*, Group 2 (cyst of *Protoperidinium americanum*, *Brigantedinium* spp., *Lejeunecysta oliva*, *Echinidinium delicatum*, *Votadinium spinosum*, cyst of *Polykrikos kofoidii*, Group 3 (*Selenopemphix quanta*, *Lejeunecysta sabrina*, *Echinidinium transparantum*, *Echinidinium aculeatum*, *Selenopemphix nephroides*), Group 4 (*Lejeunecysta paratenella*, *Echinidinium* spp., *Xandarodinium xanthum*, *Quinquecuspis concreta*) and fresh-water algae, heterotrophic and autotrophic taxa; samples scores for RDA axes 1 and 2; number of taxa identified in each sample.

## 4.6 Discussion

Dinocyst assemblages are affected by various factors such as preservation, dilution and transport, which may bias the paleoceanographic and paleoenvironmental reconstruction. Although organic-walled dinocyst associations have been shown to be related to sea surface conditions such as temperature, salinity, nutrient levels and productivity, they may be altered pre- and post-depositionally due to species-selective degradation associated with variable bottom water oxygen concentrations (Zonneveld et al., 1997, 2001b, 2007, 2008). Preservation experiments have shown that the heterotrophic taxa such as the cysts of *Protoperidinium* species are more susceptible to oxygenic degradation in comparison to autotrophic taxa. The autotrophic taxa, such as *O. centrocarpum* and *Spiniferites* species, are moderately sensitive, and *Impagidinium* cysts are extremely resistant. The oxygen concentrations of bottom waters on the Namaqua shelf along the west coast of South Africa are highly depleted with values of 2 mL/L or less, especially during the upwelling season (Jarre et al., 2015; Monteiro and van der Plas, 2006). Our data exhibit high relative abundance of the “sensitive” protoperidiniaceans (composed mainly of *Brigantedinium* spp., *Echinidinium* spp., *S. quanta*) of up to 99% of the dinocyst assemblages in the surface sediment samples and 98% in the fossil samples. The high abundance of the protoperidiniaceans in combination with the lack of observed cyst degradation suggests that no significant selective dissolution of protoperidiniacean species over other species occurred in our study sites with the exception of one surface sample (30.60°S). This sample is characterized by a much lower content of heterotrophic taxa (~66%) in comparison with other surface samples from the mudbelt (average of ~92%). Considering that the sample is actually located under the Namaqua cell, we expect a similar assemblage as that of the other three samples (located at 29.70°S, 29.93°S and 29.94°S). The discrepancy might be attributed to somewhat higher bottom water oxygen concentrations at the site at 30.60°S (Jarre et al., 2015) enhancing selective degradation of heterotrophic taxa. Except for this site, the variation in relative abundances, concentrations and accumulation rates of heterotrophic taxa should reliably indicate the variability in nutrient availability and productivity of the overlying surface waters.

Due to the high sinking velocity of dinocyts and the relatively shallow water depth of the study area, the effect of lateral transport on dinocysts is probably small (Holzwarth et al., 2007). Still, the southern Benguela region is highly dynamic including surface and bottom currents. No reworked palynomorphs (including dinocysts, pollen and spores) were observed suggesting that the dinocyst signal is not disturbed by transport, re-suspension and re-deposition of the sediments. The lack of dinocysts characteristic of southern water masses such as *Selenopemphix antarctica* and *Impagidinium pallidum* indicates that large-scale

transport from the south with cold Subantarctic Water and Antarctic Bottom Water can be excluded (Holzwarth et al., 2007; Zonneveld et al., 2001a). However, the relatively high abundances of *O. centrocarpum* and *S. mirabilis* might be related to an effect of warm Indian Ocean waters via the Agulhas Current (Davey, 1971; Davey and Rogers, 1975). Dinocysts may also be transported by bottom currents such as the poleward countercurrent. However, the low occurrences of *Lingulodinium machaerophorum* and *Nematosphaeropsis labyrinthus* (Holzwarth et al., 2007; Zonneveld et al., 2001a) characterizing the northern Benguela region indicate negligible transport of dinocysts by bottom currents.

Other transport processes such as sediment relocation, winnowing and displacement within nepheloid layers are considered to be insignificant for the distribution of dinocysts in this shallow area (Holzwarth et al., 2007). The modern pollen distribution in the mudbelt indicates that sediments of the core GeoB8331-4 are affected by terrestrial input from the Orange River (Zhao et al., 2016a). The dilution with fluvial sediments could have affected the dinocyst accumulation rates but would have had little effect on the relative abundances in dinocyst associations. The variations of the dinocyst accumulation rates are greatly influenced by the sedimentation rates. The highest dinocyst accumulation rates (mainly of heterotrophic taxa) correspond to the lowest dinocyst concentrations around 500 cal. yr BP probably due to dilution by fluvial sediments. Variations in sedimentation rates of core GeoB8331-4 might be related to changes in sediment supply, accommodation space, or shifts in the mudbelt depo-center associated with sea level change. Sea level rose from ca. 45 m below mean sea level at 11,000 cal. yr BP to the maximum of around 3 m above present-day at ca. 6500 cal. yr BP and then dropped by around 3 m to its present level since 5500 cal. yr BP (Herbert and Compton, 2007 and references therein). This resulted in a landward shift of the mudbelt deposition from deeper water to shallow water. *Impagidinium* spp., which are usually restricted to the slope and open ocean sediments (Holzwarth et al., 2007; Zonneveld et al., 2001a), might reflect some information about sea level change. However, the very low presence of *Impagidinium* spp. (less than 1%) throughout the record as well as the small variability in pollen/dinocyst ratio prior to 6500 cal. yr BP suggest that sea level change during the Holocene did not significantly influence the dinocyst assemblages.

### 4.6.1 Modern dinocyst distributions in relation to environmental factors

Dinocyst concentrations in the marine surface samples of the mudbelt increase from north to south showing a similar pattern as the pollen concentrations (Zhao et al., 2016a). The same trend in the concentration of both terrestrial and marine elements suggests a predominant control by high sediment input of the Orange River diluting the samples nearest to its mouth.

Holzwarth et al. (2007) also found that the samples collected near the Orange River mouth contain less dinocysts in comparison to other samples from the mudbelt. However, since the dinocyst concentrations might also be related to sea surface productivity (Devillers and de Vernal, 2000), the gradient of dinocyst concentrations could also reflect the different levels of productivity between upwelling cells in the southern Benguela region. The four samples of the central mudbelt are located under the Namaqua cell and the five samples of the southern mudbelt, in particular the southernmost one, are affected by the Cape Columbine cell.

The sediments under the two upwelling cells differ in their dinocyst composition and near the Cape Columbine cell the number of taxa is higher. The autotrophic taxa, in particular *O. centrocarpum* and *Spiniferites* cysts, are much more abundant in the Cape Columbine cell than in the Namaqua cell. One possible explanation is the higher seasonality of the Cape Columbine cell where the stratified conditions during upwelling relaxation are favorable for the growth of autotrophic taxa. Another explanation is intrusion by warm water from Agulhas rings, which might reach the Cape Columbine cell but not as far north as the Namaqua cell. Although *O. centrocarpum*, *Spiniferites* spp. and *S. ramosus* are cosmopolitan taxa (Dale, 1996; Wall et al., 1977; Zonneveld et al., 2013), Davey (1971), Davey and Rogers (1975) and Wall et al. (1977) found high concentrations of *O. centrocarpum* in southern Benguela shelf sediments influenced by the warm Agulhas water. Published interpretations of the occurrence of *S. ramosus* are contradictory. Davey and Rogers (1975) proposed that *S. ramosus* was related to the occurrence of cold, upwelled nutrient-rich water, while Esper et al. (2004) inferred that extension of Agulhas waters might be responsible for high percentages of *S. ramosus*. The studies of modern distributions (Holzwarth et al., 2007; Zonneveld et al., 2001a), however, suggest that *S. ramosus* is characteristic for the region influenced by the Benguela Current rather than upwelling.

*P. kofoidii*, which has been related with nutrient-rich environments (Marret, 1994), has high percentages in the southern mudbelt together with *P. schwartzii* and *E. aculeatum*. Zonneveld et al. (2001a) concluded that high abundance of *P. kofoidii* probably reflect warm and nutrient-rich environments. *E. aculeatum* generally dominates in areas with mixed waters and enhanced nutrient concentrations associated with active upwelling (Marret and Zonneveld, 2003). Bouimetarhan et al. (2009) and Zonneveld et al. (2001a) found that this taxon might also be associated with river outflow.

*L. oliva* has often been used as a proxy for river outflow (Bouimetarhan et al., 2009; Holzwarth et al., 2007; Zonneveld et al., 2001a). It is indeed abundant in the northern mudbelt near the Orange River mouth but is even more abundant in the central mudbelt where only ephemeral rivers (e.g., Buffels and Groen River) reach the ocean. Cyst of *P. americanum* and *Q. concreta* which are also interpreted as proxies for fluvial influences

(Bouimetarhan et al., 2009; Holzwarth et al., 2007), have high percentages in both the northern and central mudbelt. However, Pospelova et al. (2008) found that the dominance of cyst of *P. americanum* is associated with high productivity and high nutrient levels rather than river discharge.

Other heterotrophic taxa including *Brigantedinium* spp., *Echinidinium* spp., *E. delicatum*, *E. transparantum* and *S. quanta* are evenly distributed in the mudbelt. *Brigantedinium* spp. generally dominates dinocyst associations in areas with nutrient-rich waters and active upwelling (Marret and Zonneveld, 2003; Pospelova et al., 2008; Zonneveld et al., 2013) containing lots of food such as diatoms (Wall et al., 1977). Although distinguishing between different taxa of *Echinidinium* and other “spiny brown cysts” is difficult (Radi et al., 2013), they have been illustrated to be the main components in the vicinity of active upwelling (Marret and Zonneveld, 2003; Wall et al., 1977). In contrast to core sediments, abundances of *L. paratenella* are low in the modern mudbelt sediments. This taxon has been found in Upper Cenozoic marine sediments from the continental slope and rise off New Jersey by de Verteuil (1996) and the marine surface sediments from Saldanha Bay near the Cape Columbine cell by Joyce et al. (2005), but ecological affinities are still uncertain.

We compare the dinocyst distribution in modern marine surface sediments from the Namaqualand mudbelt with the dinocyst groups classified by RDA analysis on samples from the core GeoB8331-4. From the ordination of the environmental factors, we infer that RDA 2 probably reflects the temperature gradients in nutrient-rich environments with higher values indicating warm waters, while RDA 1 might reflect the gradient of fluvial input with higher values indicating strong river discharge and freshwater influx (Figure 4.8). The taxa in Group 1 (blue) are positively related to SST and TIC and found in the southern mudbelt near the Cape Columbine cell, which is characterized by high seasonality and a possible influence of warm Agulhas waters. Group 1 is thus considered to be indicative of warm and stratified waters with high seasonality. Taxa forming Group 2 (brown) are positively related to the ratios of K/Al and Fe/Ca and have higher relative abundances in marine surface sediments influenced by the Orange River discharge. Group 2, therefore, probably indicate changes in fluvial influx. The taxa in Group 3 (green) are more or less evenly distributed in the mudbelt except for *E. aculeatum*, which has a higher presence in the southern mudbelt. This group, ordinated in the center of the axis RDA 1, might indicate an ecological transition from Group 1 to Group 2. The taxa of Group 4 (pink) have in common that they are not well represented in the marine surface sediments and do not show a clear trend along the mudbelt. Groups 3 and 4 have a positive relationship with TOC and a negative relationship with SST and might be indicative for cold and nutrient-rich waters linked to active upwelling.

Fresh-water algae such as *Pediastrum* sp. are not common in the marine surface sediments, but are well presented in the core samples. The variation of fresh-water algae, which were probably brought into the shallow marine environment by rivers, can provide some information about the river discharge (Lezine et al., 2005; Medeanic, 2006; Mudie et al., 2010).

### 4.6.2 Holocene oceanic environmental changes

To verify our interpretations, we cross-validate our results with a combination of different proxies and conduct an interdisciplinary approach for the reconstruction of paleoceanographic changes in our study area. This includes the results of pollen and elemental ratios of K/Al and Fe/Ca, TOC, TIC, and BSi content (%) from the same core (GeoB8331-4) after Hahn et al. (2016) and Zhao et al. (2016b). The alkenone-derived sea surface temperature (SST) record was established by Leduc et al. (2010) from sediments of the same core.

The aeolian transport of terrigenous material to the mudbelt is of minor importance (Eckardt and Kuring, 2005) and most of the sediment carried to the mudbelt by the Orange River is derived from Karoo sedimentary rocks. The erosion products of the Karoo sedimentary rocks contain abundant illite, K-feldspar, quartz and smectite showing high K concentration (Compton and Maake, 2007). Therefore, the ratio of K/Al has been suggested to indicate changes in K-rich fine sediments as well as the amount of fluvial input by the Orange River and other local rivers (Weldeab et al., 2013). Fe represents variations of the terrigenous fraction in the hemipelagic muds, whereas Ca is assumed to represent the marine carbonate content of the sediment. Thus, Fe/Ca has been used to trace changes in terrigenous input versus marine carbonate contributions (Adegbie et al., 2003; Collins et al., 2011; Govin et al., 2012).

#### *4.6.2.1 Warm and stratified water: local signal or strengthening of the Agulhas leakage?*

Prior to 8400 cal. yr BP, high relative abundance of Group 1 taxa suggests warm and stratified conditions, which is also shown by the maximum ratio of A/H and most positive RDA2 values (Figure 4.7). The most important question here is where the signal of the warm water is coming from: from a local source or from the Agulhas leakage? Our first argument is the high relative abundance of Fynbos vegetation (Figure 4.8g) prior to 7800 cal. yr BP suggesting warmer and more humid conditions along the west coast, in particular in the Cape region, and a northward shift of southern westerlies (Zhao et al., 2016b). The northward shift of the southern westerlies would suppress southeast trade winds and thus result in less upwelling, which is indicated by maximum SSTs during this period (Figure 4.8h)

(Leduc et al., 2010). As an alternative, we consider that *O. centrocarpum* might be associated with warm Agulhas waters (Davey, 1971; Davey and Rogers, 1975), which would imply that Agulhas water flowed as far north as site GeoB8331-4 at 29°S. The latter scenario is unlikely for two reasons. Firstly, a northward shift of the southern westerlies would block the inflow of the warm Agulhas water, which would reduce the Agulhas leakage resulting in lower SST. However, from modeling studies, it is not clear whether the shifts in the southern westerlies, southeast trade winds, as well as the local winds do have an effect on the strength of the Agulhas leakage (de Boer et al., 2013; Kohfeld et al., 2013). Secondly, eddies of the Agulhas Current do not propagate onto the continental shelf but are retained at the slope (Pilo et al., 2015). The cross-shelf distributions of temperature, salinity, water masses and dissolved oxygen in St. Helena Bay located in the southern part of the southern Benguela region showed different forcing mechanisms between the inshore and offshore environments. Upwelling dynamics dominate closer to the coast reflecting the seasonal nature of upwelling in the southern Benguela (Lamont et al., 2015). Therefore, we assume it is unlikely that our study area can receive warm water from the Agulhas leakage, and that the warm and stratified water conditions during this period should be attributed to reduced upwelling (or upwelling relaxation) as the result of a northward shift of the southern westerlies.

Maximum dinocyst concentrations, which mainly consist of autotrophic taxa during this period, suggest a full-oceanic environment with minor fluvial input suitable for dinoflagellates in general (Kim and Lim, 2014) and autotrophic dinoflagellates in particular. This inference is corroborated by high values of TIC (Figure 4.8k). The dominance of autotrophic taxa suggests that surface water conditions during this period are not favorable for the growth of heterotrophic dinoflagellates, which is probably due to low nutrient supply from both upwelling and terrestrial sources. Low nutrient availability is confirmed by the minimum values of TOC and BSi (Figure 4.8k and 4.8l) suggesting the absence of diatom blooms. Diatom analysis by Hahn et al. (2016) indeed found poor diatom preservation prior to 8,500 cal. yr BP. Low representation of fresh-water algae during this period also suggests a lower fluvial input by the Orange River corresponding with the low ratios of K/Al and Fe/Ca (Figure 4.8j). Herbert and Compton (2007) also found that the core site received relatively little terrestrial material during the early Holocene. Low river discharge of the Orange River during the early Holocene can be attributed to lower rainfall in the summer rainfall zone (SRZ) evidenced by both pollen and geochemical records (Hahn et al., 2016; Zhao et al., 2016b).

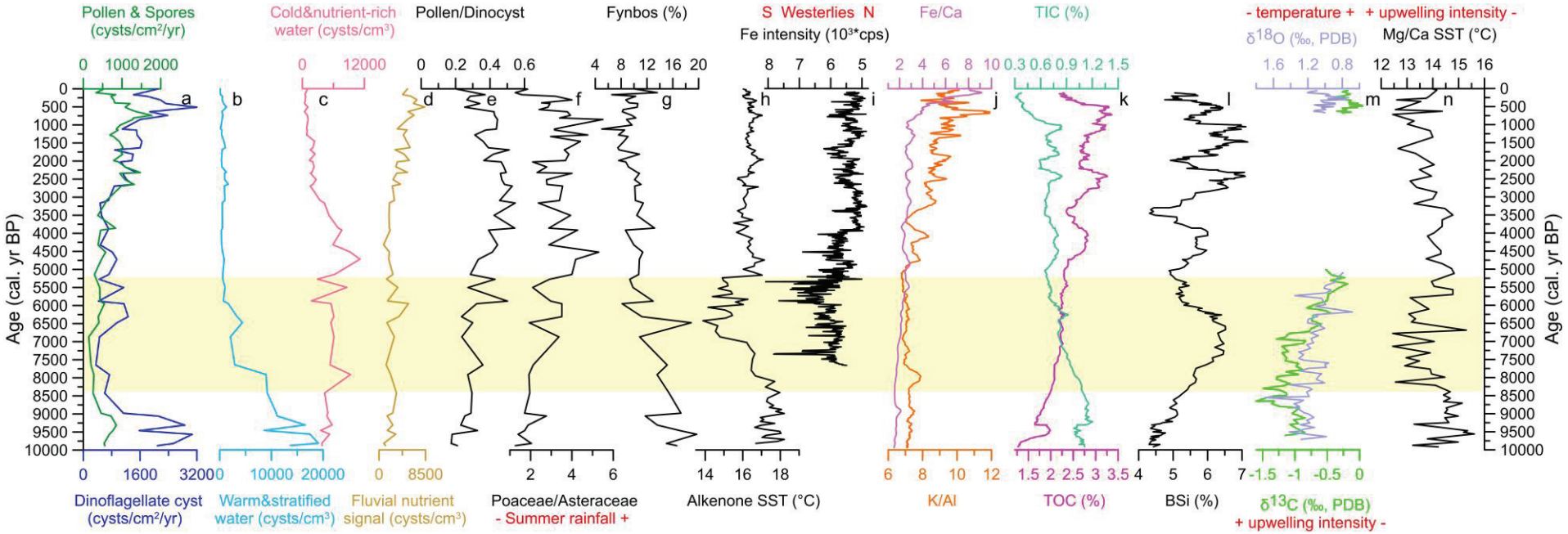


**Figure 4.8** A comparison of (a) accumulation rates (cysts/cm$^2$/yr) of pollen and spores (green, Zhao et al., 2016b) and dinoflagellate cyst (blue), (b) cysts from warm and stratified water, (c) cysts from cold and nutrient-rich water, (d) cysts indicating fluvial nutrient influence, (e) the ratio of pollen over dinoflagellate cysts (pollen/dinocyst), (f) the ratio of Poaceae over Asteraceae (Zhao et al., 2016b), (g) relative abundance of Fynbos pollen (%) (Zhao et al., 2016b), (h) alkenone-derived sea surface temperature (SST, °C) (Leduc et al., 2010), (i) iron concentrations (Fe intensity, cps) from the Chilean continental margin at 41°S (Lamy et al., 2001), (j) element ratios of K/Al (orange) and Fe/Ca (violet) (Hahn et al., 2016), (k) total organic carbon (TOC, %, magenta) and total inorganic carbon (TIC, %, green) (Hahn et al., 2016), (l) biogenic silica (BSi, %) (Hahn et al., 2016), (m) $\delta^{13}C$ (green) and $\delta^{18}O$ (blue) analyzed in *Neogloboquadrina pachyderma* (sinistra) in core GeoB8332-4 (Weldeab et al., 2013) and (n) Mg/Ca temperature record of ODP1084B (Farmer et al., 2005). With exception of the Chilean Fe record, $\delta^{13}C$ and $\delta^{18}O$ records in core GeoB8332-4 and Mg/Ca SST record of ODP1084B, all proxy have been determined on sediments of core GeoB8331-4.

#### *4.6.2.2 Cold and nutrient-rich water with active upwelling*

Since the early middle Holocene (from 8400 cal. yr BP), a notable change in the composition of the dinocyst assemblage shown by the decrease of the A/H ratio and the increase in number of taxa indicates a reorganization in the dinoflagellate assemblage (Figure 4.7). *O. centrocarpum*, which can be regarded as a cosmopolitan species, is presently dominant along the fringes of the Benguela upwelling (Zonneveld et al., 2013). High relative abundances of *O. centrocarpum* give way to a strong increase of *L. paratenella* (belonging to Group 4) after 8400 cal. yr BP possibly indicating a shift of the dominant environment from the edge of the upwelling (Petrick et al., 2015) to much colder and well mixed waters. However, it must be kept in mind that the ecological affinities of *L. paratenella* are not known in detail. A shift to colder and well mixed water is also indicated by most negative RDA2 values and a sharp decline in alkenone-derived SST (Leduc et al., 2010). Iron concentrations from the Chilean continental margin at 41°S provide a record of the latitudinal position of the southern westerlies suggesting a southward shift of the southern westerlies between 8400-5300 cal. yr BP (Figure 4.8i) (Lamy et al., 2001). Although a different behavior of the southern westerlies might exist in Africa, this record could still give us information about the latitudinal position of the southern westerlies. This southward shift would allow the southeastern trade winds to induce upwelling-related high productivity along the coast. Intensified upwelling with cold ocean surface waters caused dry conditions along the west coast of South Africa, which is indicated by an expansion of the Succulent Karoo at the expense of Fynbos vegetation (Zhao et al., 2016b). Between two maxima, low values of *L. paratenella* correspond to higher values of *Brigantedinium* spp. and *S. quanta*. This is probably due to minimum SST conditions since *Brigantedinium* spp. and *S. quanta* (*Protoperidinium* species) are known to be characteristic of cold and nutrient-rich waters (Bringué et al., 2014; Zonneveld et al., 2013). The timing of this upwelling intensification is consistent with cold intervals (8400-5800 cal. yr BP) seen in the northern Benguela region suggesting an increase in upwelling intensity in the entire BUS (Figure 4.8n) (Farmer et al., 2005). In contrast, Weldeab et al. (2013) proposed that upwelling gradually weakened during the period between 9000 and 5000 cal. yr BP (Figure 4.8m) based on data of the neighboring core GeoB8332-4. The inference of a weaker upwelling and warmer surface waters, which we dispute, are based on increasing $\delta^{13}C$ and decreasing $\delta^{18}O$ of *Neogloboquadrina pachyderma* (sinistral). We argue that the variability of $\delta^{13}C$ should be interpreted with caution due to the complex sources of dissolved inorganic carbon (DIC). Weldeab et al. (2013) presumed little influence of riverine DIC at the core site in comparison to remineralized marine organic carbon. The similarity of terrestrial plant waxes and their compound specific $\delta^{13}C$ compositions between the Orange River and mudbelt surface

sediments, however, indicates a considerable terrestrial contribution from the Orange River (Herrmann et al., 2016) corroborated by the pollen distribution in the mudbelt (Zhao et al., 2016a).

The general decline in dinocyst concentrations during this period probably indicates, on the one hand, a transition from an oceanic-like environment to a neritic environment similar to the present-day conditions (Kim and Lim, 2014). This is reflected by the shift from autotrophic to heterotrophic dinocyst taxa. TOC and BSi generally increase and TIC decreases indicating an increasing contribution of terrigenous material as the deposition center of the Orange River shifted to the core site when sea level rose (Compton, 2006; Hahn et al., 2016; Herbert and Compton, 2007). On the other hand, the decline in dinocyst concentrations might also be attributed by dilution of increased fresh-water influx (Piasecki, 1980). This is indicated by a higher representation of fresh-water algae and a steady increase of Fe/Ca. This interpretation is corroborated by the increase of Poaceae/Asteraceae ratio after 7600 cal. yr BP suggesting increased summer rainfall in the SRZ which would intensify the Orange River discharge.

#### *4.6.2.3 Warm and nutrient–rich water related to strong river discharge*

Since 3100 cal. yr BP, an increase in fluvial indicator taxa (Group 2) and some increase in fresh-water algae (Figure 4.7) indicate stronger river discharge until 640 years ago, when declines of *Pediastrum* sp., *Brigantedinium* spp., and cyst of *P. americanum* set in. Previous studies (Hahn et al., 2016; Mabote et al., 1997; Zhao et al., 2016a) suggest that terrigenous material in the northern mudbelt is mainly derived from the Orange River. Hence, the fresh-water influx from the Orange River is considered to be the main source of nutrients to the northern mudbelt. Increased summer rainfall in the SRZ indicated by high ratios of Poaceae/Asteraceae (Figure 4.8f) (Zhao et al., 2016b) between 2000-1000 cal. yr BP would have resulted in stronger river discharge as indicated by the increased K/Al ratios. The strong river discharge, in turn, brings more nutrients that favor the growth of heterotrophic dinoflagellates (e.g., *Brigantedinium* spp., cyst of *P. americanum*, *S. quanta*, *L. oliva* and *V. spinosum*), which are known to feed on other phytoplankton such as diatoms and small dinoflagellates (Graham and Wilcox, 2000). This interpretation is supported by the elevated contents of TOC and BSi between 3100 and 640 cal. yr BP.

On the other hand, high nutrient input coupled to more freshwater might lead to low cyst concentrations due to competition with diatoms during enhanced productivity (Dale and Fjellså, 1994). The lowest dinocyst concentrations are recorded in core GeoB8331-4 for the late Holocene when BSi reaches maximum values. After 640 cal. yr BP, the decline in the representation of heterotrophic taxa, fresh-water algae, as well as TOC and BSi would reflect

a decline in summer rainfall in the SRZ. This would bring lower river discharge to the northern mudbelt supplying less nutrients to the core site. However, the strong increase in Fe/Ca after 850 cal. yr BP might be attributed to the anthropogenic impact resulting in a tenfold increase in Orange River sediment loads during this period (Compton et al., 2010; Hahn et al., 2016). The temperature record at ODP1084B (Farmer et al., 2005) does not show a warming trend but an overall cooling trend after ca. 5000 cal. yr BP. Particularly, the large increase in relative abundance of *Neogloboquadrina pachyderma* (sinistral) after ca. 4000 cal. yr BP suggests intensified upwelling. Weldeab et al. (2013) provide evidence from Nd and Sr isotope records revealing humid conditions in the WRZ, which is consistent with pollen data of GeoB8331-4 showing relatively wet conditions for the last 700-200 years. The accompanied declining SST and strong upwelling off the Orange River mouth during this period are also proposed by Weldeab et al. (2013). They attribute it to the northerly position of the southern westerlies which may enhance the precipitation in the WRZ and block the inflow of the Agulhas leakage, thus reducing the SST and enhancing the upwelling. Conversely, our record indicates that the SST was dominated by upwelling dynamics rather than warm waters of Agulhas leakage which would unlikely have reached our core site (discussed in section 5.2.1).

## 4.7 Conclusions

Organic-walled dinoflagellate cysts from marine surface sediments and the gravity core GeoB8331-4 off southwestern Africa were used to reconstruct Holocene paleoceanographic and paleoenvironmental changes in the southern Benguela upwelling region. Our results highlight that it is unlikely that the core site off northern Namaqualand received warm waters via the Agulhas leakage during the Holocene. The changes in sea surface temperatures are mainly attributed to stronger/weaker upwelling intensity due to a southward/northward shift of the southern westerly wind belt, respectively. Freshwater influx by the Orange River was found to play a critical role in controlling paleo-productivity changes during the late Holocene (3100 cal. yr BP- 640 cal. yr BP). The findings based on dinocysts are supported by previous palaeoenviromental reconstructions using pollen and geochemical data from the same core, suggesting that the significantly different oceanographic conditions mainly shown by dinocyst results are associated with climate changes on land. This multiproxy approach indicates that the terrestrial and marine records generated from the same sediment sequence enable a better understanding of the mechanisms driving variability in the Holocene of South Africa and provide significant insight into land-ocean linkages.

## 4.8 Acknowledgements

This study was funded by the German Federal Ministry of Education and Research (BMBF) (Grant/Award Number: '03G0840A'). The investigations were conducted within the collaborative project 'Regional Archives for Integrated Investigations' (RAiN), which is embedded in the international research programme SPACES (Science Partnership for the Assessment of Complex Earth System Processes). We thank the captain, the crew, and the scientists of the *Meteor* cruise M57-1 for recovering the studied samples, and the GeoB core repository in MARUM (Center for Marine Environmental Sciences) for retaining the samples. Thanks to GLOMAR (Bremen International Graduate School for Marine Sciences) for supporting the first author's PhD project. We would like to thank Karin Zonneveld for her help with the dinoflagellate cyst identification. Gesine Mollenhauer and Nicole Herrmann are thanked for helpful discussion. We thank the two anonymous reviewers for their helpful and constructive comments.

# Chapter 5 Synthesis and outlook

## 5.1 Synthesis

The main aim of this thesis was to investigate the Holocene palaeoclimatic, palaeovegetation and palaeoceanographic changes in South Africa and the southern Benguela upwelling system in order to better understand the mechanisms of climate and oceanography evolution in this region. This thesis was based on records of pollen, microcharcoal and organic-walled dinocysts of 12 marine surface sediment samples and two marine sites (two gravity cores and two multicores) retrieved from the Namaqualand mudbelt offshore of the west coast of South Africa.

Our investigation on spatial pollen distribution in marine surface sediments along the Namaqualand mudbelt (Chapter 2) indicates representation of different vegetation communities in western South Africa. Pollen concentrations show a marked north-south increased gradient. This is partly correlated with the latitudinal vegetation biomass changes (from north to south, Desert-Succulent Karoo-Fynbos), while the low pollen concentration in the northern mudbelt is probably more the effect of dilution with silt and clay from the Orange River. The distinctive pollen composition in the mudbelt surface sediments suggests that the Orange River which flows mostly through the SRZ is a major contributor of pollen to the northern mudbelt, while to the southern mudbelt pollen is probably transported by winds and rivers from the WRZ. These conclusions are supported by the fossil pollen compositions in two marine gravity cores from the northern and southern mudbelt, respectively, demonstrating that pollen records of marine sediments in the mudbelt have the potential to be a tool for palaeovegetation reconstruction in this region.

Both pollen (Chapter 3) and organic-walled dinocysts (Chapter 4) records display three main periods during the Holocene indicating contrasting climate development between the WRZ and SRZ of South Africa as well as significantly distinct oceanographic conditions in the southern Benguela upwelling system. The first period occurred between ca. 9900- 7800 cal. yr BP characterized by lower summer rainfall with less grass in the SRZ but relatively wet conditions with the presence of Renosterveld vegetation in the WRZ. Warm and stratified waters in the southern Benguela upwelling system during this period were indicated by high abundance of autotrophic taxa, which was probably the result of reduced upwelling due to the northward position of the southern westerlies. The second period occurred between ca.7800-2400 cal. yr BP when a higher summer rainfall with more grasses dominated in the SRZ, while warmer and drier conditions prevailed in the WRZ indicated by the decline of Fynbos vegetation accompanied with an expansion of Succulent Karoo vegetation. The

higher summer rainfall was attributed to increased austral summer insolation toward the middle Holocene. Drier conditions in the WRZ were possibly affected by a southward shift of the southern westerlies. This was supported by the dinocyst records characterized by high abundance of active upwelling-related taxa and the quick decline of stratified water-related taxa. The southward shift of the southern westerlies during this period would not suppress southeast trade winds, and thus induce an upwelling-related high productivity. The last period (ca. 2400 cal. yr BP-modern) showed a more stable climate in the WRZ in comparison to that of the SRZ with higher aridity in particular after 850 cal. yr BP. Meantime, a strong river discharge with high nutrient supply from the Orange River was indicated by high representations of fluvial-related taxa during this period until 640 cal. yr BP. This corroborates the quick decline of grass pollen suggesting decreased summer rainfall in the SRZ and hereafter lower river discharge of the Orange River.

Therefore, the specific research questions addressed at the beginning of this thesis could be answered:

(1) What are the possible sources of mudbelt pollen and to what degree can pollen distribution of the mudbelt reflect the adjacent continental vegetation?

There are three different pollen sources from north to south of the mudbelt: for the northern mudbelt, the Orange River is the major pollen source; for the central mudbelt, offshore berg winds and local ephemeral Namaqualand rivers have a large contribution in comparison to the Orange River; for the southern mudbelt, the Fynbos vegetation is the main pollen source. The distinctive pollen spectra reflect a good correlation with the extend of the terrestrial biomes, suggesting that pollen records from marine sediments in the mudbelt can be utilized as a reliable tool for the palaeovegetation reconstruction in this region. Please see details in Chapter 2.

(2) How did the Holocene vegetation and climate vary in the winter and summer rainfall zones of South Africa?

A high temporal resolution Holocene vegetation and hydrological variability in the two rainfall zones was reconstructed, please see details in Chapter 3.

(3) Were the variabilities in the two zones consistent? If not, what were their mechanisms, respectively?

Apparently contrasting climate developments were detected in the two rainfall zones. For the SRZ, the higher/lower rainfall conditions were mainly dominated by the higher/lower austral summer insolation, while for the WRZ, it is more attributable to the northward/southward position of the southern westerlies. Please see details in Chapter 3.

(4) How was the land-sea interaction during the Holocene?

According to an interdisciplinary study combining the analysis of pollen, dinoflagellate cysts and geochemical data, a clear link was found showing significantly distinct oceanographic conditions associated with climate changes on land. During the early Holocene, a weak upwelling was detected probably caused by a northward position of the southern westerlies, which induces relatively wet conditions in the WRZ indicated by the presence of Renosterveld vegetation. Towards the middle Holocene, the southward shift of the southern westerlies gave way to the prevailing southeast trade winds in the southern Benguela region inducing active upwelling which caused drier conditions in the WRZ. This was also shown by a decline of Fynbos vegetation accompanied with an increasing Succulent Karoo vegetation in the WRZ. During the early period of late Holocene, higher summer rainfall in the SRZ indicated by abundant grasses resulted in a strong river discharge of the Orange River which was also indicated by high representation of fluvial-related taxa. Therefore, terrestrial and marine records generated from the same sediment sequence enable better understanding of the mechanisms driving Holocene climate variability in South Africa and provide significant insight into the land-ocean linkages.

## 5.2 Outlook

The fourth manuscript based on organic-walled dinocyst records of gravity core GeoB8323-2 for the last 2300 years is currently in preparation. The preliminary results probably indicate an unparalleled development of oceanographic conditions between the southern and northern part of the southern Benguela upwelling system. The possible mechanisms might need more investigation.

Although a good spatial pollen distribution along the mudbelt was presented in this thesis which will be valuable for later palynological studies in southern Africa, only 12 marine surface sediments in the inner shelf (mudbelt) along the west coast of South Africa were investigated. Therefore, to better reconstruct the palaeoclimate of southern Africa and fully understand the correlation between terrestrial and marine archives, it is necessary to study more marine surface sediments (including more samples from the mudbelt and extension to the middle and outer shelf) as well as more terrestrial surface sediments over South Africa in particular along the west coast and the Orange River.

Due to the age limitation of the gravity core GeoB8323-2, only the period for the last 2200 years is available for the regional comparison with the gravity core GeoB8331-4. Concerning the similarity in dinocyst assemblage of the lower part (227-285 cm) in GeoB8323-2 with the lowest part (ca. 9900-8400 cal. yr BP) of that in GeoB8331-4, our initial idea was that the

sediment sequence from 227 to 285 cm in GeoB8323-2 could be matched to the lower sequence of GeoB8331-4. Unfortunately, the absence of molluscs below 227 cm in the core GeoB8323-2 made it impossible to establish a new age model. The $^{14}C$ dates based on bulk sediment TOC are ca. 500 years old compared to the ages based on molluscs, which is not ideal for the age model establishment. Therefore, to fully obtain a regional comparison between the SRZ and WRZ, high-resolution and long continuous marine records in the southern mudbelt covering the whole Holocene should be retrieved in a future expedition.

In this thesis, the spatial dinocyst distribution in marine surface sediments and fossil dinocyst records were investigated only qualitatively. Concerning the quantitative reconstruction with the Modern Analogue Technique in other ocean areas, it would be interesting to first establish a modern dinocyst dataset and then apply it to our fossil records.

# References


Adegbie, A., Schneider, R., Röhl, U., Wefer, G., 2003. Glacial millennial-scale fluctuations in central African precipitation recorded in terrigenous sediment supply and freshwater signals offshore Cameroon. Palaeogeography, Palaeoclimatology, Palaeoecology 197, 323-333.

Andrews, W.R.H., Hutchings, L., 1980. Upwelling in the Southern Benguela Current. Progress in Oceanography 9, 1-81.

Baker, A., Routh, J., Blaauw, M., Roychoudhury, A.N., 2014. Geochemical records of palaeoenvironmental controls on peat forming processes in the Mfabeni peatland, Kwazulu Natal, South Africa since the Late Pleistocene. Palaeogeography, Palaeoclimatology, Palaeoecology 395, 95-106.

Basson, M., Theron, T., Little, P., Luger, M., 1998. Olifants/Doring River Basin study: main report. Report PG000/00/0198.

Baxter A.J., 1996. Late Quaternary Palaeoenvironments of the Sandveld, Western Cape Province, South Africa. PhD Thesis, University of Cape Town, South Africa.

Baxter, A.J., Meadows, M.E., 1994. Palynological evidence for the impact of colonial settlement within lowland Fynbos: A high-resolution study from the Verlorenvlei, southwestern Cape Province, South Africa. Historical Biology 9, 61-70.

Berger, A., Loutre, M.F., 1991. Insolation values for the climate of the last 10 million years. Quaternary Science Reviews 10, 297-317.

Biastoch, A., Boning, C.W., Schwarzkopf, F.U., Lutjeharms, J.R.E., 2009. Increase in Agulhas leakage due to poleward shift of Southern Hemisphere westerlies. Nature 462, 495-498.

Birch, G., Day, R., Du Plessis, A., 1991. Nearshore Quaternary sediments on the west coast of southern Africa. Bulletin of the Geological Survey of South Africa 101.

Birch, G.F., 1977. Surficial sediments on the continental margin off the west coast of South Africa. Marine Geology 23, 305-337.

Bonnefille, R., Riollet, G., 1980. Pollen des savanes d'Afrique orientale (in French). Éditions du Centre national de la recherche scientifique, Paris.

Bouimetarhan, I., Marret, F., Dupont, L., Zonneveld, K., 2009b. Dinoflagellate cyst distribution in marine surface sediments off West Africa (17–6°N) in relation to sea-surface conditions, freshwater input and seasonal coastal upwelling. Marine Micropaleontology 71, 113-130.

Bousman, B., Scott, L., 1994. Climate or overgrazing?: the palynological evidence for vegetation change in the eastern Karoo. South African Journal of Science 90, 575-578.

Bousman, C.B., 1998. The Chronological Evidence for the Introduction of Domestic Stock into Southern Africa. African Archaeological Review 15, 133-150.

Bredenkamp, G., Granger, J.E., van Rooyen, N., 1996. Vegetation of South Africa, Lesotho and Swaziland. Department of Environmental Affairs & Tourism, Pretoria.

Breman, E., Gillson, L., Willis, K., 2012. How fire and climate shaped grass-dominated vegetation and forest mosaics in northern South Africa during past millennia. The Holocene 22, 1427-1439.

Brook, G.A., Scott, L., Railsback, L.B., Goddard, E.A., 2010. A 35 ka pollen and isotope record of environmental change along the southern margin of the Kalahari from a stalagmite and animal dung deposits in Wonderwerk Cave, South Africa. Journal of Arid Environments 74, 870-884.

Caley, T., Peeters, F.J.C., Biastoch, A., Rossignol, L., van Sebille, E., Durgadoo, J., Malaize, B., Giraudeau, J., Arthur, K., Zahn, R., 2014. Quantitative estimate of the paleo-Agulhas leakage. Geophysical Research Letters 41, 1238-1246.

Campbell, B.M., Moll, E.J., 1977. The forest communities of Table Mountain, South Africa. Vegetatio 34, 105-115.

Chase, B.M., Boom, A., Carr, A.S., Meadows, M.E., Reimer, P.J., 2013. Holocene climate change in southernmost South Africa: rock hyrax middens record shifts in the southern westerlies. Quaternary Science Reviews 82, 199-205.

Chase, B.M., Lim, S., Chevalier, M., Boom, A., Carr, A.S., Meadows, M.E., Reimer, P.J., 2015. Influence of tropical easterlies in southern Africa's winter rainfall zone during the Holocene. Quaternary Science Reviews 107, 138-148.

Chase, B.M., Meadows, M.E., 2007. Late Quaternary dynamics of southern Africa's winter rainfall zone. Earth-Science Reviews 84, 103-138.

Chase, B.M., Meadows, M.E., Carr, A.S., Reimer, P.J., 2010. Evidence for progressive Holocene aridification in southern Africa recorded in Namibian hyrax middens: Implications for African Monsoon dynamics and the ‘‘African Humid Period’’. Quaternary Research 74, 36-45.

Chase, B.M., Meadows, M.E., Scott, L., Thomas, D.S.G., Marais, E., Sealy, J., Reimer, P.J., 2009. A record of rapid Holocene climate change preserved in hyrax middens from southwestern Africa. Geology 37, 703-706.

Chase, B.M., Scott, L., Meadows, M.E., Gil-Romera, G., Boom, A., Carr, A.S., Reimer, P.J., Truc, L., Valsecchi, V., Quick, L.J., 2012. Rock hyrax middens: A palaeoenvironmental archive for southern African drylands. Quaternary Science Reviews 56, 107-125.

Chase, B.M., Thomas, D.S.G., 2006. Late Quaternary dune accumulation along the western margin of South Africa: distinguishing forcing mechanisms through the analysis of migratory dune forms. Earth and Planetary Science Letters 251, 318-333.

Chevalier, M., Chase, B.M., 2015. Southeast African records reveal a coherent shift from high- to low-latitude forcing mechanisms along the east African margin across last glacial–interglacial transition. Quaternary Science Reviews 125, 117-130.

Clark, J.S., 1988. Stratigraphic charcoal analysis on petrographic thin sections: application to fire history in northwestern Minnesota. Quaternary Research 30, 81-91.

Clark, R.L., 1982. Point count estimation of charcoal in pollen preparations and thin sections of sediments. Pollen et spores 24, 23-35.

Cockcroft, M.J., Wilkinson, M.J., Tyson, P.D., 1987. The application of a present-day climatic model to the late Quaternary in southern Africa. Climatic Change 10, 161-181.

Coetzee, J., 1976. A report on a pollen analytical investigation of recent river mouth sediments on the South West African coast. Palaeoecology of Africa 9, 131-135.

Collins, J.A., Schefuß, E., Govin, A., Mulitza, S., Tiedemann, R., 2014. Insolation and glacial–interglacial control on southwestern African hydroclimate over the past 140 000 years. Earth and Planetary Science Letters 398, 1-10.

Collins, J.A., Schefusz, E., Heslop, D., Mulitza, S., Prange, M., Zabel, M., Tjallingii, R., Dokken, T.M., Huang, E., Mackensen, A., Schulz, M., Tian, J., Zarriess, M., Wefer, G., 2011. Interhemispheric symmetry of the tropical African rainbelt over the past 23,000 years. Nature Geoscience 4, 42-45.

Compton, J.S., 2006. The mid-Holocene sea-level highstand at Bogenfels Pan on the southwest coast of Namibia. Quaternary Research 66, 303-310.

Compton, J.S., Herbert, C.T., Hoffman, M.T., Schneider, R.R., Stuut, J.-B., 2010. A tenfold increase in the Orange River mean Holocene mud flux: implications for soil erosion in South Africa. The Holocene 20, 115-122.

Compton, J.S., Maake, L., 2007. Source of the suspended load of the upper Orange River, South Africa. South African Journal of Geology 110, 339-348.

Cooremans, B., 1989. Pollen production in central southern Africa. Pollen et spores 31, 61-78.

Cortese, G., Abelmann, A., Gersonde, R., 2004. A glacial warm water anomaly in the subantarctic Atlantic Ocean, near the Agulhas Retroflection. Earth and Planetary Science Letters 222, 767-778.

Cowling, R.M., Cartwright, C.R., Parkington, J.E., Allsopp, J.C., 1999a. Fossil wood charcoal assemblages from Elands Bay Cave, South Africa: implications for Late Quaternary vegetation and climates in the winter-rainfall Fynbos biome. Journal of Biogeography 26, 367-378.

Cowling, R.M., Esler, K.J., Rundel, P.W., 1999b. Namaqualand, South Africa – an overview of a unique winter-rainfall desert ecosystem. Plant Ecology 142, 3-21.

Cowling, R.M., Richardson, D.M., Pierce, S.M., 1997. Vegetation of southern Africa. Cambridge University Press, Cambridge.

Dale, B., 1996. Dinoflagellate cyst ecology: modeling and geological applications, in: Jansonius, J., McGregor, D.C. (Eds.), Palynology: principles and applications. American Association of Stratigraphic Palynologists Foundation, Salt Lake City, pp. 1249-1275.

Dale, B., Dale, A.L., Jansen, J.H.F., 2002. Dinoflagellate cysts as environmental indicators in surface sediments from the Congo deep-sea fan and adjacent regions. Palaeogeography, Palaeoclimatology, Palaeoecology 185, 309-338.

Dale, B., Fjellså, A., 1994. Dinoflagellate Cysts as Paleoproductivity Indicators: State of the Art, Potential, and Limits, in: Zahn, R., Pedersen, T., Kaminski, M., Labeyrie, L. (Eds.), Carbon Cycling in the Glacial Ocean: Constraints on the Ocean's Role in Global Change. Springer Berlin Heidelberg, pp. 521-537.

Daniau, A.-L., Goñi, M.F.S., Martinez, P., Urrego, D.H., Bout-Roumazeilles, V., Desprat, S., Marlon, J.R., 2013. Orbital-scale climate forcing of grassland burning in southern Africa. Proceedings of the National Academy of Sciences 110, 5069-5073.

Davey, R., 1971. Palynology and palaeo-environmental studies, with special reference to the continental shelf sediments of South Africa. Proceedings of the Second Planktonic Conference. Edizioni Tecnoscienza, Roma, pp. 331-347.

Davey, R.J., Rogers, J., 1975. Palynomorph distribution in Recent offshore sediments along two traverses off South West Africa. Marine Geology 18, 213-225.

de Boer, A.M., Graham, R.M., Thomas, M.D., Kohfeld, K.E., 2013. The control of the Southern Hemisphere Westerlies on the position of the Subtropical Front. Journal of Geophysical Research: Oceans 118, 5669-5675.

de Vernal, A., Eynaud, F., Henry, M., Hillaire-Marcel, C., Londeix, L., Mangin, S., Matthiessen, J., Marret, F., Radi, T., Rochon, A., Solignac, S., Turon, J.L., 2005. Reconstruction of sea-surface conditions at middle to high latitudes of the Northern Hemisphere during the Last Glacial Maximum (LGM) based on dinoflagellate cyst assemblages. Quaternary Science Reviews 24, 897-924.

de Vernal, A., Rochon, A., Turon, J.L., Matthiessen, J., 1997. Organic-walled dinoflagellate cysts: Palynological tracers of sea-surface conditions in middle to high latitude marine environments. Geobios 30, 905-920.

de Vernal, A., Turon, J.-L., Guiot, J., 1994. Dinoflagellate cyst distribution in high-latitude marine environments and quantitative reconstruction of sea-surface salinity, temperature, and seasonality. Canadian Journal of Earth Sciences 31, 48-62.

de Verteuil, L., 1996. Data report: Upper Cenozoic dinoflagellate cysts from the continental slope and rise off New Jersey, in: Mountain, G., Miller, K., Blum, P., Poag, C., Twichell, D. (Eds.), Proceedings of the Ocean Drilling Program: Scientific results. College Station, Texas, pp. 439-454.

Devillers, R., de Vernal, A., 2000. Distribution of dinoflagellate cysts in surface sediments of the northern North Atlantic in relation to nutrient content and productivity in surface waters. Marine Geology 166, 103-124.

Dewar, G., Reimer, P.J., Sealy, J., Woodborne, S., 2012. Late-Holocene marine radiocarbon reservoir correction (ΔR) for the west coast of South Africa. The Holocene 22, 1481-1489.

Dupont, L., 1999. Pollen and spores in marine sediments from the east Atlantic- A view from the ocean into the African continent, in: Fischer, G., Wefer, G. (Eds.), Use of Proxies in Paleoceanography: Examples from the South Atlantic. Springer-Verlag, Berlin Heidelberg, pp. 523-546.

Dupont, L., Behling, H., Jahns, S., Marret, F., Kim, J.-H., 2007. Variability in glacial and Holocene marine pollen records offshore from west southern Africa. Vegetation History and Archaeobotany 16, 87-100.

Dyer, R.A., 1975. The genera of southern African flowering plants. Department of agricultural technical services, Pretoria.

Dyez, K.A., Zahn, R., Hall, I.R., 2014. Multicentennial Agulhas leakage variability and links to North Atlantic climate during the past 80,000 years. Paleoceanography 29, 1238-1248.

Eckardt, F., Kuring, N., 2005. SeaWiFS identifies dust sources in the Namib Desert. International Journal of Remote Sensing 26, 4159-4167.

Ekblom, A., Gillson, L., Risberg, J., Holmgren, K., Chidoub, Z., 2012. Rainfall variability and vegetation dynamics of the lower Limpopo Valley, Southern Africa, 500 AD to present. Palaeogeography, Palaeoclimatology, Palaeoecology 363, 69-78.

Esper, O., Versteegh, G.J.M., Zonneveld, K.A.F., Willems, H., 2004. A palynological reconstruction of the Agulhas Retroflection (South Atlantic Ocean) during the Late Quaternary. Global and Planetary Change 41, 31-62.

Evers, T.M., 1975. Recent Iron Age research in the eastern Transvaal, South Africa. The South African Archaeological Bulletin 30, 71-83.

Faegri, K., Iversen, J., 1989. Textbook of pollen analysis in: Faegri, K., Kaland, P., Krzywinski, K. (Eds.). Wiley, New York.

Farmer, E.C., Demenocal, P.B., Marchitto, T.M., 2005. Holocene and deglacial ocean temperature variability in the Benguela upwelling region: Implications for low-latitude atmospheric circulation. Paleoceanography 20.

Fensome, R., MacRae, R., Williams, G., 2008. DINOFLAJ2, version 1. American Association of Stratigraphic Palynologists, Data Series 1

Fischer, G., Wefer, G., 1996. Long-term observation of particle fluxes in the Eastern Atlantic: seasonality, changes of flux with depth and comparison with the sediment record, in: Wefer, G., Berger, W., Siedler, W.H., Webb, D. (Eds.), The South Atlantic: Present and Past Circulation. Springer-Verlag, Berlin Heidelberg, pp. 325-344.

Franzese, A.M., Hemming, S.R., Goldstein, S.L., Anderson, R.F., 2006. Reduced Agulhas Leakage during the Last Glacial Maximum inferred from an integrated provenance and flux study. Earth and Planetary Science Letters 250, 72-88.

Gajewski, K., Lézine, A.-M., Vincens, A., Delestan, A., Sawada, M., 2002. Modern climate–vegetation–pollen relations in Africa and adjacent areas. Quaternary Science Reviews 21, 1611-1631.

Goldblatt, P., Manning, J.C., 2002. Plant diversity of the Cape region of southern Africa. Annals of the Missouri Botanical Garden 89, 281-302.

Gordon, A.L., Weiss, R.F., Smethie, W.M., Warner, M.J., 1992. Thermocline and intermediate water communication between the south Atlantic and Indian oceans. Journal of Geophysical Research: Oceans 97, 7223-7240.

Govin, A., Holzwarth, U., Heslop, D., Ford Keeling, L., Zabel, M., Mulitza, S., Collins, J.A., Chiessi, C.M., 2012. Distribution of major elements in Atlantic surface sediments (36°N–49°S): Imprint of terrigenous input and continental weathering. Geochemistry, Geophysics, Geosystems 13.

Graham, L., Wilcox, L., 2000. Algae, Prentice-Hall, Upper Saddle River, New Jersey, USA.

Granger, R., 2016. Palaeoenvironmental reconstruction of late Holocene climate dynamics in Southwest Africa using a multi-proxy characterization of Namaqualand mudbelt sediments. Master thesis, University of Cape Town.

Gray, C.E.D., 2009. Characterising the Namaqualand Mudbelt: Chronology, Palynology and Palaeoenvironments. PhD Thesis, University of Cape Town, South Africa.

Gray, C.E.D., Meadows, M.E., Lee-Thorp, J.A., Rogers, J., 2000. Characterising the Namaqualand mudbelt of southern Africa: chronology, palynology and palaeoenvironments. South African Geographical Journal 82, 137-142.

Grimm, E., 2011. TILIA software version 1.7. 16. Illinois State Museum, Research and Collection Center. Springfield USA.

Hahn, A., Compton, J.S., Meyer-Jacob, C., Kristen, K.L., Lucassen, F., Pérey Mazo, M., Schefuß, E., Zabel, M., 2016. Holocene paleoclimatic record from the South African Namaqualand mudbelt: a source to sink approach. Quaternary International 404, 121-135.

Head, M., 1996. Modern dinoflagellate cysts and their biological affinities. Palynology: principles and applications 3, 1197-1248.

Head, M.J., Seidenkrantz, M.-S., Janczyk-Kopikowa, Z., Marks, L., Gibbard, P.L., 2005. Last Interglacial (Eemian) hydrographic conditions in the southeastern Baltic Sea, NE Europe, based on dinoflagellate cysts. Quaternary International 130, 3-30.

Heinrich, S., Zonneveld, K.A.F., Bickert, T., Willems, H., 2011. The Benguela upwelling related to the Miocene cooling events and the development of the Antarctic Circumpolar Current: Evidence from calcareous dinoflagellate cysts. Paleoceanography 26, PA3209.

Herbert, C.T., Compton, J.S., 2007. Geochronology of Holocene sediments on the western margin of South Africa. South African Journal of Geology 110, 327-338.

Herrmann, N., Boom, A., Carr, A.S., Chase, B.M., Granger, R., Hahn, A., Zabel, M., Schefuß, E., 2016. Sources, transport and deposition of terrestrial organic material: A case study from southwestern Africa. Quaternary Science Reviews 149, 215-229.

Heusser, L.E., 1983. Pollen distribution in the bottom sediments of the western North Atlantic Ocean. Marine Micropaleontology 8, 77-88.

Hijmans, R.J., Cameron, S.E., Parra, J.L., Jones, P.G., Jarvis, A., 2005. Very high resolution interpolated climate surfaces for global land areas. International Journal of Climatology 25, 1965-1978.

Holmgren, K., Lee-Thorp, J.A., Cooper, G.R.J., Lundblad, K., Partridge, T.C., Scott, L., Sithaldeen, R., Siep Talma, A., Tyson, P.D., 2003. Persistent millennial-scale climatic variability over the past 25,000 years in Southern Africa. Quaternary Science Reviews 22, 2311-2326.

Holzwarth, U., Esper, O., Zonneveld, K., 2007. Distribution of organic-walled dinoflagellate cysts in shelf surface sediments of the Benguela upwelling system in relationship to environmental conditions. Marine Micropaleontology 64, 91-119.

Holzwarth, U., Esper, O., Zonneveld, K.A.F., 2010. Organic-walled dinoflagellate cysts as indicators of oceanographic conditions and terrigenous input in the NW African upwelling region. Review of Palaeobotany and Palynology 159, 35-55.

Hooghiemstra, H., Lézine, A.-M., Leroy, S.A.G., Dupont, L., Marret, F., 2006. Late Quaternary palynology in marine sediments: A synthesis of the understanding of pollen distribution patterns in the NW African setting. Quaternary International 148, 29-44.

Hopley, P.J., Weedon, G.P., Marshall, J.D., Herries, A.I.R., Latham, A.G., Kuykendall, K.L., 2007. High- and low-latitude orbital forcing of early hominin habitats in South Africa. Earth and Planetary Science Letters 256, 419-432.

Houghton, J.T., Jenkins, G.J., Ephraums, J.J., 1990. Climate Change: The IPCC Assessment. 202.

Huffman, T.N., 1996. Archaeological evidence for climatic change during the last 2000 years in southern Africa. Quaternary International 33, 55-60.

Hutchings, L., van der Lingen, C.D., Shannon, L.J., Crawford, R.J.M., Verheye, H.M.S., Bartholomae, C.H., van der Plas, A.K., Louw, D., Kreiner, A., Ostrowski, M., Fidel, Q., Barlow, R.G., Lamont, T., Coetzee, J., Shillington, F., Veitch, J., Currie, J.C., Monteiro, P.M.S., 2009. The Benguela Current: An ecosystem of four components. Progress in Oceanography 83, 15-32.

Inthorn, M., Wagner, T., Scheeder, G., Zabel, M., 2006. Lateral transport controls distribution, quality, and burial of organic matter along continental slopes in high-productivity areas. Geology 34, 205-208.

Jarre, A., Hutchings, L., Crichton, M., Wieland, K., Lamont, T., Blamey, L., Illert, C., Hill, E., Berg, M., 2015. Oxygen-depleted bottom waters along the west coast of South Africa, 1950-2011. Fisheries Oceanography 24, 56-73.

Joyce, L.B., Pitcher, G.C., du Randt, A., Monteiro, P.M.S., 2005. Dinoflagellate cysts from surface sediments of Saldanha Bay, South Africa: an indication of the potential risk of harmful algal blooms. Harmful Algae 4, 309-318.

Keil, R.G., Montlucon, D.B., Prahl, F.G., Hedges, J.I., 1994. Sorptive preservation of labile organic matter in marine sediments. Nature 370, 549-552.

Kim, S.Y., Lim, D.I., 2014. Signatures of the late Holocene Neoglacial cold event and their marine-terrestrial linkage in the northwestern Pacific margin. Progress in Oceanography 124, 54-65.

Klapwijk, M., 1974. A preliminary report on Pottery from the north-eastern Transvaal, South Africa. The South African Archaeological Bulletin 29, 19-23.

Klein, R.G., 1991. Size variation in the Cape dune Molerat (Bathyergus suillus) and late Quaternary climatic change in the southwestern Cape Province, South Africa. Quaternary Research 36, 243-256.

Kohfeld, K., Graham, R., de Boer, A., Sime, L., Wolff, E., Le Quéré, C., Bopp, L., 2013. Southern Hemisphere westerly wind changes during the Last Glacial Maximum: paleo-data synthesis. Quaternary Science Reviews 68, 76-95.

Kristen, I., Fuhrmann, A., Thorpe, J., Röhl, U., Wilkes, H., Oberhänsli, H., 2007. Hydrological changes in southern Africa over the last 200 Ka as recorded in lake sediments from the Tswaing impact crater. South African Journal of Geology 110, 311-326.

Kristen, I., Wilkes, H., Vieth, A., Zink, K.G., Plessen, B., Thorpe, J., Partridge, T.C., Oberhansli, H., 2010. Biomarker and stable carbon isotope analyses of sedimentary organic matter from Lake Tswaing: evidence for deglacial wetness and early Holocene drought from South Africa. Journal of Paleolimnology. 44 (1), 143-160.

Lamont, T., Hutchings, L., van den Berg, M.A., Goschen, W.S., Barlow, R.G., 2015. Hydrographic variability in the St. Helena Bay region of the southern Benguela ecosystem. Journal of Geophysical Research: Oceans 120, 2920-2944.

Lamy, F., Hebbeln, D., Röhl, U., Wefer, G., 2001. Holocene rainfall variability in southern Chile: a marine record of latitudinal shifts of the Southern Westerlies. Earth and Planetary Science Letters 185, 369-382.

Leduc, G., Herbert, C.T., Blanz, T., Martinez, P., Schneider, R., 2010. Contrasting evolution of sea surface temperature in the Benguela upwelling system under natural and anthropogenic climate forcings. Geophysical Research Letters 37, L20705.

Lewis, J., Dodge, J., Powell, A., 1990. Quaternary dinoflagellate cysts from the upwelling system offshore Peru, Hole 686B, ODP Leg 1121, in: Suess, E., von Huene, R. (Eds.), Proceedings of the Ocean Drilling Program, Scientific Results, pp. 323-328.

Lezine, A.M., Duplessy, J.C., Cazet, J.P., 2005. West African monsoon variability during the last deglaciation and the Holocene: Evidence from fresh water algae, pollen and isotope data from core KW31, Gulf of Guinea. Palaeogeography, Palaeoclimatology, Palaeoecology 219, 225-237.

Mabote, M.E., Rogers, J., Meadows, M.E., 1997. Sedimentology of terrigenous mud from the Orange River delta and the inner shelf off Namaqualand, South Africa. South African Geographical Journal 79, 108-114.

MacDonald, G.M., Larsen, C.P., Szeicz, J., Moser, K., 1991. The reconstruction of boreal forest fire history from lake sediments: a comparison of charcoal, pollen, sedimentological, and geochemical indices. Quaternary Science Reviews 10, 53-71.

Maher, L.J., 1972. Nomograms for computing 0.95 confidence limits of pollen data. Review of Palaeobotany and Palynology 13, 85-93.

Maher, L.J., 1981. Statistics for microfossil concentration measurements employing samples spiked with marker grains. Review of Palaeobotany and Palynology 32, 153-191.

Marret, F., 1994. Distribution of dinoflagellate cysts in recent marine sediments from the east Equatorial Atlantic (Gulf of Guinea). Review of Palaeobotany and Palynology 84, 1-22.

Marret, F., de Vernal, A., 1997. Dinoflagellate cyst distribution in surface sediments of the southern Indian Ocean. Marine Micropaleontology 29, 367-392.

Marret, F., Zonneveld, K.A.F., 2003. Atlas of modern organic-walled dinoflagellate cyst distribution. Review of Palaeobotany and Palynology 125, 1-200.

Martin, A., 1968. Pollen analysis of Groenvlei lake sediments, Knysna (South Africa). Review of Palaeobotany and Palynology 7, 107-144.

Mayer, L.M., 1994. Surface area control of organic carbon accumulation in continental shelf sediments. Geochimica et Cosmochimica Acta 58, 1271-1284.

McCarthy, F.M., Mudie, P.J., 1998. Oceanic pollen transport and pollen: dinocyst ratios as markers of late Cenozoic sea level change and sediment transport. Palaeogeography, Palaeoclimatology, Palaeoecology 138, 187-206.

Meadows, M., Sugden, J., 1991. A vegetation history of the last 14,000 years on the Cederberg, south-western Cape Province. South African Journal of Science 87, 34-43.

Meadows, M.E., Baxter, A.J., 1999. Late Quaternary palaeoenvironments of the southwestern Cape, South Africa: a regional synthesis. Quaternary International 57, 193-206.

Meadows, M.E., Baxter, A.J., 2001. Holocene vegetation history and palaeoenvironments at Klaarfontein Springs, Western Cape, South Africa. The Holocene 11, 699-706.

Meadows, M.E., Baxter, A.J., Parkington, J., 1996. Late Holocene environments at verlorenvlei, Western Cape Province, South Africa. Quaternary International 33, 81-95.

Meadows, M.E., Chase, B.M., Seliane, M., 2010. Holocene palaeoenvironments of the Cederberg and Swartruggens mountains, Western Cape, South Africa: Pollen and stable isotope evidence from hyrax dung middens. Journal of Arid Environments 74, 786-793.

Meadows, M.E., Dingle, R.V., Rogers, J., Mills, E.G., 1997. Radiocarbon chronology of Namaqualand mudbelt sediments: problems and prospects. South African Journal of Science 93, 321-327.

Meadows, M.E., Rogers, J., Lee-Thorp, J.A., Bateman, M.D., Dingle, R.V., 2002. Holocene geochronology of a continental shelf mudbelt off southwestern Africa. The Holocene 12, 59-67.

Medeanic, S., 2006. Freshwater algal palynomorph records from Holocene deposits in the coastal plain of Rio Grande do Sul, Brazil. Review of Palaeobotany and Palynology 141, 83-101.

Metwally, A.A., Scott, L., Neumann, F.H., Bamford, M.K., Oberhänsli, H., 2014. Holocene palynology and palaeoenvironments in the Savanna Biome at Tswaing Crater, central South Africa. Palaeogeography, Palaeoclimatology, Palaeoecology 402 (0), 125-135.

Milliman, J.D., Rutkowski, C.M., Meybeck, M., 1995. River discharge to the sea: a global river index (GLORI). LOICZ reports and studies. School of Marine Science, Virginia Institute of Marine Science, College of William and Mary. pp. 90.

Montade, V., Nebout, N.C., Kissel, C., Mulsow, S., 2011. Pollen distribution in marine surface sediments from Chilean Patagonia. Marine Geology 282, 161-168.

Monteiro, P.M., van der Plas, A.K., 2006. Low oxygen water (LOW) variability in the Benguela system: Key processes and forcing scales relevant to forecasting. Large Marine Ecosystems 14, 71-90.

Moss, P.T., Kershaw, A.P., Grindrod, J., 2005. Pollen transport and deposition in riverine and marine environments within the humid tropics of northeastern Australia. Review of Palaeobotany and Palynology 134, 55-69.

Mucina, L., Rutherford, M.C., 2006. The vegetation of South Africa, Lesotho and Swaziland. South African National Biodiversity Institute.

Mudie, P.J., Marret, F., Rochon, A., Aksu, A.E., 2010. Non-pollen palynomorphs in the Black Sea corridor. Vegetation History and Archaeobotany 19, 531-544.

Nelson, G., 1989. Poleward motion in the Benguela area, in: Neshyba, S.J., Mooers, C.N.K., Smith, R.L., Baeber, R.T. (Eds.), Poleward flows along eastern ocean boundaries. Springer, New York, pp. 110-130.

Nelson, G., Hutchings, L., 1983. The Benguela upwelling area. Progress in Oceanography 12, 333-356.

Neumann, F., Botha, G., Scott, L., 2014. 18,000 years of grassland evolution in the summer rainfall region of South Africa: evidence from Mahwaqa Mountain, KwaZulu-Natal. Vegetation History and Archaeobotany, 1-17.

Neumann, F.H., Scott, L., Bamford, M.K., 2011. Climate change and human disturbance of Fynbos vegetation during the late Holocene at Princess Vlei, Western Cape, South Africa. The Holocene 21, 1137-1149.

Neumann, F.H., Scott, L., Bousman, C.B., van As, L., 2010. A Holocene sequence of vegetation change at Lake Eteza, coastal KwaZulu-Natal, South Africa. Review of Palaeobotany and Palynology 162, 39-53.

Neumann, F.H., Stager, J.C., Scott, L., Venter, H.J.T., Weyhenmeyer, C., 2008. Holocene vegetation and climate records from Lake Sibaya, KwaZulu-Natal (South Africa). Review of Palaeobotany and Palynology 152, 113-128.

Norström, E., Neumann, F.H., Scott, L., Smittenberg, R.H., Holmstrand, H., Lundqvist, S., Snowball, I., Sundqvist, H.S., Risberg, J., Bamford, M., 2014. Late Quaternary vegetation dynamics and hydro-climate in the Drakensberg, South Africa. Quaternary Science Reviews 105, 48-65.

Norström, E., Scott, L., Partridge, T.C., Risberg, J., Holmgren, K., 2009. Reconstruction of environmental and climate changes at Braamhoek wetland, eastern escarpment South Africa, during the last 16,000 years with emphasis on the Pleistocene-Holocene transition. Palaeogeography, Palaeoclimatology, Palaeoecology 271, 240-258.

Oboh-Ikuenobe, E.F., de Villiers, S.E., 2003. Dispersed organic matter in samples from the western continental shelf of Southern Africa: palynofacies assemblages and depositional environments of Late Cretaceous and younger sediments. Palaeogeography, Palaeoclimatology, Palaeoecology 201, 67-88.

O'Connor, T.G., Bredenkamp, G.J., 1997. Grassland, in: Cowling, R.M., Richardson, D.M., Pierce, S.M. (Eds.), Vegetation of South Africa. Cambridge University Press, Cambridge, pp. pp.215-245.

Partridge, T.C., Demenocal, P.B., Lorentz, S.A., Paiker, M.J., Vogel, J.C., 1997. Orbital forcing of climate over South Africa: A 200,000-year rainfall record from the pretoria saltpan. Quaternary Science Reviews 16, 1125-1133.

Peeters, F.J.C., Acheson, R., Brummer, G.-J.A., de Ruijter, W.P.M., Schneider, R.R., Ganssen, G.M., Ufkes, E., Kroon, D., 2004. Vigorous exchange between the Indian and Atlantic oceans at the end of the past five glacial periods. Nature 430, 661-665.

Peterson, R.G., Stramma, L., 1991. Upper-level circulation in the South Atlantic Ocean. Progress in Oceanography 26, 1-73.

Petrick, B.F., McClymont, E.L., Marret, F., van der Meer, M.T.J., 2015. Changing surface water conditions for the last 500 ka in the Southeast Atlantic: Implications for variable influences of Agulhas leakage and Benguela upwelling. Paleoceanography 30.

Piasecki, S., 1980. Dinoflagellate cyst stratigraphy of the Miocene Hodde and Gram Formations, Denmark. Bulletin of the Geological Society of Denmark 29, 53-76.

Pilo, G., Mata, M., Azevedo, J., 2015. Eddy Surface properties and propagation at Southern Hemisphere western boundary current systems. Ocean Science 11, 629-641.

Pospelova, V., de Vernal, A., Pedersen, T.F., 2008. Distribution of dinoflagellate cysts in surface sediments from the northeastern Pacific Ocean (43–25°N) in relation to sea-surface temperature, salinity, productivity and coastal upwelling. Marine Micropaleontology 68, 21-48.

Pospelova, V., Pedersen, T.F., de Vernal, A., 2006. Dinoflagellate cysts as indicators of climatic and oceanographic changes during the past 40 kyr in the Santa Barbara Basin, southern California. Paleoceanography 21.

Pospelova, V., Price, A.M., Pedersen, T.F., 2015. Palynological evidence for late Quaternary climate and marine primary productivity changes along the California margin. Paleoceanography 30, 877-894.

Quick, L.J., Chase, B.M., Meadows, M.E., Scott, L., Reimer, P.J., 2011. A 19.5 kyr vegetation history from the central Cederberg Mountains, South Africa: Palynological evidence from rock hyrax middens. Palaeogeography, Palaeoclimatology, Palaeoecology 309, 253-270.

Radi, T., Bonnet, S., Cormier, M.-A., de Vernal, A., Durantou, L., Faubert, É., Head, M.J., Henry, M., Pospelova, V., Rochon, A., Van Nieuwenhove, N., 2013. Operational taxonomy and (paleo-)autecology of round, brown, spiny dinoflagellate cysts from the Quaternary of high northern latitudes. Marine Micropaleontology 98, 41-57.

Rau, A.J., 2002. A late Quaternary history of Agulhas-Benguela interactions from two sediment cores on the western continental slope of South Africa. PhD Thesis, University of Cape Town, South Africa.

Rau, A.J., Rogers, J., Lutjeharms, J.R.E., Giraudeau, J., Lee-Thorp, J.A., Chen, M.T., Waelbroeck, C., 2002. A 450-kyr record of hydrological conditions on the western Agulhas Bank Slope, south of Africa. Marine Geology 180, 183-201.

Reason, C.J.C., Rouault, M., 2005. Links between the Antarctic Oscillation and winter rainfall over western South Africa. Geophysical Research Letters 32, L07705.

Reimer, P.J., Bard, E., Bayliss, A., Beck, J.W., Blackwell, P.G., Bronk Ramsey, C., Buck, C.E., Cheng, H., Edwards, R.L., Friedrich, M., 2013. IntCal13 and Marine13 radiocarbon age calibration curves 0-50,000 years cal BP. Radiocarbon 55, 1869-1887.

Richardson, D.M., 2000. Ecology and biogeography of Pinus. Cambridge University Press, Cambridge.

Rogers, J., 1977. Sedimentation on the continental margin off the Orange river and the Namib desert. PhD Thesis, University of Cape Town, South Africa.

Rogers, J., Bremner, J.M., 1991. The Benguela ecosystem; Part VII, Marine-geological aspects. Oceanography and Marine Biology: An Annual Review 29, 1-85.

Rogers, J., Rau, A., 2006. Surficial sediments of the wave-dominated Orange River Delta and the adjacent continental margin off south-western Africa. African Journal of Marine Science 28, 511-524.

Rossignol, M., 1962. Analyse pollinique de sédiments marins Quaternaires en Israël. II. Sédiments Pleistocènes. Pollen Spores 4, 121-148.

Schefuß, E., Kuhlmann, H., Mollenhauer, G., Prange, M., Pätzold, J., 2011. Forcing of wet phases in southeast Africa over the past 17,000 years. Nature 480, 509-512.

Schell, I.I., 1968. On the relation between the winds off southwest Africa and the Benguela Current and Agulhas Current penetration in the South Atlantic. Deutsche Hydrografische Zeitschrift 21, 109-117.

Schneider, R., Bleil, U., Buschhoff, H., Compton, J.S., Enneking, K., Frederichs, T., Herbert, C.T., Hessler, S., Hilgenfeldt, C., Kahle, G., Kim, J.-H., Machutchon, M., McMillan, I., Meyer-Schack, B., Ochsenhirt, W.-T., Rau, A.J., Rogers, J., Schacht, R., Schewe, F., Schnieders, L., Schulz, H.D., Spilker, S., Veitch, J., Weldeab, S., Wien, K., Wilke, I., Zahn, R., Zaric, S., Zatloukal, N., 2003. Report and preliminary results of Meteor cruise M 57-1, Cape Town – Walvis Bay, 20.01. 2003–08.02. 2003. University of Bremen, Germany

Schnepf, E., Elbrächter, M., 1992. Nutritional strategies in dinoflagellates: a review with emphasis on cell biological aspects. European journal of protistology 28, 3-24.

Scott, A.C., Damblon, F., 2010. Charcoal: Taphonomy and significance in geology, botany and archaeology. Palaeogeography, Palaeoclimatology, Palaeoecology 291, 1-10.

Scott, L., 1982. Late Quaternary fossil pollen grains from the Transvaal, South Africa. Review of Palaeobotany and Palynology 36, 241-278.

Scott, L., 1987. Late Quaternary forest history in Venda, Southern Africa. Review of Palaeobotany and Palynology 53, 1-10.

Scott, L., Bousman, C.B., Nyakale, M., 2005. Holocene pollen from swamp, cave and hyrax dung deposits at Blydefontein (Kikvorsberge), Karoo, South Africa. Quaternary International 129, 49-59.

Scott, L., Cooremans, B., 1992. Pollen in recent Procavia (hyrax), Petromus (dassie rat) and bird dung in South Africa. Journal of Biogeography, 205-215.

Scott, L., Neumann, F.H., Brook, G.A., Bousman, C.B., Norström, E., Metwally, A.A., 2012. Terrestrial fossil-pollen evidence of climate change during the last 26 thousand years in Southern Africa. Quaternary Science Reviews 32, 100-118.

Scott, L., Woodborne, S., 2007a. Pollen analysis and dating of Late Quaternary faecal deposits (hyraceum) in the Cederberg, Western Cape, South Africa. Review of Palaeobotany and Palynology 144 (3–4), 123-134.

Scott, L., Woodborne, S., 2007b. Vegetation history inferred from pollen in Late Quaternary faecal deposits (hyraceum) in the Cape winter-rain region, and its bearing on past climates in South Africa. Quaternary Science Reviews 26 (7-8), 941-953.

Shannon, L.V., 1985. The Benguela ecosystem. I: Evolution of the Benguela physical features and processes. Oceanography and Marine Biology 23, 105-182.

Shannon, L.V., Nelson, G., 1996. The Benguela: large scale features and processes and system variability, in: Wefer, G., Berger, W.H., Siedler, G., Webb, D. (Eds.), The South Atlantic: Present and Past Circulation. Springer-Verlag, Berlin Heidelberg, pp. 63-210.

Shaughnessy, G., 1986. A case study of some woody plant introductions to the Cape Town area, in: Macdonald, I., Kruger, F., Ferrar, A. (Eds.), The Ecology and Management of Biological Invasions in Southern Africa. Cape Town: Oxford University Press, 1986., pp. pp. 37-34.

Shi, N., Dupont, L., Beug, H.-J., Schneider, R., 1998. Vegetation and climate changes during the last 21 000 years in S.W. Africa based on a marine pollen record. Vegetation History and Archaeobotany 7, 127-140.

Shi, N., Schneider, R., Beug, H.-J., Dupont, L., 2001. Southeast trade wind variations during the last 135 kyr: evidence from pollen spectra in eastern South Atlantic sediments. Earth and Planetary Science Letters 187, 311-321.

Stager, J.C., Mayewski, P.A., White, J., Chase, B.M., Neumann, F.H., Meadows, M.E., King, C.D., Dixon, D.A., 2012. Precipitation variability in the winter rainfall zone of South Africa during the last 1400 yr linked to the austral westerlies. Climate of the Past 8, 877-887.

Stager, J.C., Ryves, D.B., King, C., Madson, J., Hazzard, M., Neumann, F.H., Maud, R., 2013. Late Holocene precipitation variability in the summer rainfall region of South Africa. Quaternary Science Reviews 67, 105-120.

Stover, L., Riding, J., Brinkhuis, H., 1996. Mesozoic-Tertiary dinoflagellates, acritarchs and prasinophytes.

Tang, L., Mao, L., Lü, X., Ma, Q., Zhou, Z., Yang, C., Kong, Z., Batten, D.J., 2013. Palaeoecological and palaeoenvironmental significance of some important spores and micro-algae in Quaternary deposits. Chinese Science Bulletin 58, 3125-3139.

Taylor, A., 2004. A trace element study of sediments from the Olifants River estuary, the Berg River estuary, and the off-shore Mud Belt. PhD Thesis, University of Cape Town, South Africa.

Ter Braak, C., Šmilauer, P., 2012. Canoco reference manual and user's guide: software for ordination (version 5.0). Microcomputer Power, Ithaca, NY, USA.

Tinner, W., Conedera, M., Ammann, B., Gaggeler, H.W., Gedye, S., Jones, R., Sagesser, B., 1998. Pollen and charcoal in lake sediments compared with historically documented forest fires in southern Switzerland since AD 1920. The Holocene 8, 31-42.

Traverse, A., Ginsburg, R.N., 1966. Palynology of the surface sediments of Great Bahama Bank, as related to water movement and sedimentation. Marine Geology 4, 417-459.

Traverse, A., Ginsburg, R.N., 1967. Pollen and associated microfossils in the marine surface sediments of the Great Bahama Bank. Review of Palaeobotany and Palynology 3, 243-254.

Truc, L., Chevalier, M., Favier, C., Cheddadi, R., Meadows, M.E., Scott, L., Carr, A.S., Smith, G.F., Chase, B.M., 2013. Quantification of climate change for the last 20,000 years from Wonderkrater, South Africa: implications for the long-term dynamics of the Intertropical Convergence Zone. Palaeogeography, Palaeoclimatology, Palaeoecology 386, 575-587.

Tyson, P.D., Karlen, W., Holmgren, K., Heiss, G. A., 2000. The little ice age and Medieval warming in South Africa. South African Journal of Science 96, 121-126.

Tyson, P.D., 1986. Climatic change and variability in southern Africa. Oxford University Press, USA.

Tyson, P.D., Preston-Whyte, R.A., 2000. The weather and climate of southern Africa. Oxford University Press, Cape Town.

Udeze, C.U., Oboh-Ikuenobe, F.E., 2005. Neogene palaeoceanographic and palaeoclimatic events inferred from palynological data: Cape Basin off South Africa, ODP Leg 175. Palaeogeography, Palaeoclimatology, Palaeoecology 219, 199-223.

Urrego, D.H., Sánchez Goñi, M.F., Daniau, A.L., Lechevrel, S., Hanquiez, V., 2015. South-western Africa vegetation responses to atmospheric and oceanic changes during the last climatic cycle. Clim. Past Discuss. 11, 345-376.

Valsecchi, V., Chase, B.M., Slingsby, J.A., Carr, A.S., Quick, L.J., Meadows, M.E., Cheddadi, R., Reimer, P.J., 2013. A high resolution 15,600-year pollen and microcharcoal record from the Cederberg Mountains, South Africa. Palaeogeography, Palaeoclimatology, Palaeoecology 387, 6-16.

Verleye, T.J., Louwye, S., 2010. Late Quaternary environmental changes and latitudinal shifts of the Antarctic Circumpolar Current as recorded by dinoflagellate cysts from offshore Chile (41°S). Quaternary Science Reviews 29, 1025-1039.

Wall, D., Dale, B., Lohmann, G.P., Smith, W.K., 1977. The environmental and climatic distribution of dinoflagellate cysts in modern marine sediments from regions in the North and South Atlantic Oceans and adjacent seas. Marine Micropaleontology 2, 121-200.

Weijer, W., de Ruijter, W.P., Dijkstra, H.A., van Leeuwen, P.J., 1999. Impact of interbasin exchange on the Atlantic overturning circulation. Journal of Physical Oceanography 29, 2266-2284.

Weldeab, S., Stuut, J.B.W., Schneider, R.R., Siebel, W., 2013. Holocene climate variability in the winter rainfall zone of South Africa. Climate of the Past 9, 2347-2364.

Wheeler, A.D., 2010. Impacts of degradation on critically endangered Oudtshoorn Gannaveld. PhD Thesis, University of the Western Cape, South Africa.

White, F., 1983. The vegetation of Africa. Natural Resources Research 20. Paris: United Nations Scientific and Cultural Organization.

Whitlock, C., Millspaugh, S.H., 1996. Testing the assumptions of fire-history studies: an examination of modern charcoal accumulation in Yellowstone National Park, USA. The Holocene 6, 7-15.

Winter, A., Martin, K., 1990. Late Quaternary history of the Agulhas Current. Paleoceanography 5, 479-486.

Zhao, X., Dupont, L., Meadows, M.E., Wefer, G., 2016a. Pollen distribution in the marine surface sediments of the mudbelt along the west coast of South Africa. Quaternary International 404, 44-56.

Zhao, X., Dupont, L., Schefuß, E., Meadows, M.E., Hahn, A., Wefer, G., 2016b. Holocene vegetation and climate variability in the winter and summer rainfall zones of South Africa. The Holocene 26, 843-857.

Zonneveld, K.A.F., 1997. New species of organic walled dinoflagellate cysts from modern sediments of the Arabian Sea (Indian Ocean). Review of Palaeobotany and Palynology 97, 319-337.

Zonneveld, K.A., Versteegh, G.J., de Lange, G.J., 1997. Preservation of organic-walled dinoflagellate cysts in different oxygen regimes: a 10,000 year natural experiment. Marine Micropaleontology 29, 393-405.

Zonneveld, K.A., P Hoek, R., Brinkhuis, H., Willems, H., 2001a. Geographical distributions of organic-walled dinoflagellate cysts in surficial sediments of the Benguela upwelling region and their relationship to upper ocean conditions. Progress in Oceanography 48, 25-72.

Zonneveld, K.A.F., Versteegh, G.J.M., de Lange, G.J., 2001b. Palaeoproductivity and post-depositional aerobic organic matter decay reflected by dinoflagellate cyst assemblages of the Eastern Mediterranean S1 sapropel. Marine Geology 172, 181-195.

Zonneveld, K.A.F., Bockelmann, F., Holzwarth, U., 2007. Selective preservation of organic-walled dinoflagellate cysts as a tool to quantify past net primary production and bottom water oxygen concentrations. Marine Geology 237, 109-126.

Zonneveld, K.A.F., Versteegh, G., Kodrans-Nsiah, M., 2008. Preservation and organic chemistry of Late Cenozoic organic-walled dinoflagellate cysts: A review. Marine Micropaleontology 68, 179-197.

Zonneveld, K.A.F., Marret, F., Versteegh, G.J.M., Bogus, K., Bonnet, S., Bouimetarhan, I., Crouch, E., de Vernal, A., Elshanawany, R., Edwards, L., Esper, O., Forke, S., Grøsfjeld, K., Henry, M., Holzwarth, U., Kielt, J.-F., Kim, S.-Y., Ladouceur, S., Ledu, D., Chen, L., Limoges, A., Londeix, L., Lu, S.H., Mahmoud, M.S., Marino, G., Matsouka, K., Matthiessen, J., Mildenhal, D.C., Mudie, P., Neil, H.L., Pospelova, V., Qi, Y., Radi, T., Richerol, T., Rochon, A., Sangiorgi, F., Solignac, S., Turon, J.-L., Verleye, T., Wang, Y., Wang, Z., Young, M., 2013. Atlas of modern dinoflagellate cyst distribution based on 2405 data points. Review of Palaeobotany and Palynology 191, 1-197.

Zonneveld, K.A.F., Pospelova, V., 2015. A determination key for modern dinoflagellate cysts. Palynology 39, 387-409.

# Appendix I: Morphologies of terrestrial and marine palynomorphs

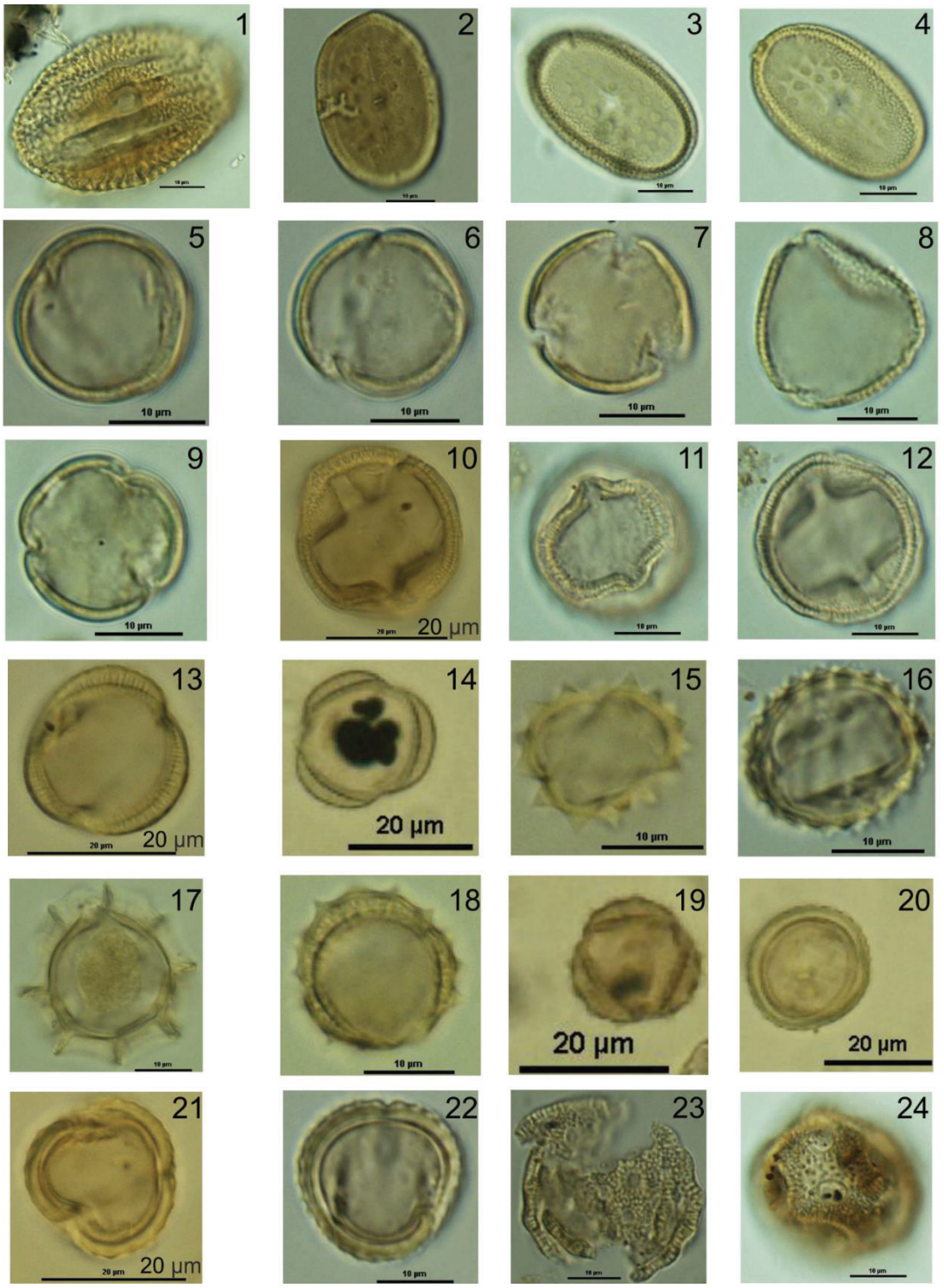


**Plate I:** 1-4. Acanthaceae: 2-4. *Justicia/Monechma*-type. 5-9. Aizoaceae. 10-12. *Anthrospermum* (Rubiaceae). 13-22. Asteraceae: 13-14. *Artemisia*-type, 15-16. Asteroideae, 17. *Pacourina*-type, 18-19. *Pentzia*-type, 20-22. *Stoebe/Elytropappus*-type. 23-24. Caryophyllaceae. The scale bars are all 10 µm except in 10, 13, 14, 19, 20 and 21 which are 20 µm.

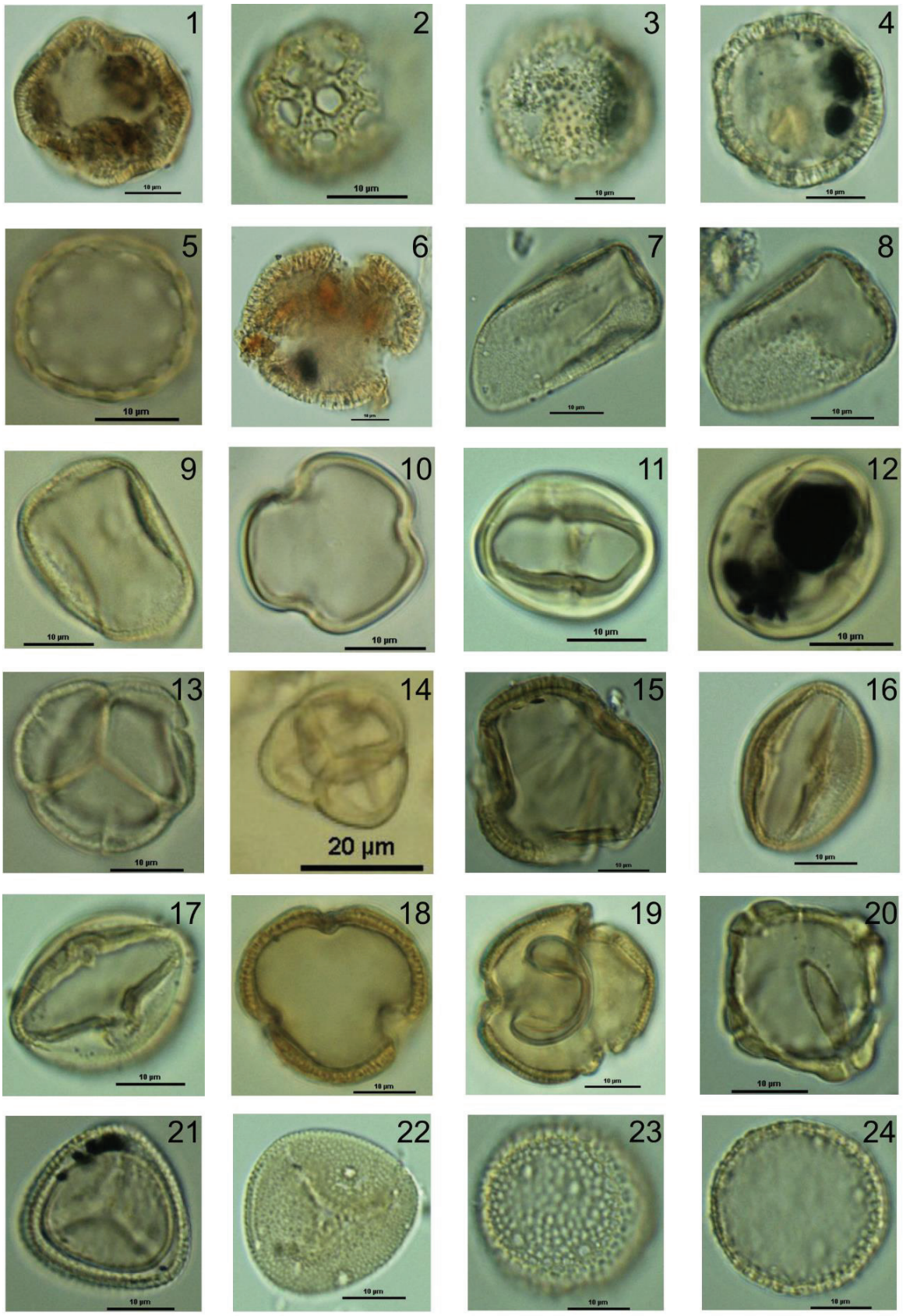


**Plate II:** 1-4. Caryophyllaceae. 5. Chenopodiaceae. 6. Convolunaceae. 7-9. Cyperaceae. 10-12. *Diospyros* (Ebenaceae). 13-14. Ericaceae. 15-19. *Euphorbia* (Euphorbiaceae). 20. Haloragaceae. 21-22. Neuradaceae. 23-24. *Passerina* (Thymelaeaceae). The scale bars are all 10 µm except in 14 which is 20 µm.

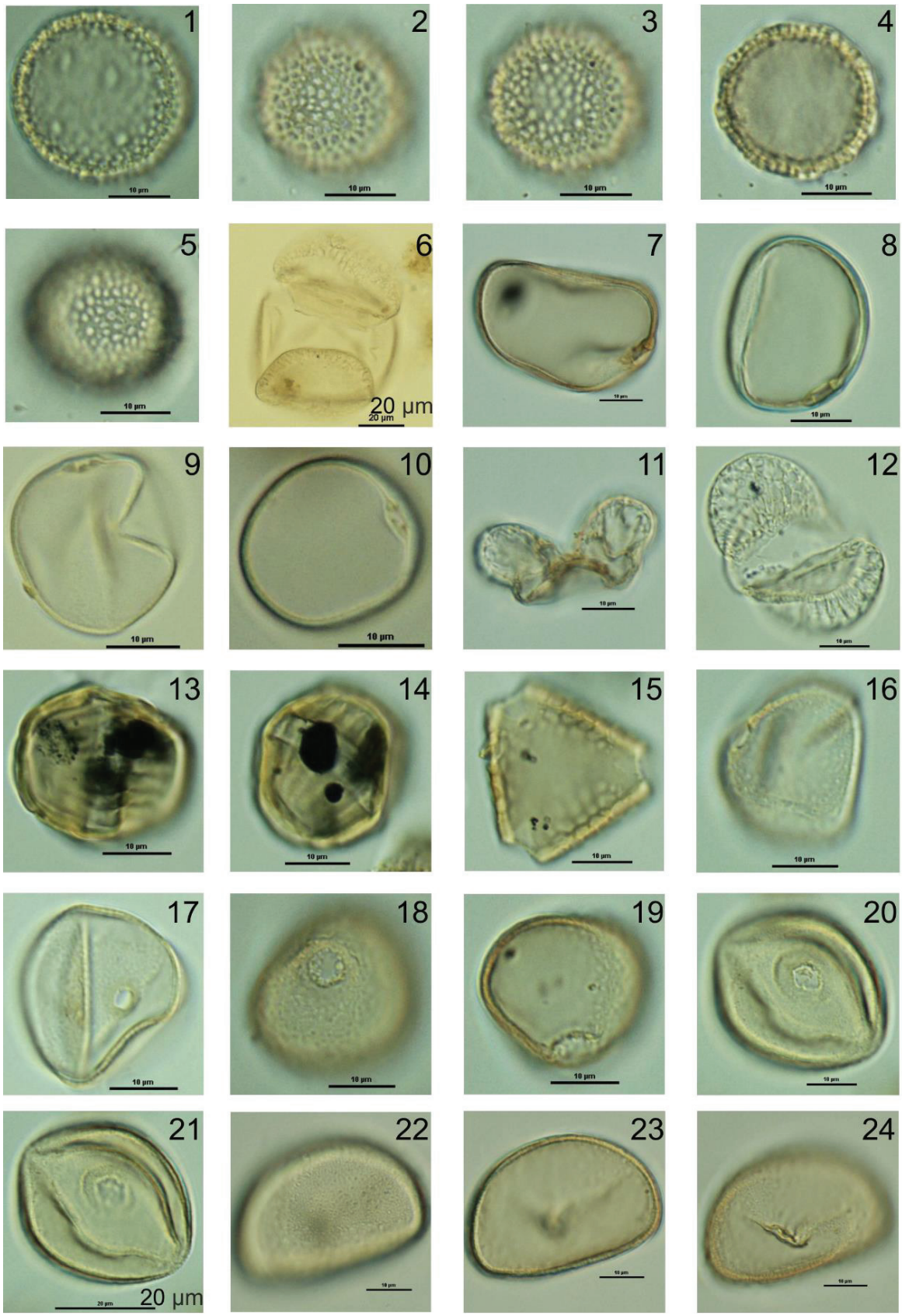


**Plate III:** 1-5. *Passerina* (Thymelaeaceae). 6. *Pinus* (Pinaceae). 7-10. Poaceae. 11-12. *Podocarpus* (Podocarpaceae). 13-14. Polygalaceae. 15. Proteaceae. 16-24. Restionaceae. The scale bars are all 10 µm except in 6 and 21 which are 20 µm.

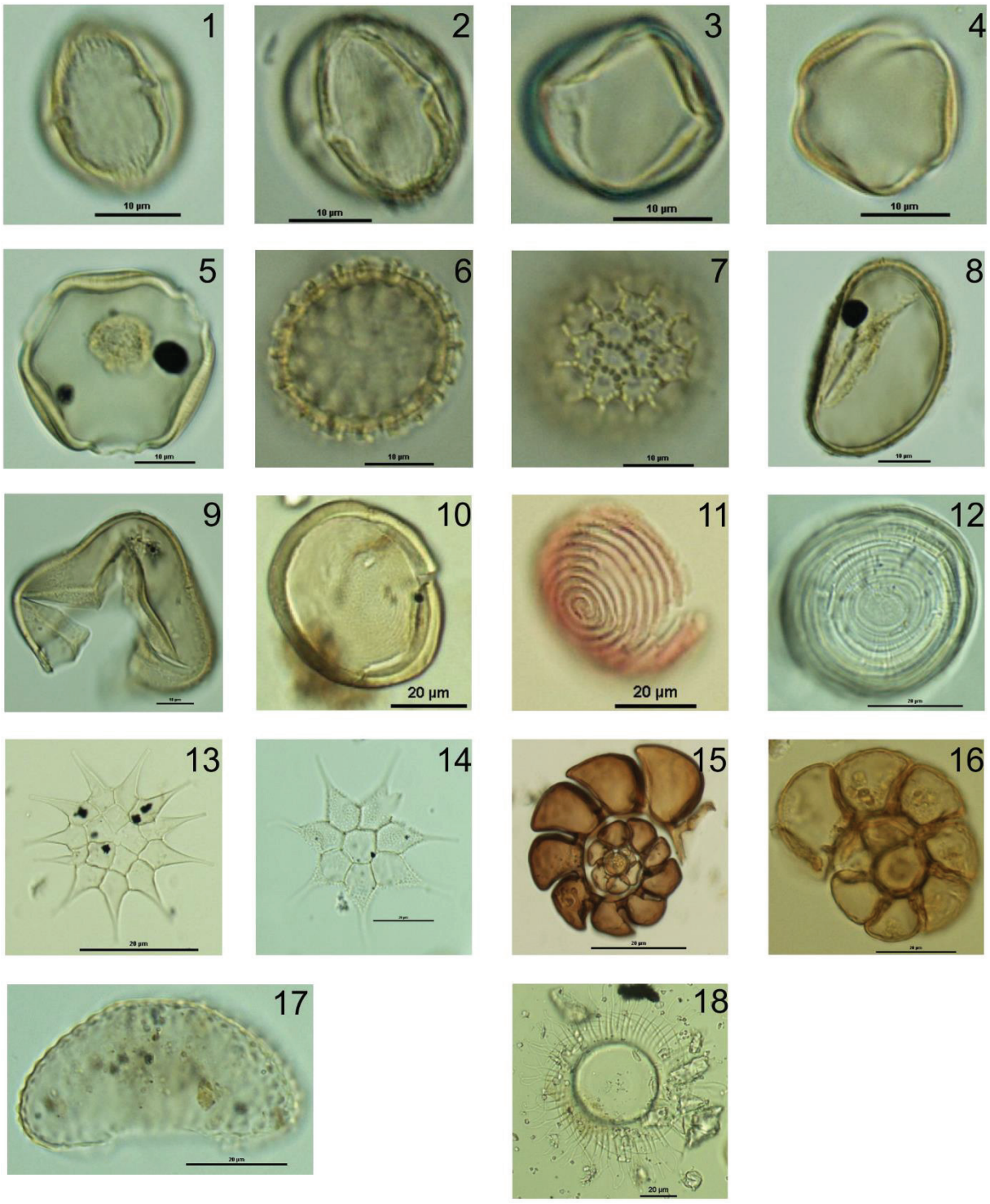


**Plate IV:** 1-3. *Rhus*-type (Anacardiaceae). 4-5. Solanaceae. 6-7. *Tribulus* (Zygophylaceae). 8. *Monolete* spore. 9. Trilete spore. 10-12. *Concentricystes* (algae). 13-14. *Pediastrum* sp. (algae). 15-16. Foraminiferal organic linings. 17. *Cosmarium* spp. (green algae). 18. *Radiosperma* cf. *R.corbiferum* (acritarch). The scale bars are all 10 µm from 1-9 and 20 µm from 10-18.

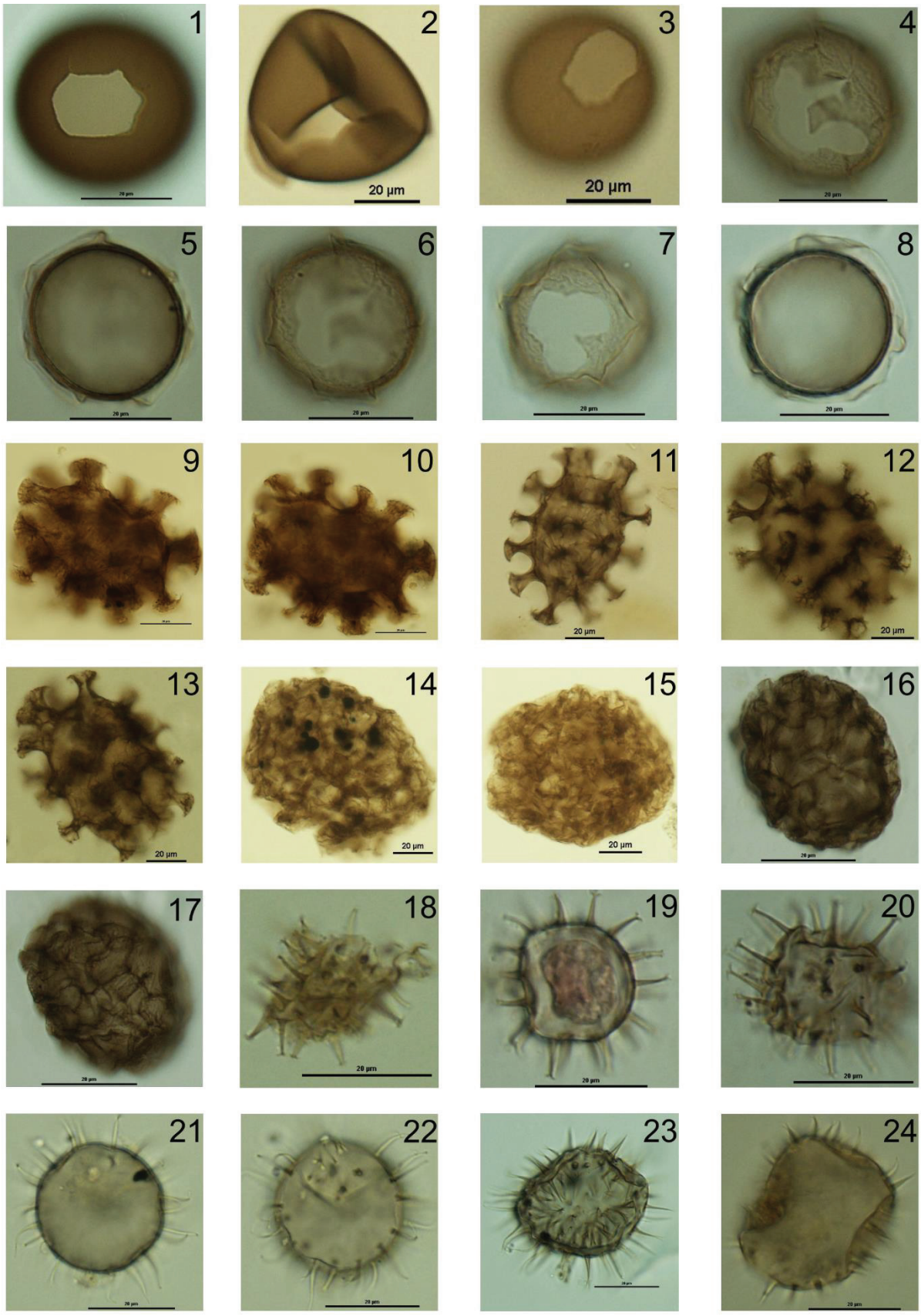


**Plate V:** 1-3. *Brigantedinium* spp. 4-8. Cyst of *Protoperidinium americanum*. 9-13. Cyst of *Polykrikos kofoidii*. 14-17. Cyst of *Polyfrikos schwartzii*. 18-20. *Echinidinium aculeatum*. 21-24. *Echinidinum transparantum*.The scale bars are all 20 µm.

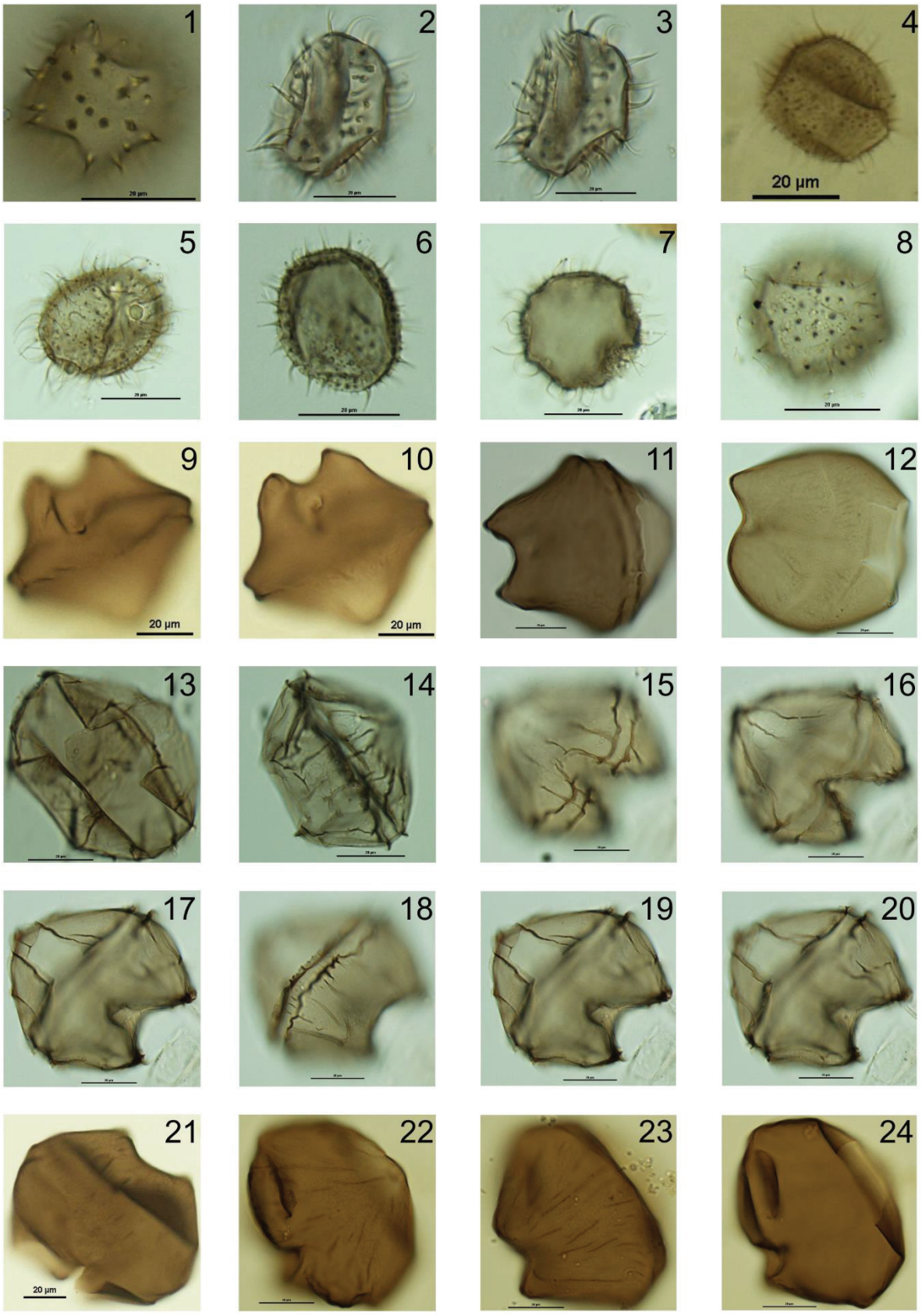


**Plate VI:** 1-3. *Echinidinum transparantum*. 4-8. *Echinidinium* spp. 9-11. *Lejeunecysta oliva*. 12. *Lejeunecysta sabrina*.13-20. *Lejeunecysta paratenella*. 21-24. *Quinquecuspis concreta*. The scale bars are all 20 µm

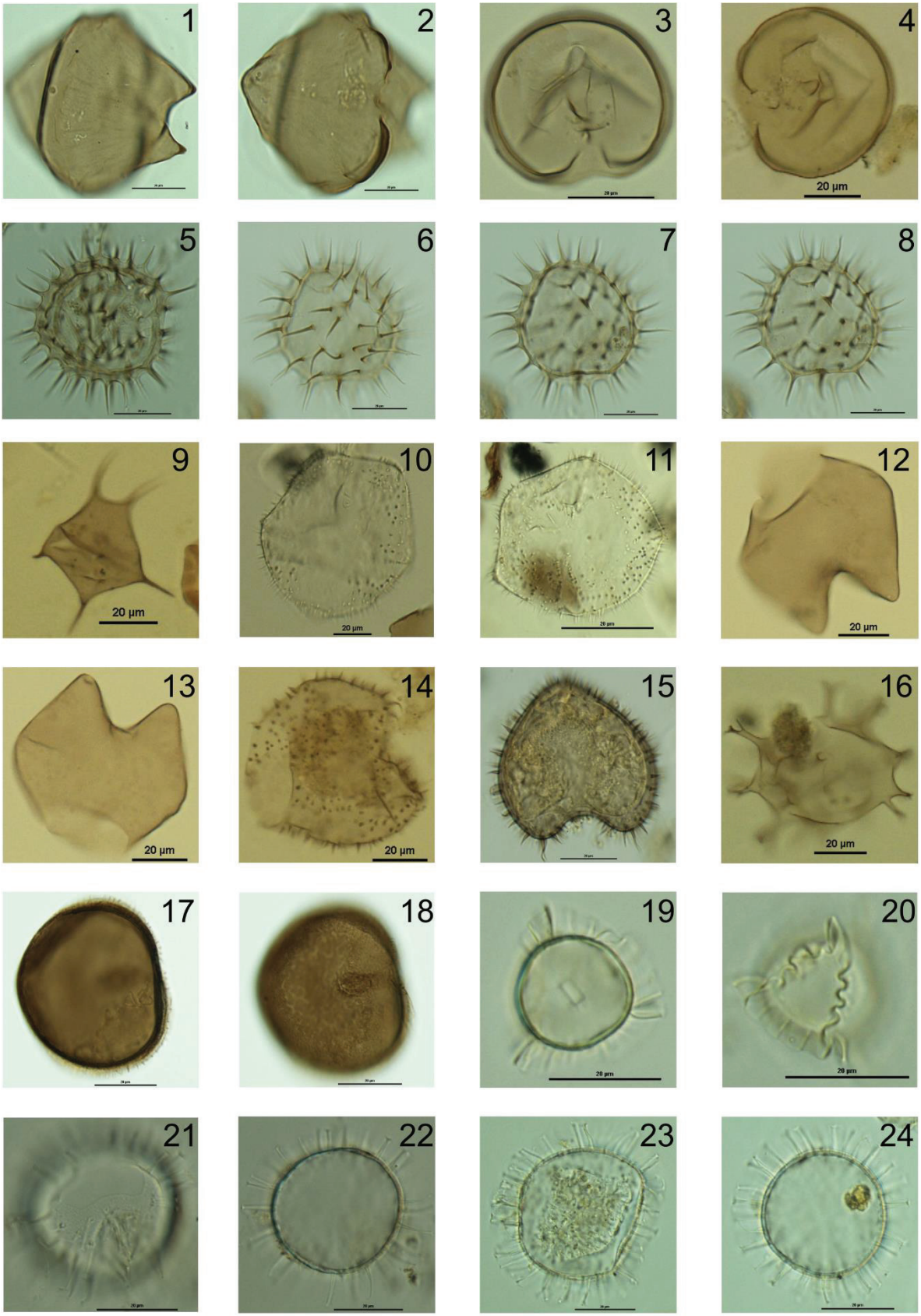


**Plate VII:** 1-2. *Quinquecuspis concreta*. 3-4. *Selenopemphix nephroides*. 5-8. *Selenopemphix quanta*. 9. *Stelladinium robustum*. 10-11. *Trinovantedinium applanatum*. 12-13. *Votadinium calvum*. 14-15. *Votadinium spinosum*. 16. *Xandarodinium xanthum*. 17-18. *Dubridinium* spp.?. 19-20. *Impagidinium* spp. 21-24. *Operculodinium centrocarpum*. The scale bars are all 20 µm.

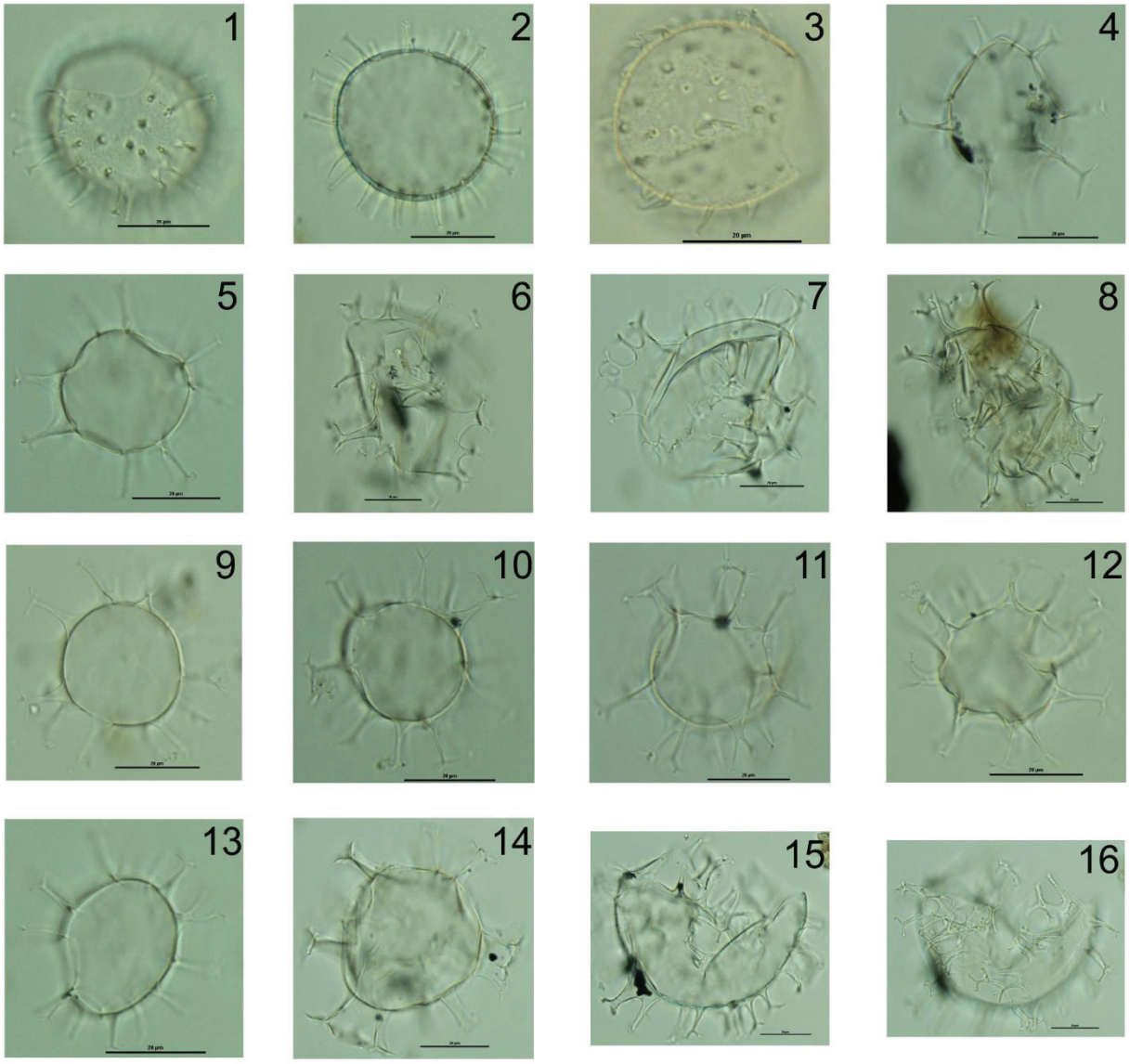


**Plate VIII:** 1-3. *Operculodinium centrocarpum*. 4. *Spiniferites bentorii*. 5. *Spiniferites membranaceus*. 6-8. *Spiniferites mirabilis*. 9-12. *Spiniferites ramosus*. 13-14. *Spiniferites* spp. 15-16. *Spiniferites* type 1. The scale bars are all 20 µm.

# Appendix II: Contributions to Chapters 2, 3 and 4, and Appendix I

**Chapter 2: Pollen distribution in the marine surface sediments of the mudbelt along the west coast of South Africa (Published in Quaternary International)**

**Xueqin Zhao, Lydie Dupont, Michael E. Meadows and Gerold Wefer**

1. Xueqin Zhao did the preparation and analyzed pollen and spores of total 12 marine surface sediment samples. She interpreted the pollen results and wrote the manuscript.

2. Dr. Lydie Dupont designed the study, supervised development of work, helped identification of pollen, data interpretation and critical manuscript revision.

3. Prof. Dr. Michael E. Meadows helped in data interpretation, provided office for manuscript writing in University of Cape Town, South Africa, and critical manuscript revision.

4. Prof. Dr. Gerold Wefer provided the research position, designed the study and revised the manuscript.

**Chapter 3: Holocene vegetation and climate variability in the winter and summer rainfall zones of South Africa (Published in The Holocene)**

**Xueqin Zhao, Lydie Dupont, Enno Schefuß, Michael E. Meadows, Annette Hahn and Gerold Wefer**

1. Xueqin Zhao did the preparation and analyzed pollen and spores of sediment samples from sites GeoB8331 (gravity core GeoB8331-4 and multicore GeoB8331-2) and GeoB8323 (gravity core GeoB8323-2 and multicore GeoB8323-1). She interpreted the pollen results and wrote the manuscript.

2. Dr. Lydie Dupont designed the study, supervised development of work, helped identification of pollen, data interpretation and critical manuscript revision.

3. Dr. Enno Schefuß helped in data interpretation and critical manuscript revision.

4. Prof. Dr. Michael E. Meadows helped in critical manuscript revision and provided office for manuscript revision in University of Cape Town, South Africa.

5. Dr. Annette Hahn helped in age model updating and data discussion, and revised the manuscript.

6. Prof. Dr. Gerold Wefer provided the research position, designed the study and revised the manuscript.

**Chapter 4: Palynological evidence for Holocene climatic and oceanographic changes off western South Africa (Published in Quaternary Science Reviews)**

**Xueqin Zhao, Lydie Dupont, Enno Schefuß, Ilham Bouimetarhan and Gerold Wefer**

1. Xueqin Zhao did the preparation and analyzed dinoflagellate cysts of total 12 marine surface samples and sediment samples from gravity core GeoB8331-4. She interpreted the dinoflagellate cyst results and wrote the manuscript.

2. Dr. Lydie Dupont designed the study, supervised development of work, helped in identification of dinoflagellate cysts, data interpretation and critical manuscript revision.

3. Dr. Enno Schefuß helped in critical manuscript revision.

4. Dr. Ilham Bouimetarhan helped to identify dinoflagellate cysts, dicussed the data and revised the manuscript.

5. Prof. Dr. Gerold Wefer provided the research position, designed the study and revised the manuscript.

**Appendix I: Morphologies of terrestrial and marine palynomorphs**

Xueqin Zhao took the photos through the microscope from the samples analyzed in this thesis.

# Acknowledgments

First of all, I would like to thank Prof. Dr. Gerold Wefer who gave me the opportunity to work on my PhD study in such an international community at the MARUM and supported me with great advices during each of my thesis committee meetings and detailed comments on each of my manuscripts.

I would like to give my deepest gratefulness to Dr. Lydie Dupont who was always there supporting me, sharing all her knowledge that I have needed and answering all the questions that I have met. Without your quick replies and extremely valuable and constructive comments on all my manuscripts, I could not have finished my PhD study in time. Your advices and encouragement when I was pregnant and thereafter gave birth my daughter always made me to calm down.

I am sincerely thankful to Dr. Enno Schefuß and Prof. Dr. Gesine Mollenhauer who gave up their time for all my thesis committee meetings with critical discussion and helpful advices.

I am also thankful to Dr. Annette Hahn who was always supportive for the age-depth model and was patient to explain the element data for me.

Many thanks to Dr. Ilham Bouimetarhan who helped me a lot on the identification of dinoflagellate cysts and gave me helpful discussion on my dinoflagellate cyst data. Also thanks to PD. Dr. Karin Zonneveld who provided me dinoflagellate cyst references.

Many thanks to Prof. Dr. Hermann Behling for his willingness to review my thesis, attending my thesis colloquium and giving me useful comments.

Many thanks to Dr. Matthias Zabel for the useful information about the RAiN project and the samples I need.

I am very happy to have worked with Nicole Hermann in the same project with helpful discussion on both of our data as well as many helps for my living life in Germany. Many thanks to Friederike Grimmer for the help of writing german abstract for this thesis. Also thanks to my other office mates, Christoph Häggi and Yanming Ruan. And Francesca Vallé and Yancheng Zhang for the help when I just started my work in MARUM.

I would like to thank GLOMAR for the funding which gave me the opportunities to attend international conferences and my research stay in Cape Town. Prof. Dr. Michael E Meadows, thanks for inviting me over to University of Cape Town for my research stay which gave me lots of discussion on my first and second manuscripts. Also thank Dr. Kelly Kirsten for finding me an accommodation in Cape Town.

In the end, I am very appreciated for the support from my family especially my parents during all my life with permanent understanding and encouragement. Most of all, I thank to my husband Weichao, without his accompanying, my study here would not even have started. Also I feel so happy to be with my precious little daughter Xixi seeing every moment in her growth.

This PhD position was funded by German Federal Ministry of Education and Research (BMBF). The investigations were conducted within the collaborative project “Regional Archives for Intergrated Investigations” (RAiN), which is embedded in the international research program SPACES (*Science Partnership for the Assessment of Complex Earth System Process*).

09 May, 2017, Bremen

Xueqin Zhao